

Selective Small Molecule Inhibition of Poly(ADP-Ribose) Glycohydrolase (PARG)

Supporting Information

*Kristin E. Finch, Claire E. Knezevic, Amanda C. Nottbohm,
Kathryn C. Partlow, and Paul J. Hergenrother**

Department of Chemistry
Roger Adams Laboratory
University of Illinois
600 S. Mathews Ave.
Urbana, IL 61802

*To whom correspondence should be addressed: hergenro@illinois.edu

Table of Contents

Supplementary Figure S1.....	S2
Supplementary Figure S2.....	S3
Supplementary Figure S3.....	S4
Supplementary Figure S4.....	S9
Supplementary Figure S5.....	S12
Supplementary Figure S6.....	S14
Supplementary Figure S7.....	S16
Supplementary Figure S8.....	S27
Supplementary Figure S9.....	S28
Supplementary Figure S10.....	S29
Supplementary Figure S11.....	S30
Supplementary Figure S12.....	S31
Supplementary Figure S13.....	S32
Supplementary Figure S14.....	S34
Supplementary Figure S15.....	S35
Supplementary Figure S16.....	S36
Supplementary Figure S17.....	S37
Supplementary Figure S18.....	S38
Supplementary Figure S19.....	S39
Supplementary Figure S20.....	S40
Supplementary Figure S21.....	S41
General Methods.....	S42
Synthesis of ³² P-PAR.....	S42
Radiometric PARG Assay.....	S43
Radiometric PARP Assay.....	S44
ARH3 protein expression.....	S44
Synthetic Protocols and Characterization.....	S44
References.....	S49
NMR Spectra.....	S50

Figure S1. Triplicate IC₅₀ data for **RBPI-1** obtained using *in vitro* ³²P-PAR degradation assay

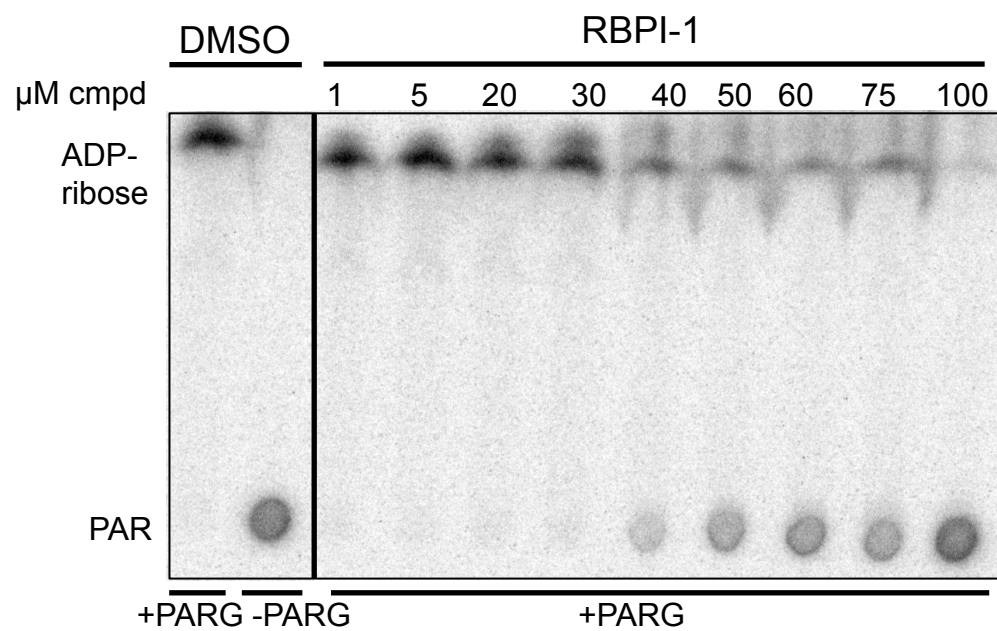
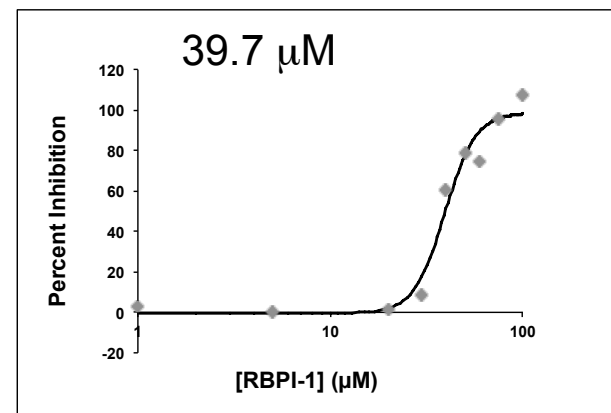
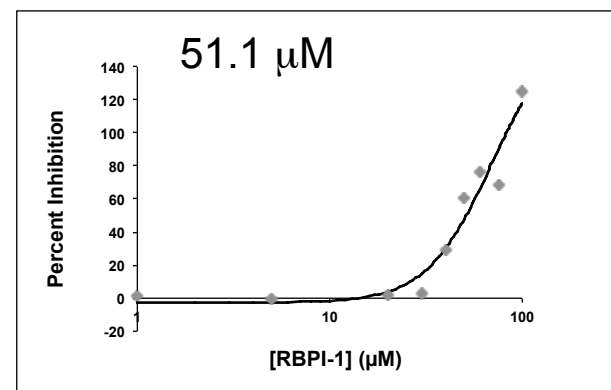
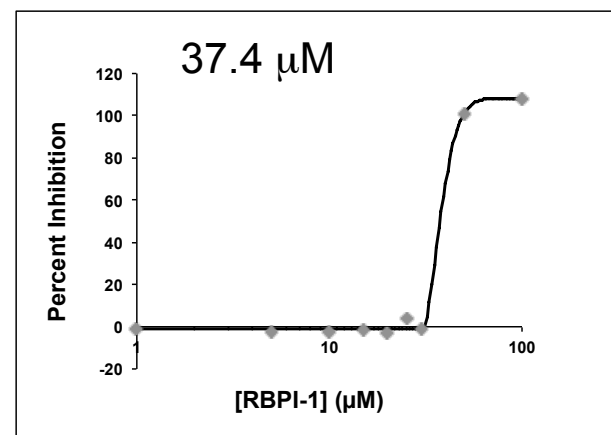
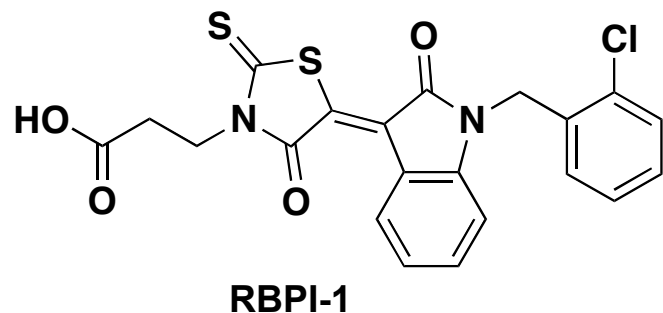


Figure S2. General synthetic route for preparation of **RBPI-1** derivative library

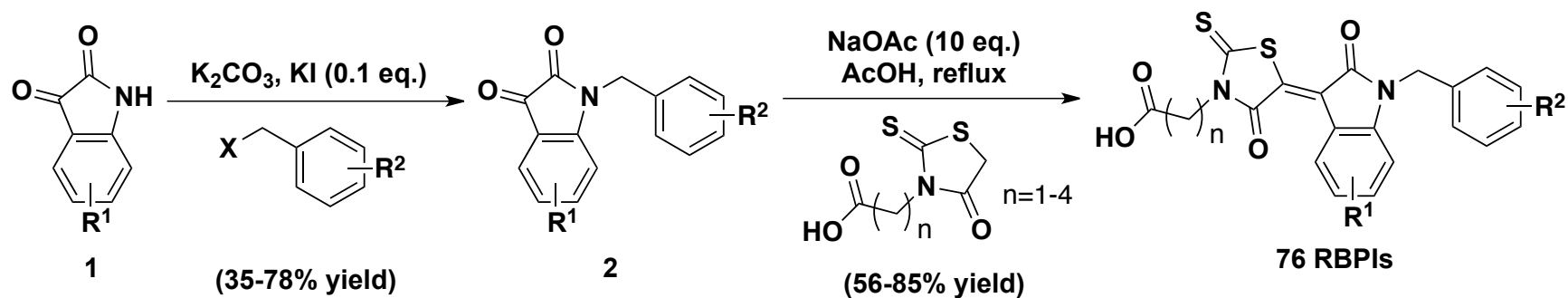


Figure S3. Structures of 76 **RBPI-1** derivative library compounds

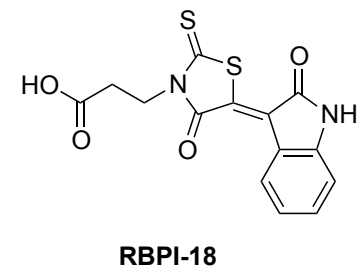
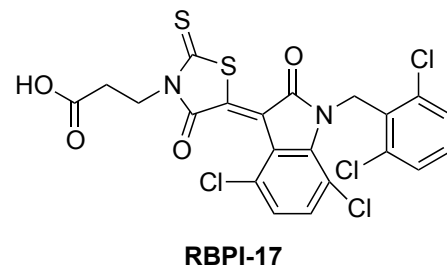
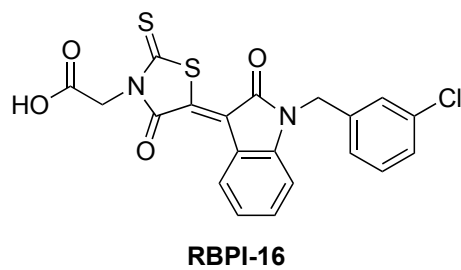
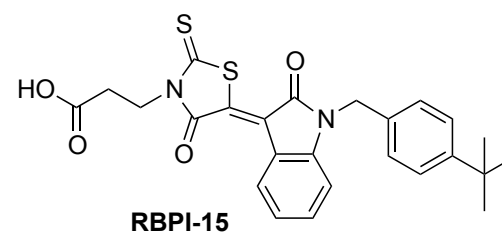
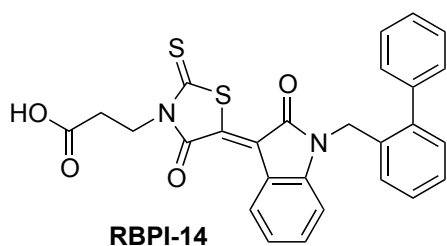
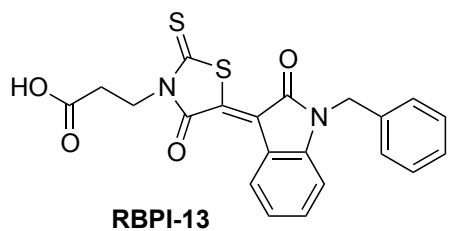
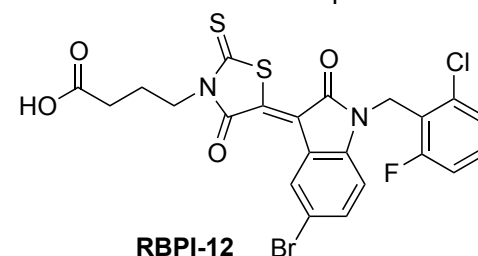
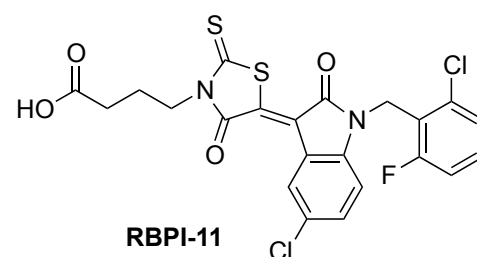
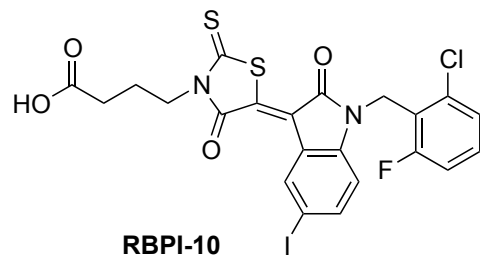
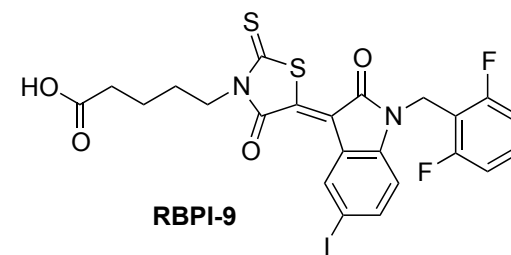
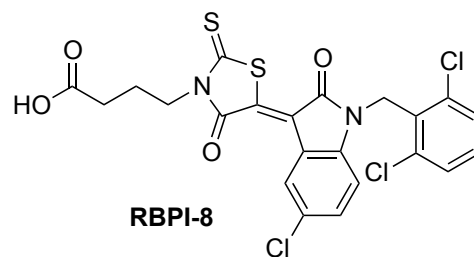
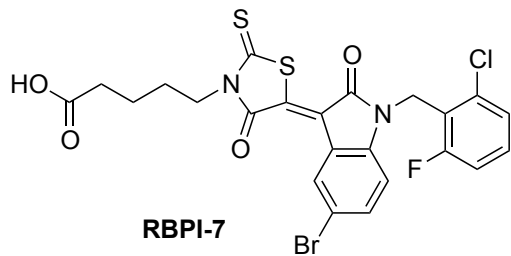
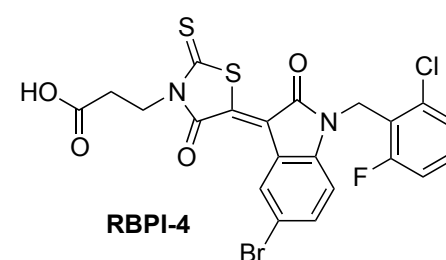
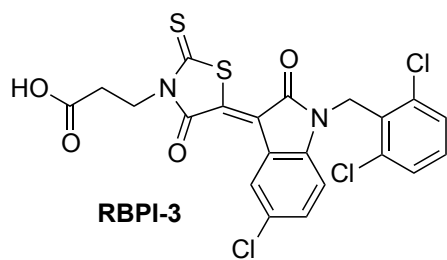
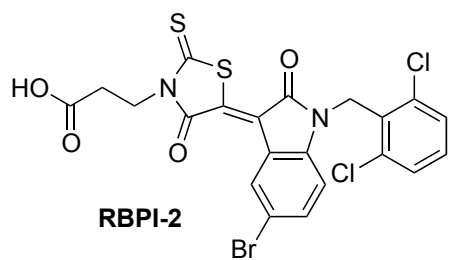


Figure S3 continued

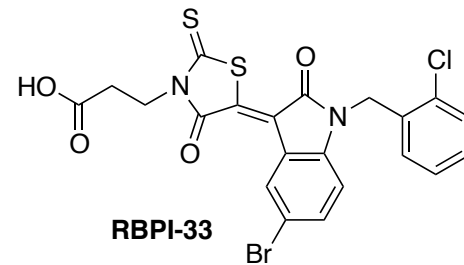
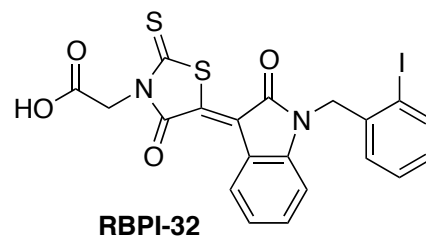
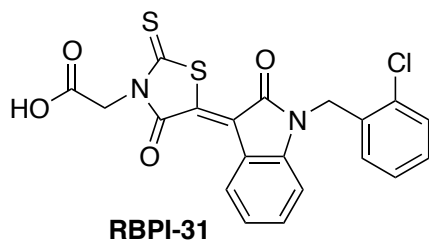
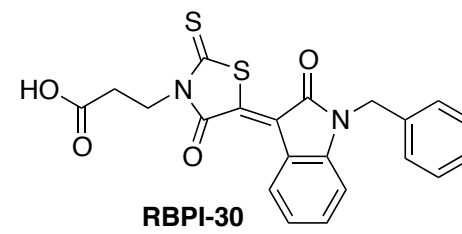
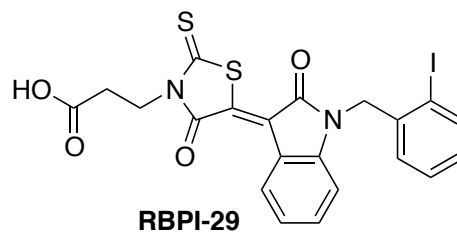
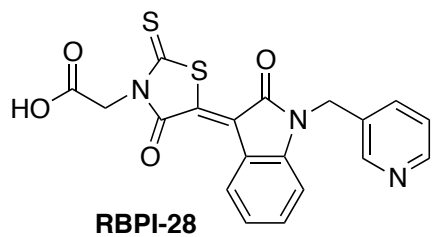
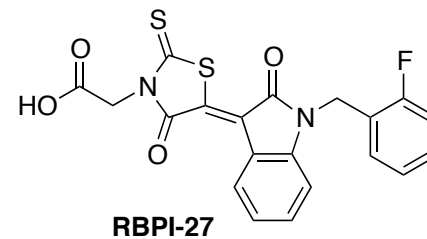
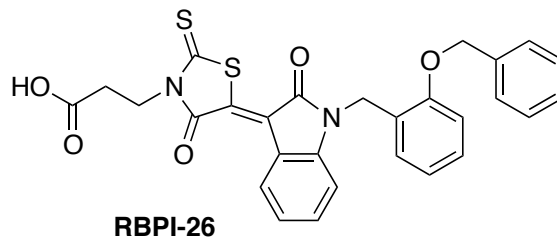
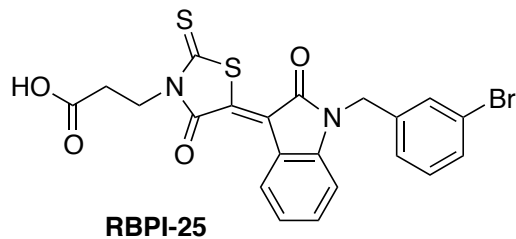
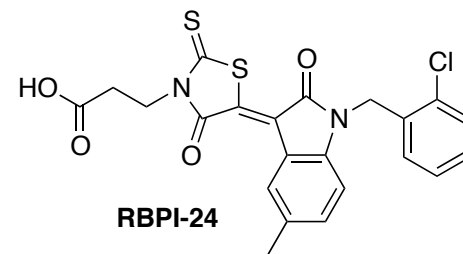
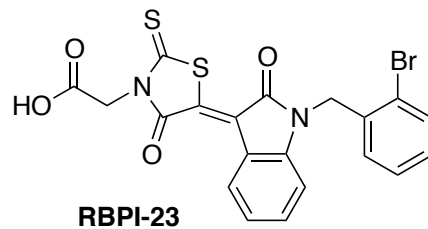
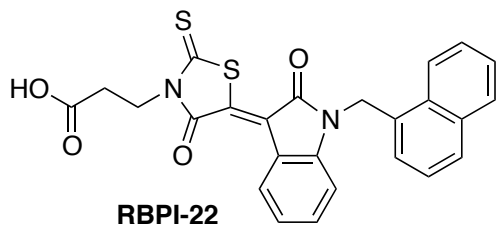
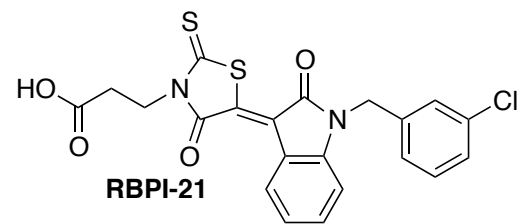
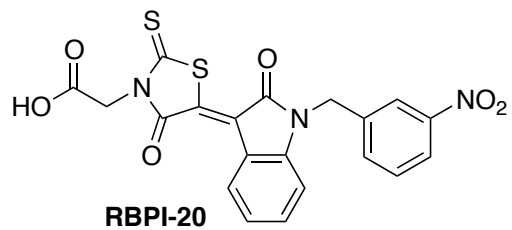
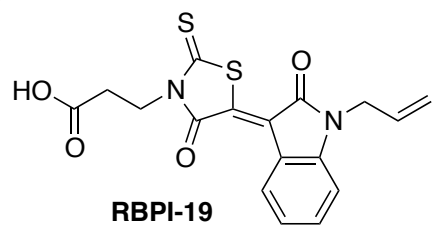
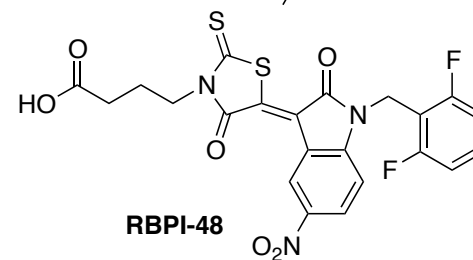
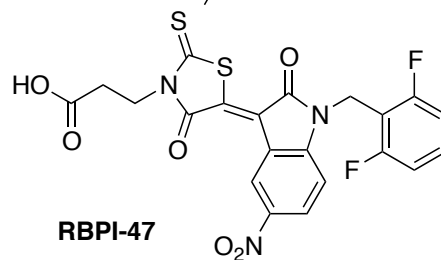
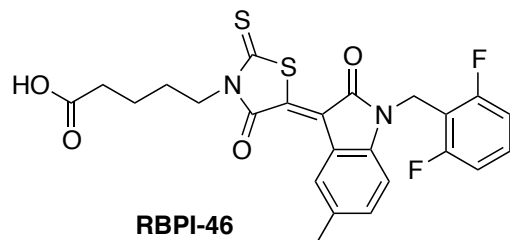
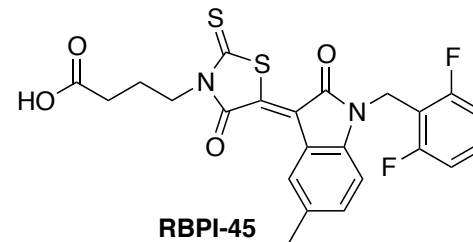
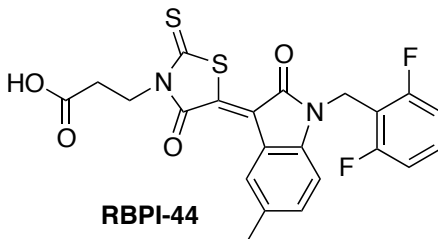
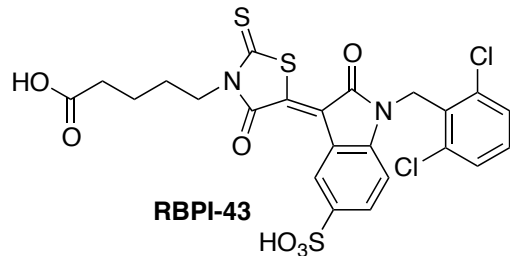
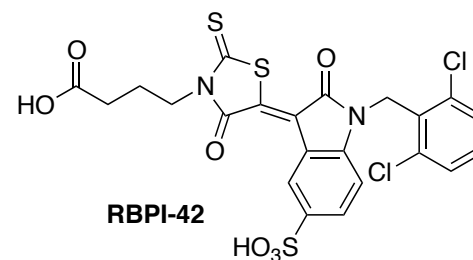
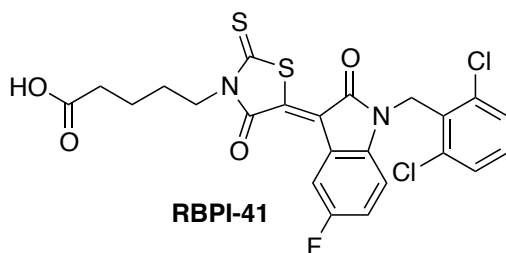
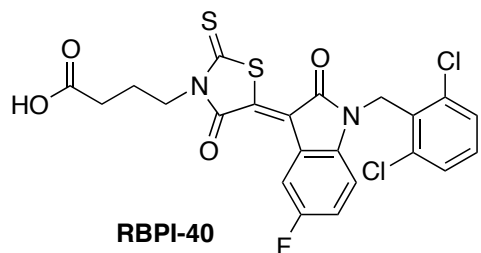
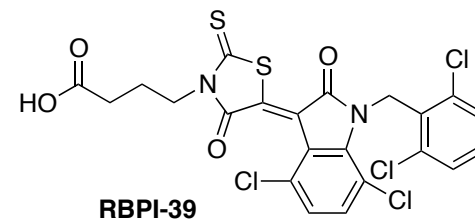
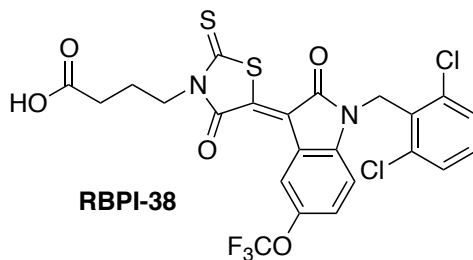
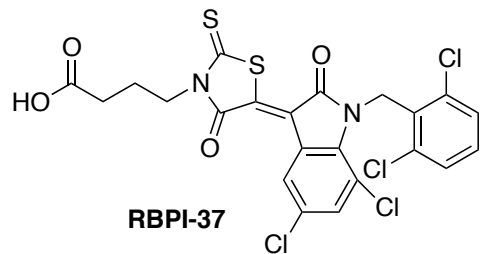
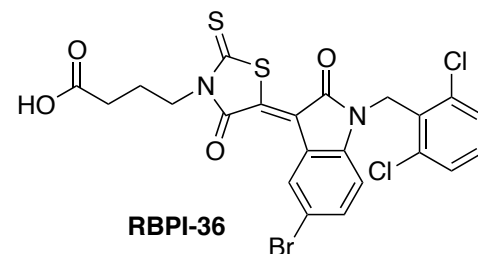
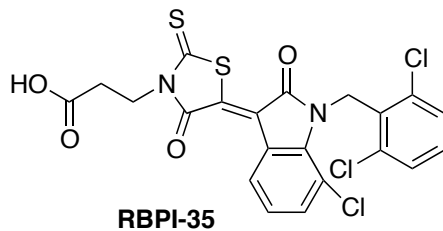
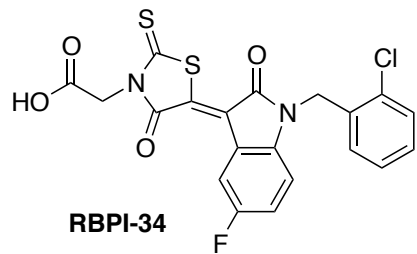


Figure S3 continued



**Figure
S3**
continued

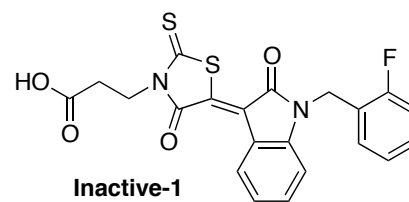
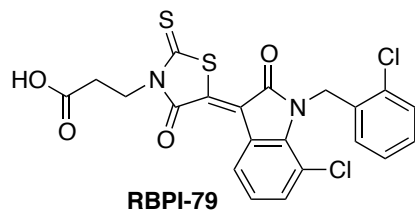
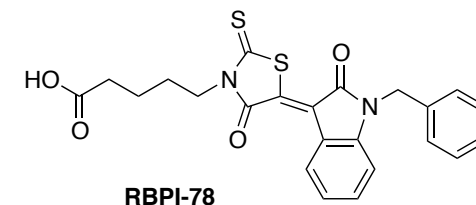
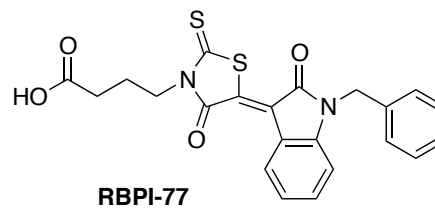
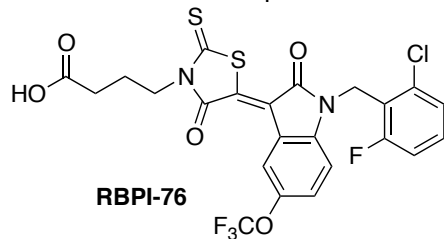
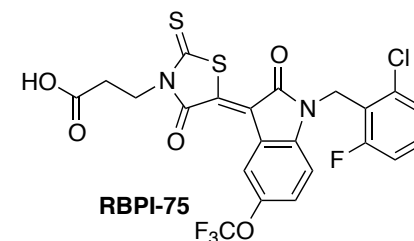
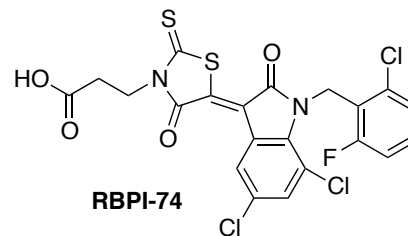
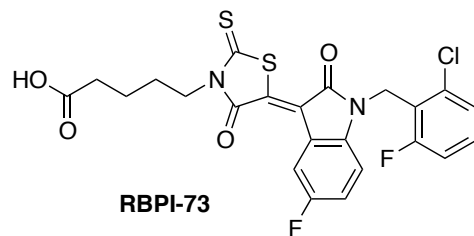
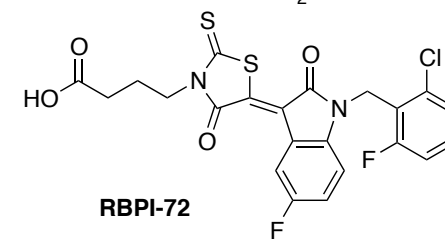
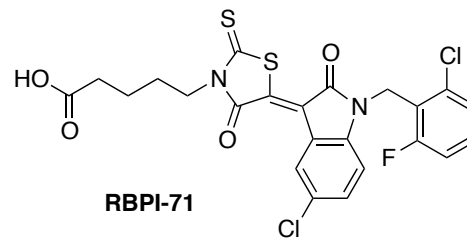
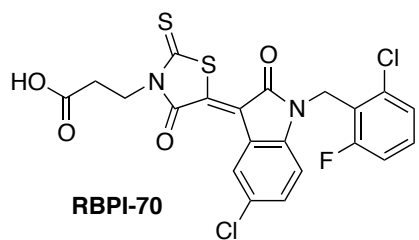
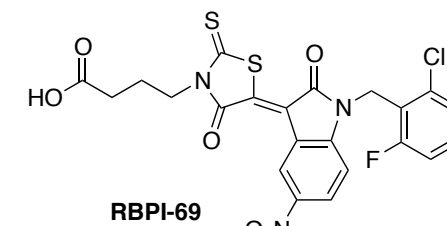
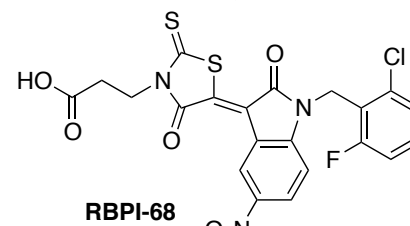
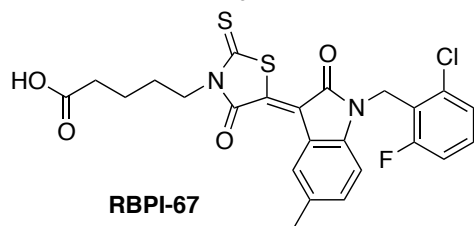
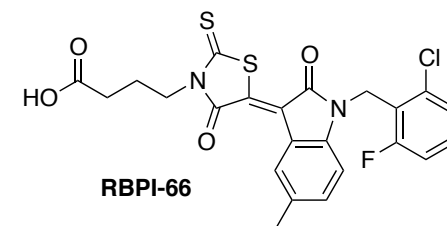
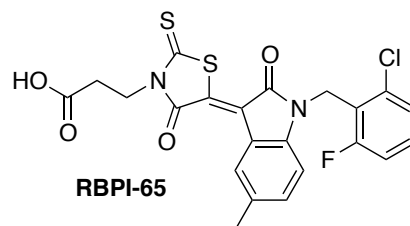
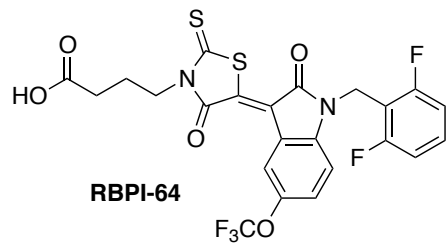


Figure S4. Library RBPIs tested at 10 μ M in *in vitro* 32 P-PAR degradation assay

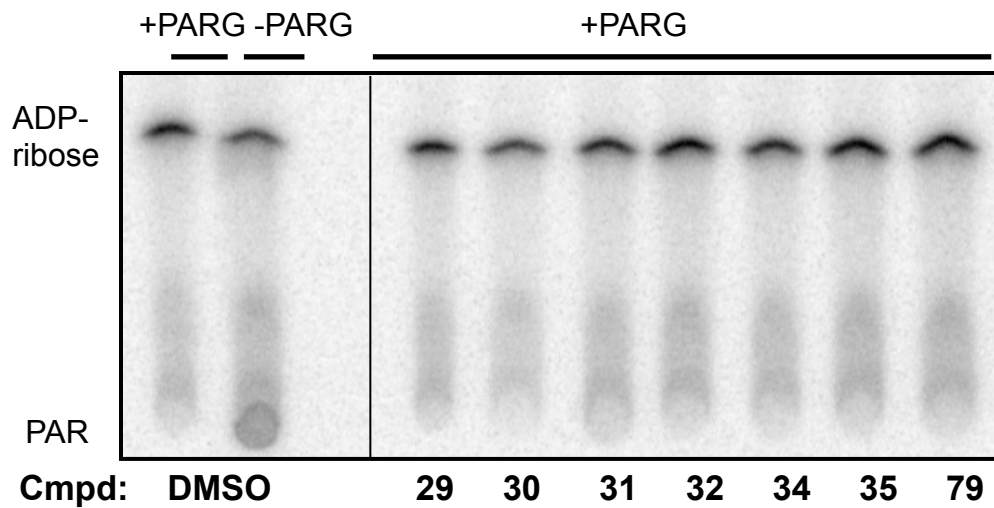
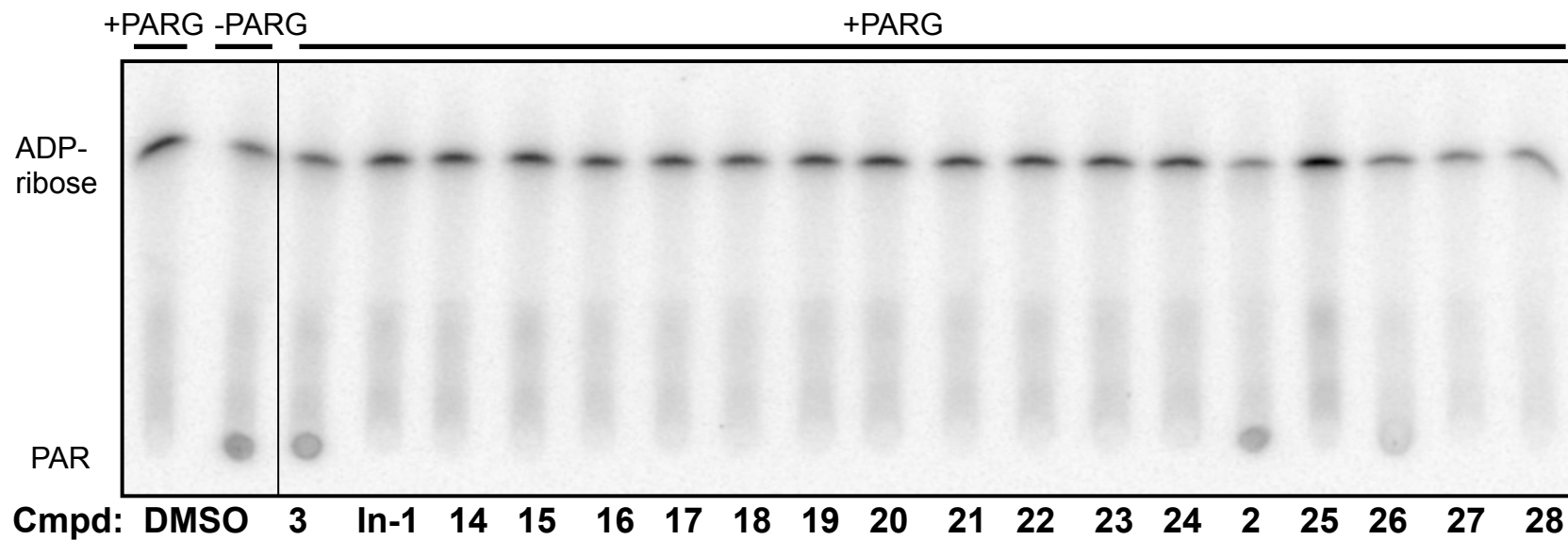


Figure S4 continued

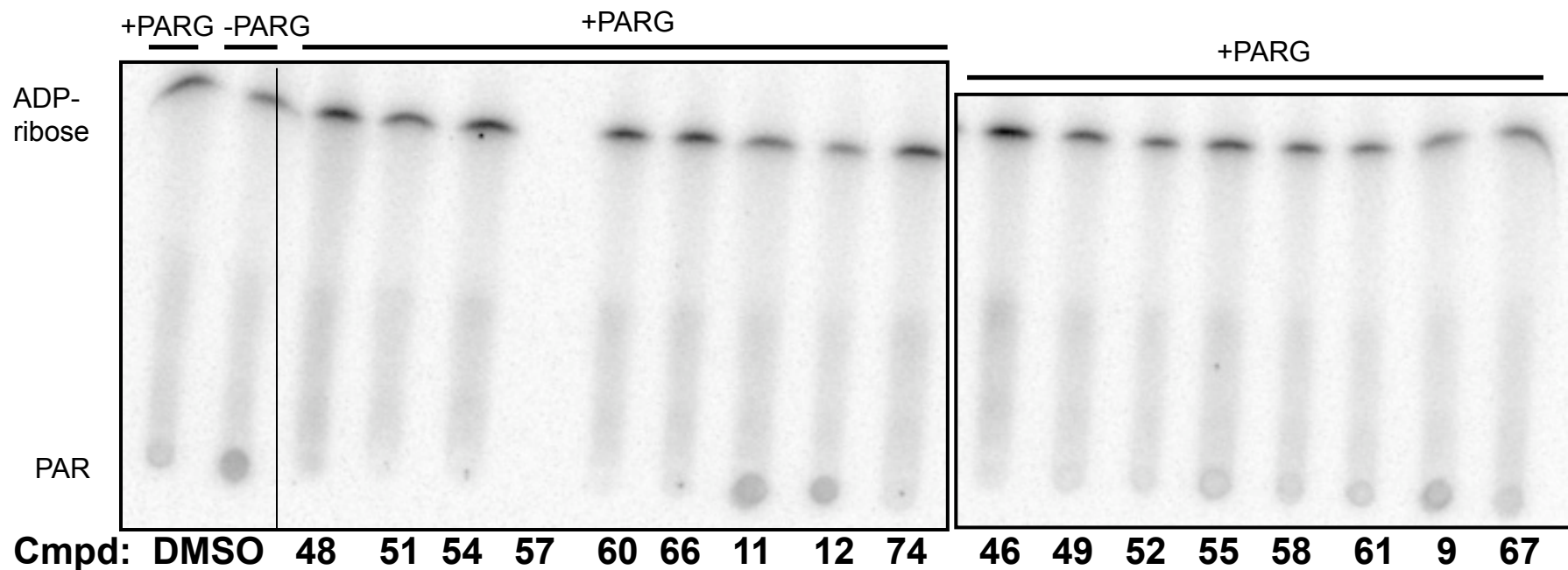
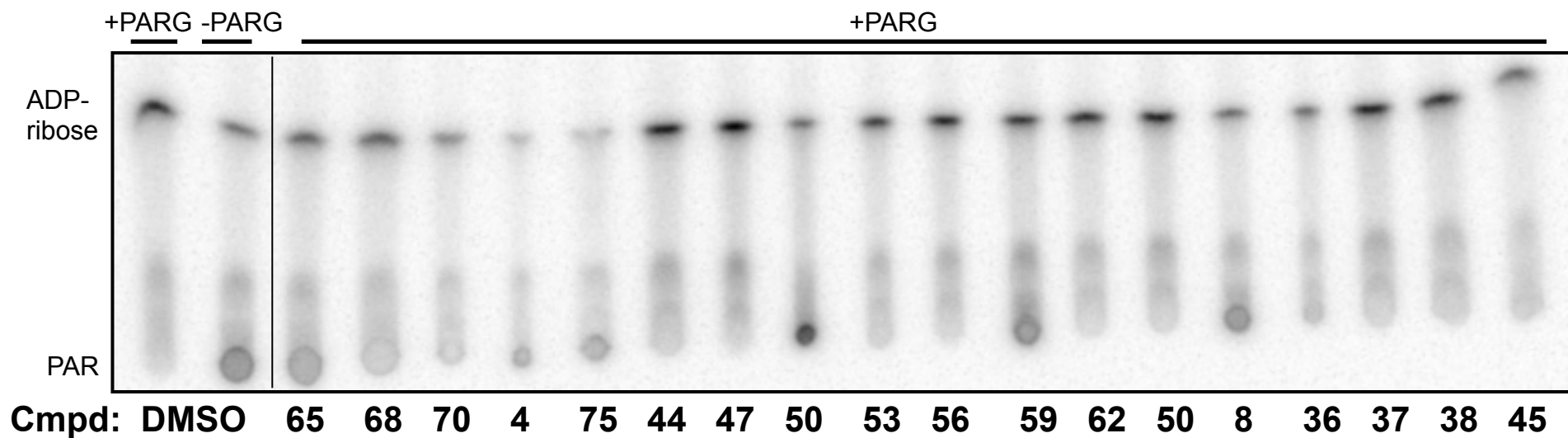


Figure S4 continued

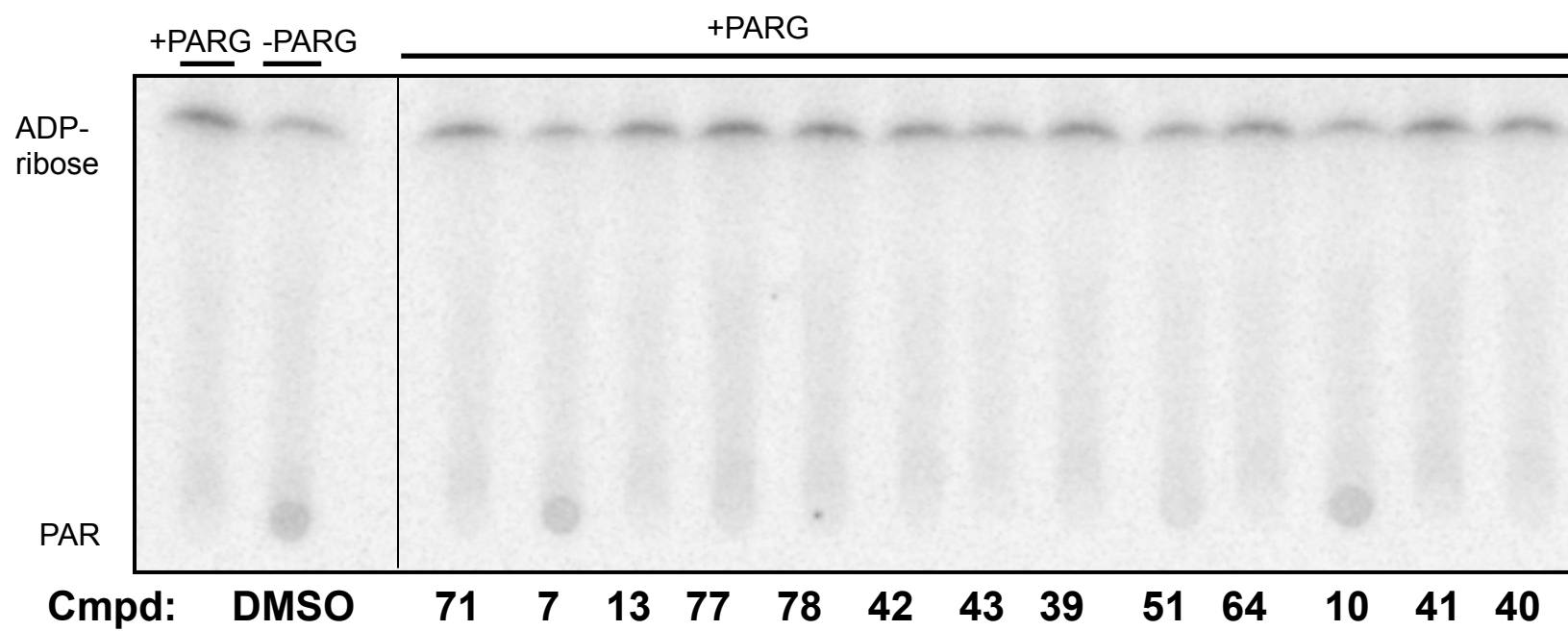


Figure S5. Library RBPIs tested at 50 μ M in *in vitro* 32 P-PAR degradation assay

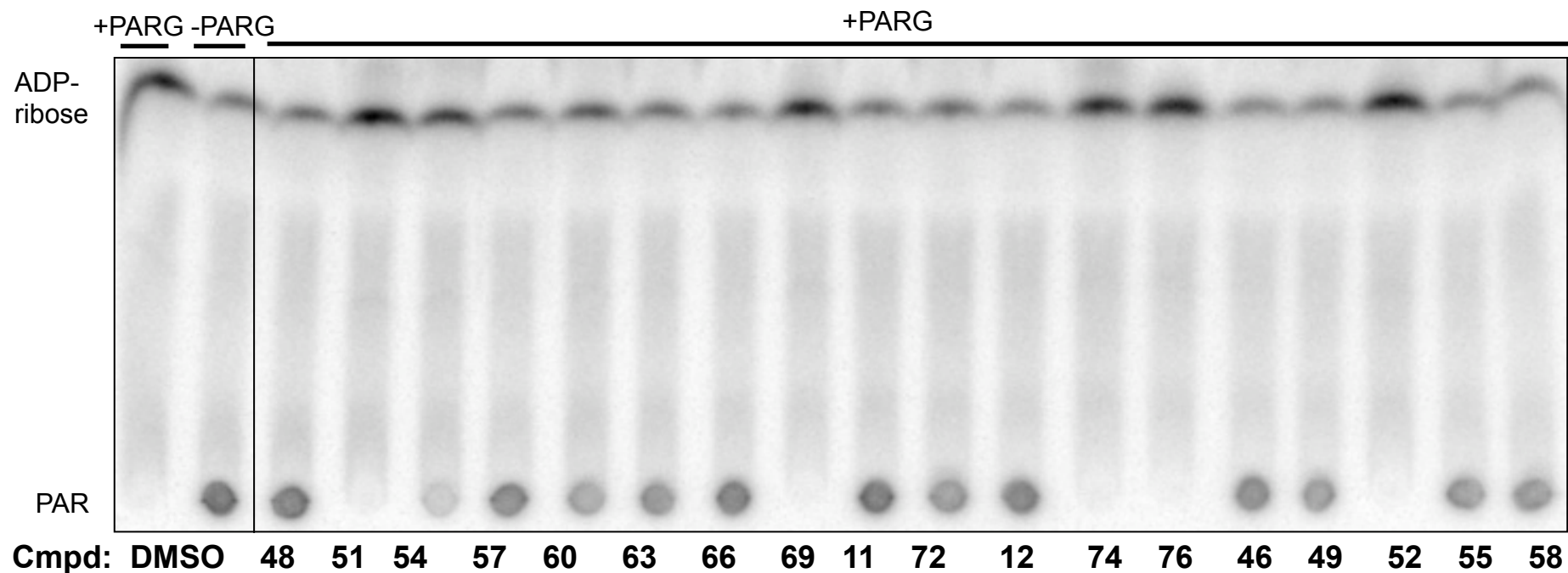
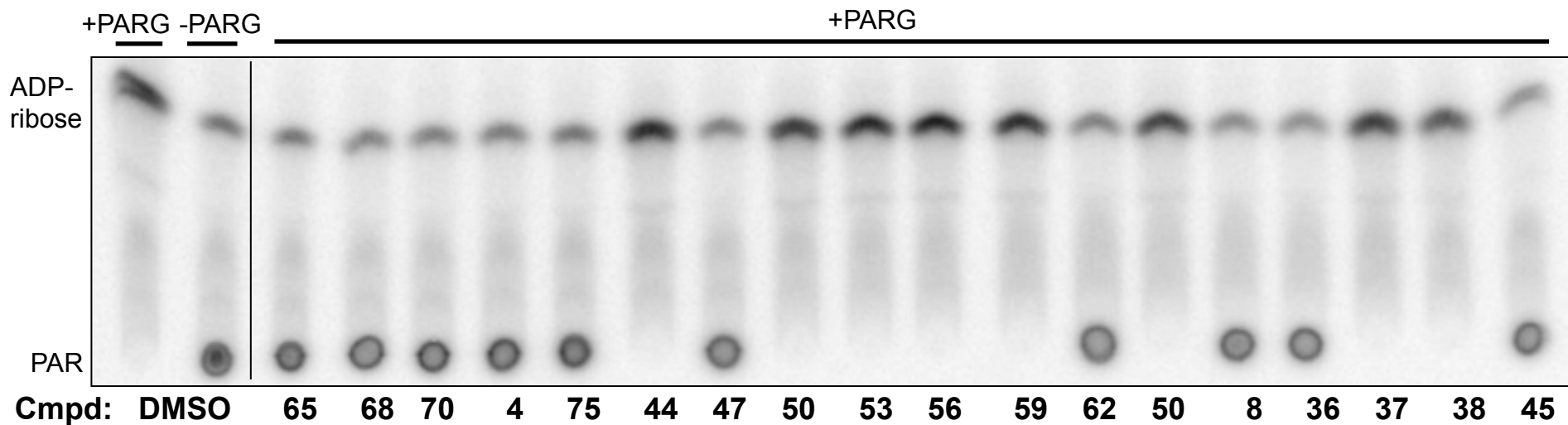
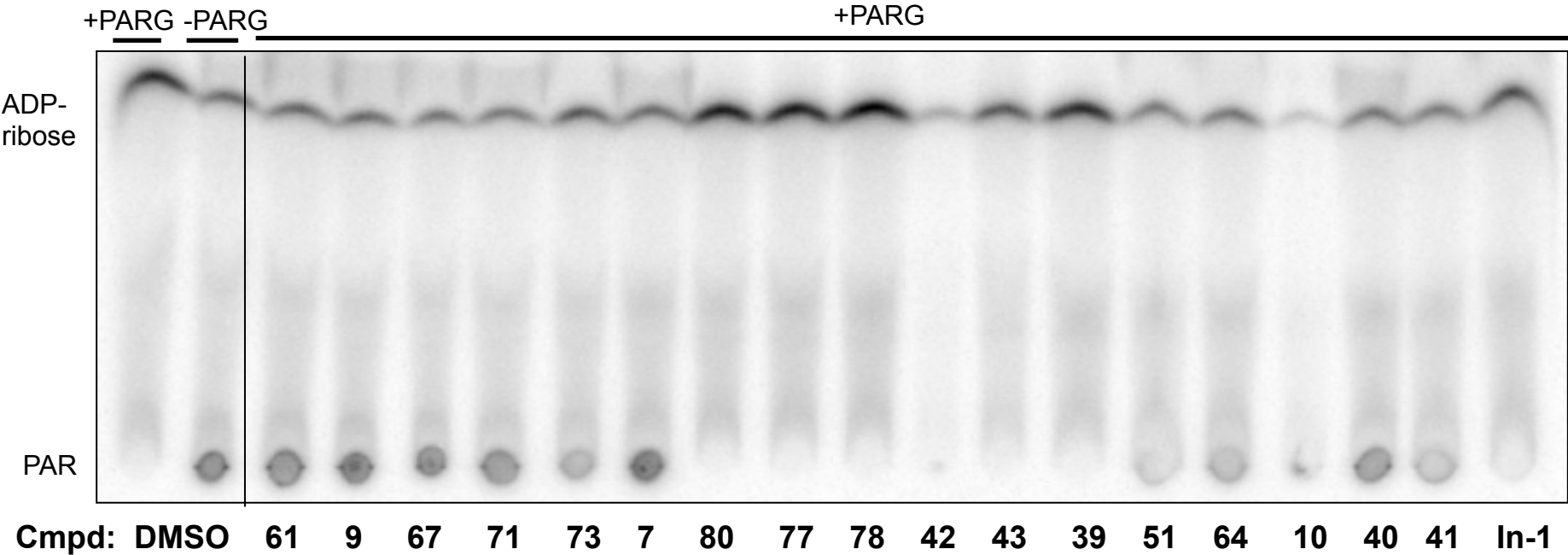


Figure S5 continued



S13 In = Inactive

Figure S6.
 IC_{50} Summary of
RBPI-7 through **RBPI-79**
obtained using *in vitro* ^{32}P -PAR
degradation assay

Compound	10 μM Screen	50 μM Screen	IC_{50} (μM)
RBPI-7	<10	<50	4.5 \pm 0.6
RBPI-8	<10	<50	3.7 \pm 1.5
RBPI-9	<10	<50	3.5 \pm 0.4
RBPI-10	<10	<50	4.2 \pm 0.9
RBPI-11	<10	<50	8.2 \pm 3.5
RBPI-12	<10	<50	6.1 \pm 1.4
Inactive-1	>10	>50	>100
RBPI-13	>10	>50	>50
RBPI-14	>10	<50	10-50
RBPI-15	>10	>50	>50
RBPI-16	>10	>50	>50
RBPI-17	>10	>50	>50
RBPI-18	>10	>50	>50
RBPI-19	>10	>50	>50
RBPI-20	>10	>50	>50
RBPI-21	>10	>50	>50
RBPI-22	>10	<50	10-50
RBPI-23	>10	>50	>50
RBPI-24	>10	<50	10-50
RBPI-25	>10	>50	>50
RBPI-26	>10	<50	10-50
RBPI-27	>10	>50	>50
RBPI-28	>10	>50	>50
RBPI-29	>10	<50	10-50
RBPI-30	>10	>50	>50
RBPI-31	>10	>50	>50
RBPI-32	>10	>50	>50
RBPI-33	>10	<50	10-50
RBPI-34	>10	>50	>50
RBPI-35	>10	>50	>50
RBPI-36	>10	<50	10-50
RBPI-37	>10	>50	>50
RBPI-38	>10	>50	>50
RBPI-39	>10	>50	>50
RBPI-40	>10	>50	>50
RBPI-41	>10	<50	10-50
RBPI-42	>10	>50	>50
RBPI-43	>10	>50	>50
RBPI-44	>10	>50	>50

Figure S6 continued

Cmpd	10 μM Screen	50 μM Screen	IC₅₀ (μM)
RBPI-45	>10	<50	10-50
RBPI-46	>10	<50	10-50
RBPI-47	>10	<50	10-50
RBPI-48	>10	<50	10-50
RBPI-49	>10	<50	10-50
RBPI-50	>10	>50	>50
RBPI-51	>10	>50	>50
RBPI-52	>10	>50	>50
RBPI-53	>10	>50	>50
RBPI-54	>10	>50	>50
RBPI-55	>10	<50	10-50
RBPI-56	>10	>50	>50
RBPI-57	>10	<50	10-50
RBPI-58	>10	<50	10-50
RBPI-59	>10	>50	>50
RBPI-60	>10	<50	10-50
RBPI-61	>10	<50	10-50
RBPI-62	>10	<50	10-50
RBPI-63	>10	<50	10-50
RBPI-64	>10	>50	>50
RBPI-65	>10	<50	10-50
RBPI-66	>10	<50	10-50
RBPI-67	>10	<50	10-50
RBPI-68	>10	<50	10-50
RBPI-69	>10	>50	>50
RBPI-70	>10	<50	10-50
RBPI-71	>10	<50	10-50
RBPI-72	>10	<50	10-50
RBPI-73	>10	>50	>50
RBPI-74	>10	>50	>50
RBPI-75	>10	<50	10-50
RBPI-76	>10	>50	>50
RBPI-77	>10	>50	>50
RBPI-78	>10	>50	>50
RBPI-79	>10	>50	>50

Figure S7. Triplicate IC_{50} curves for **RBPI-2** through **RBPI-12** obtained using *in vitro* ^{32}P -PAR degradation assay. A representative TLC plate is shown for each compound.

RBPI-2

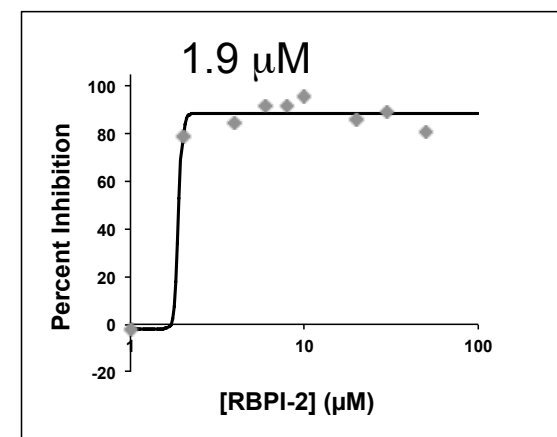
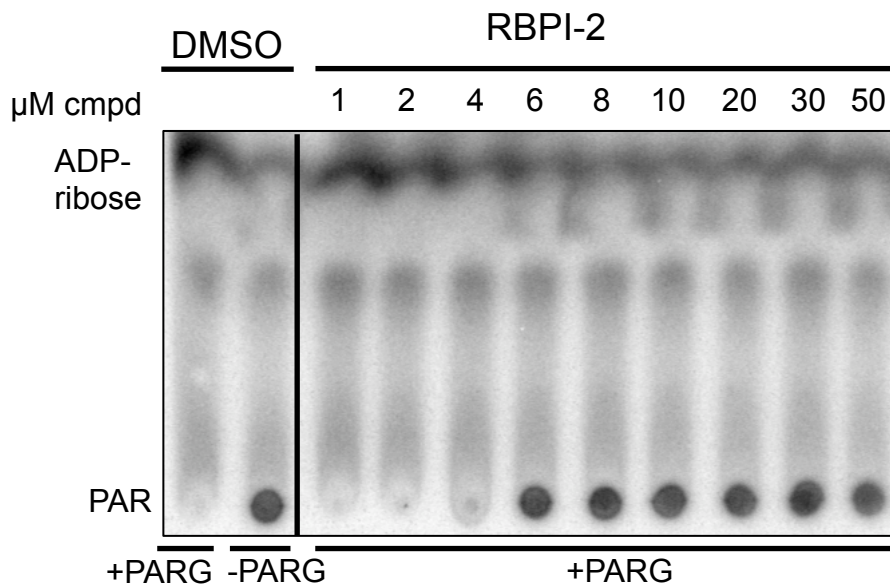
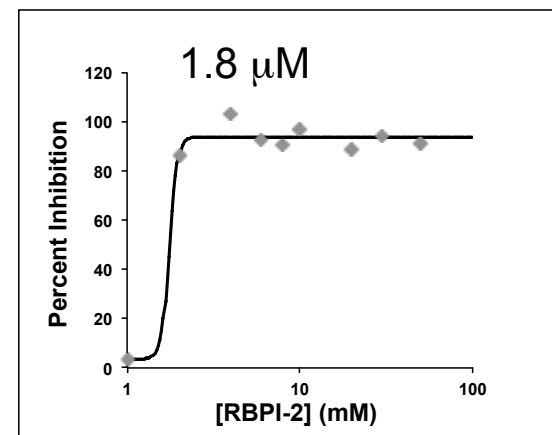
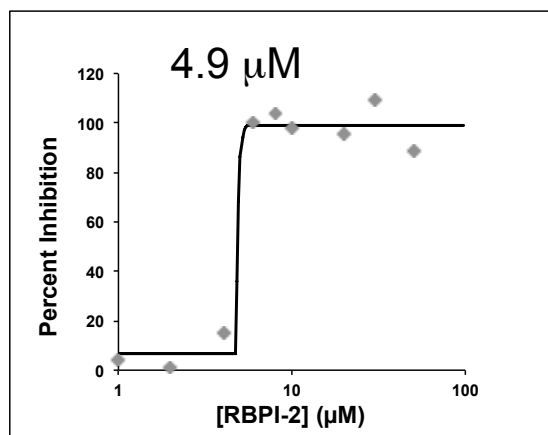
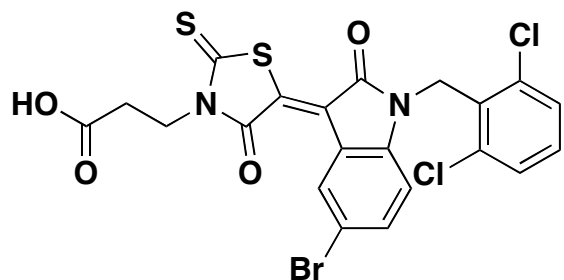


Figure S7 continued

RBPI-3

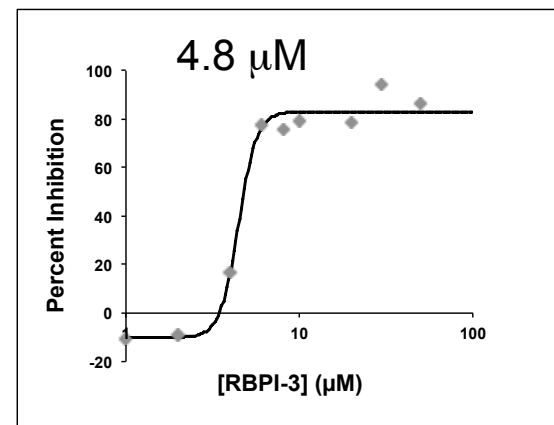
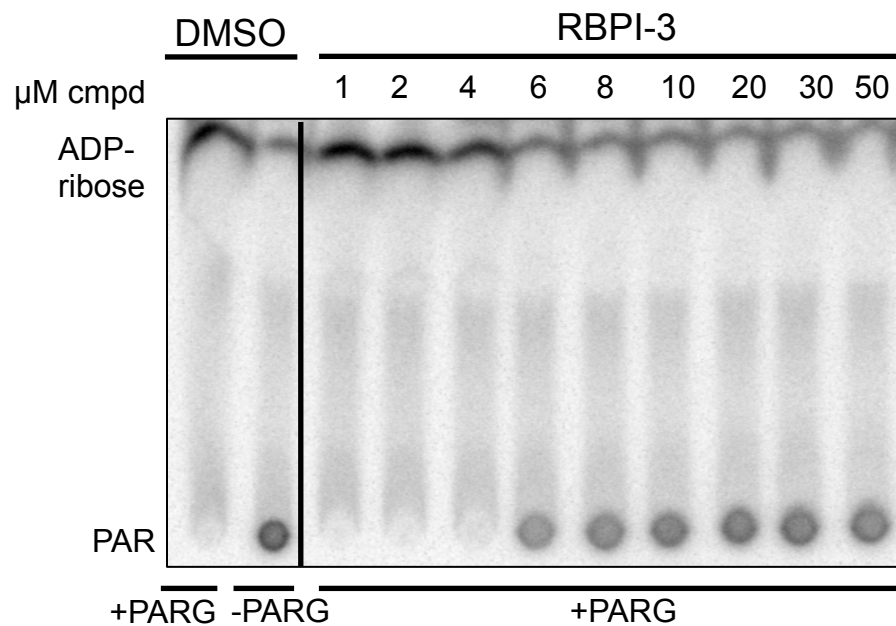
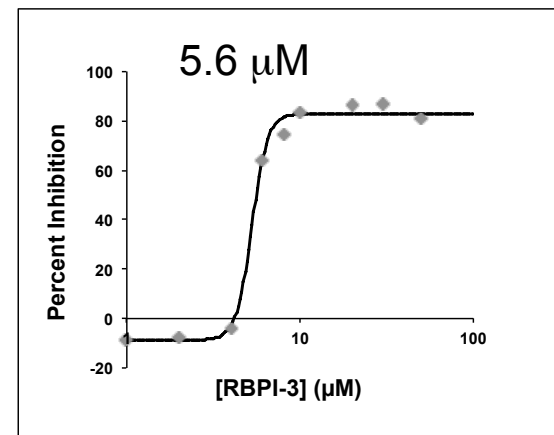
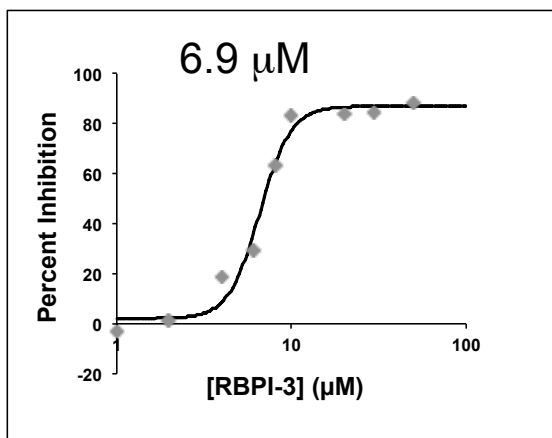
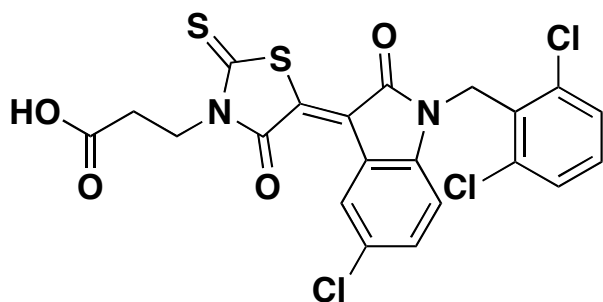


Figure S7 continued

RBPI-4

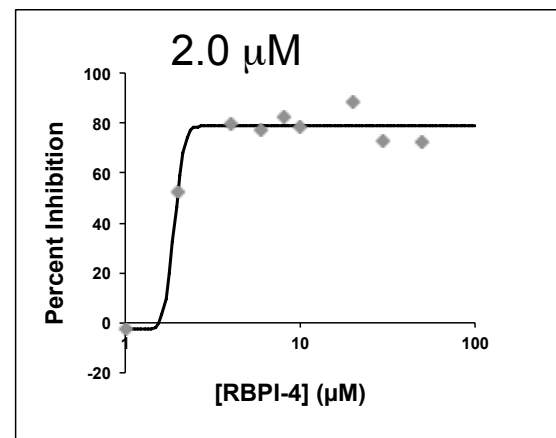
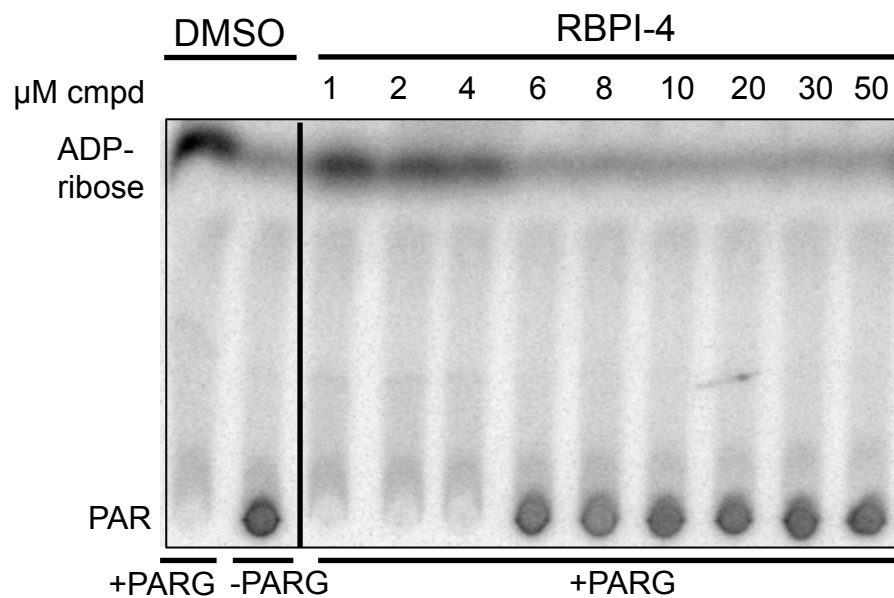
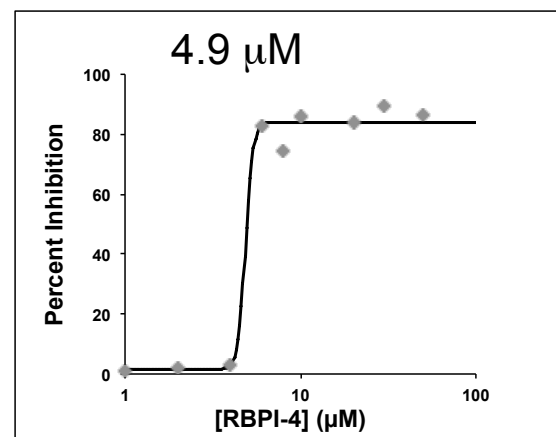
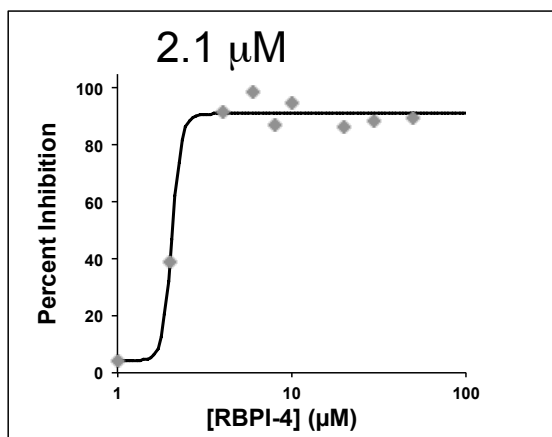
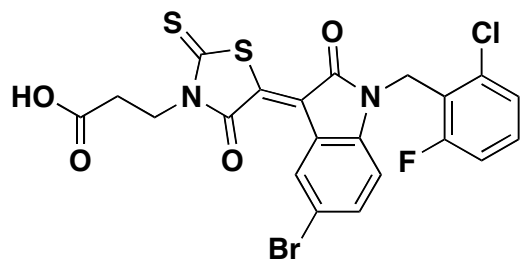


Figure S7 continued

RBPI-5

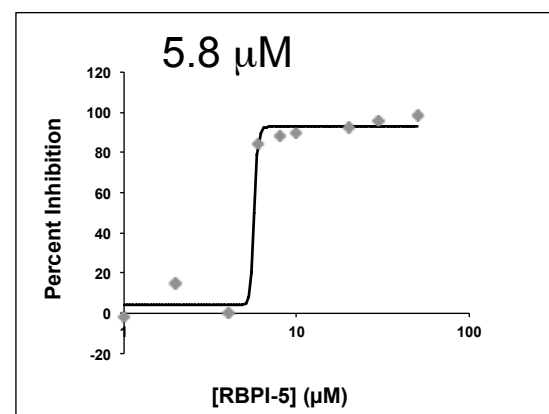
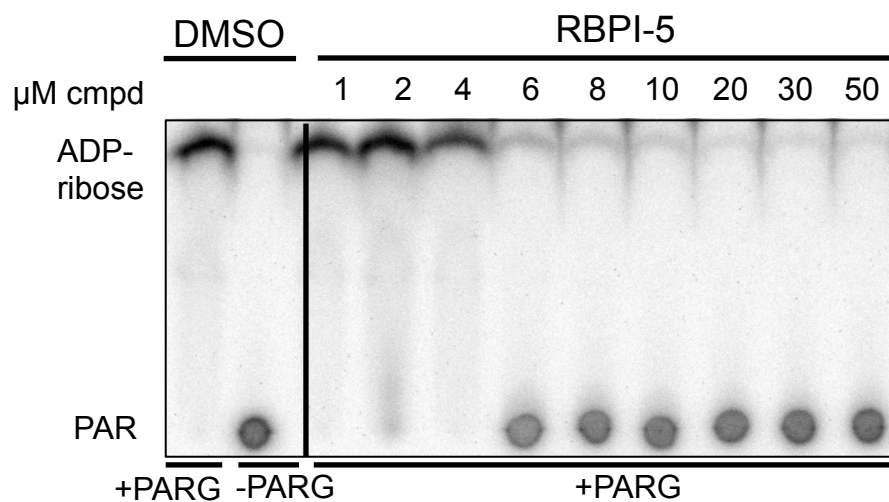
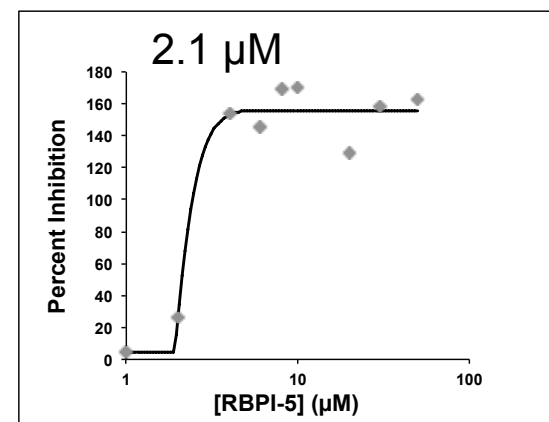
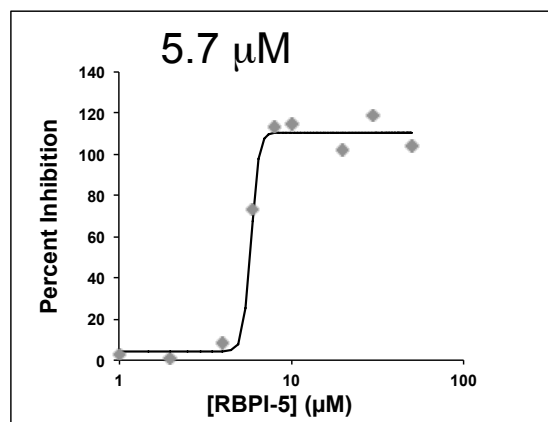
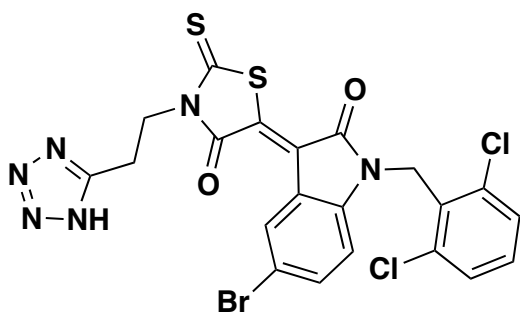


Figure S7 continued

RBPI-6

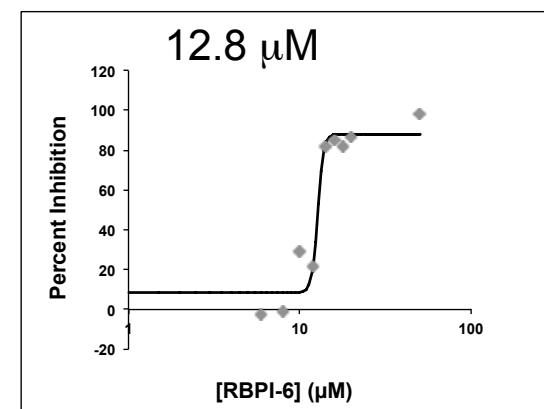
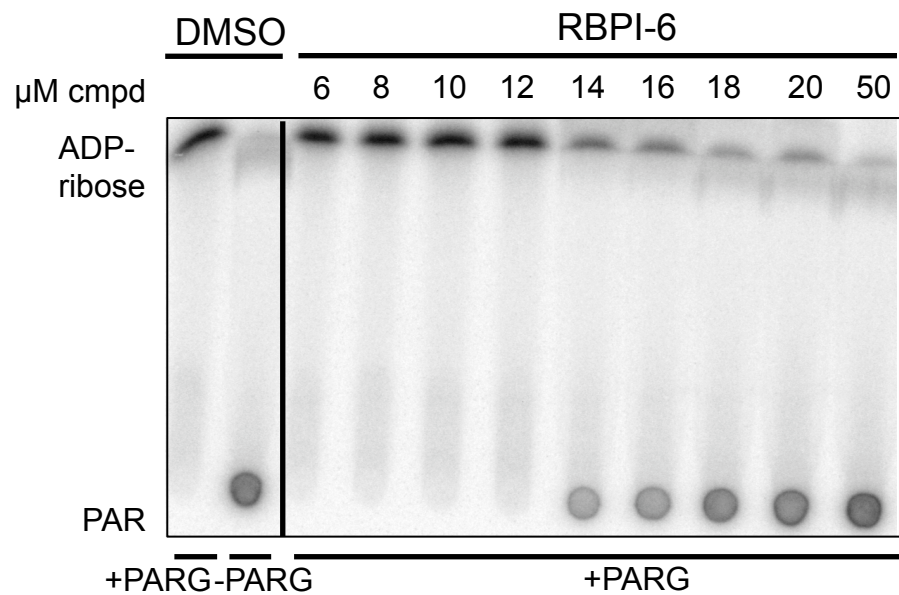
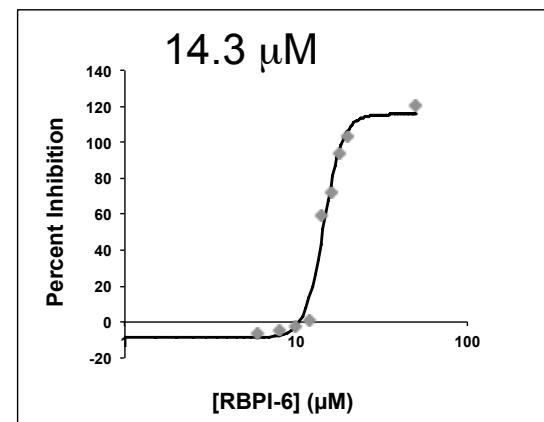
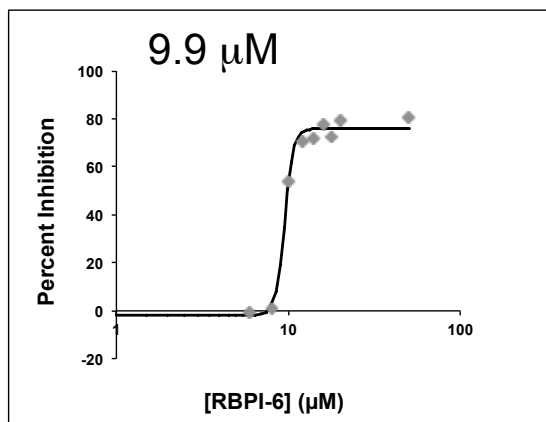
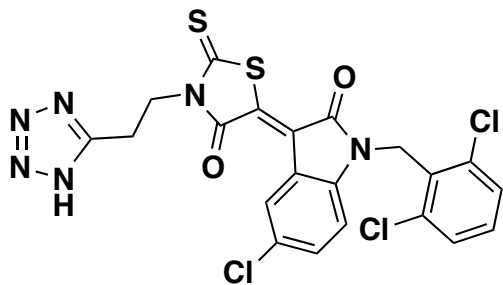


Figure S7 continued

RBPI-7

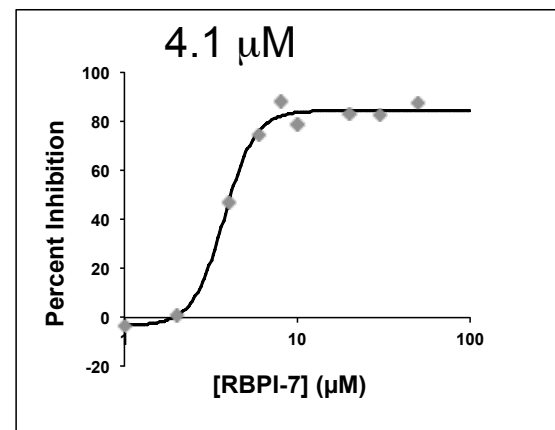
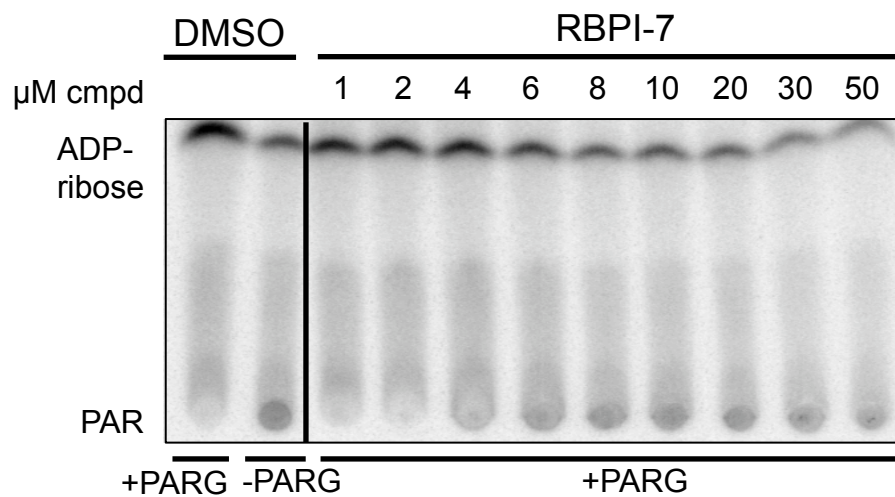
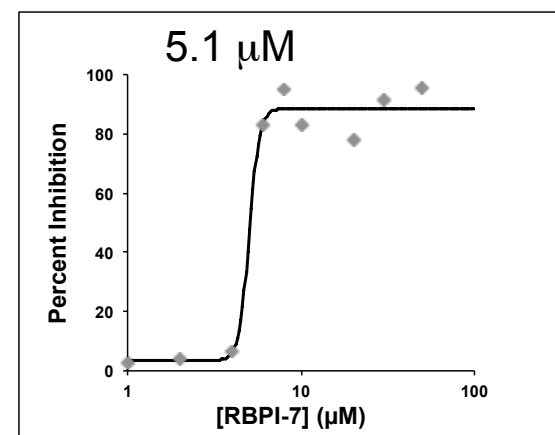
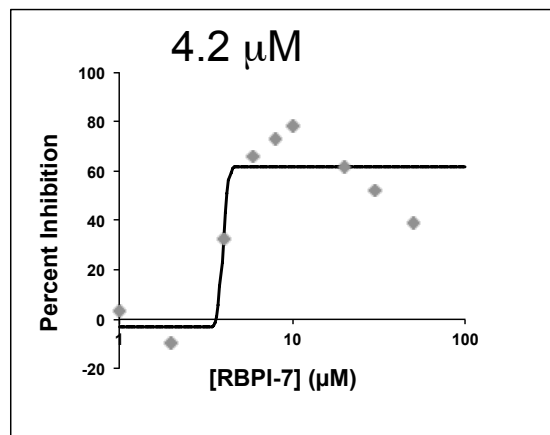
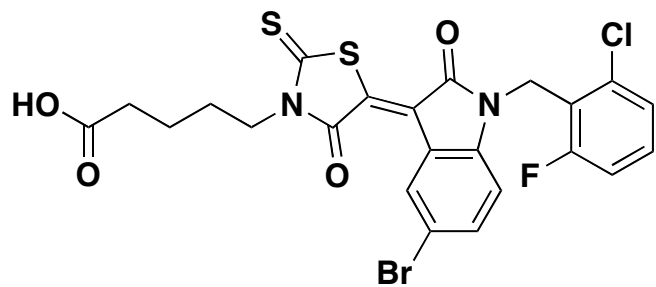


Figure S7 continued

RBPI-8

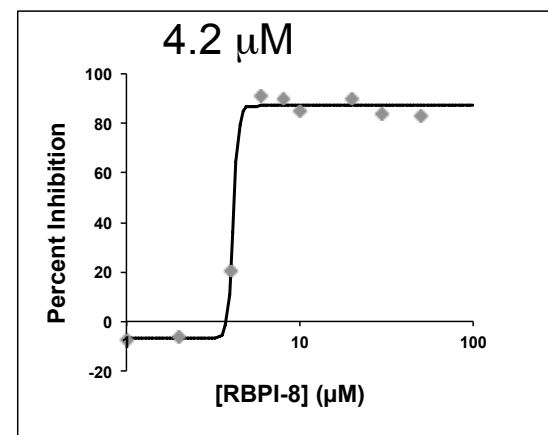
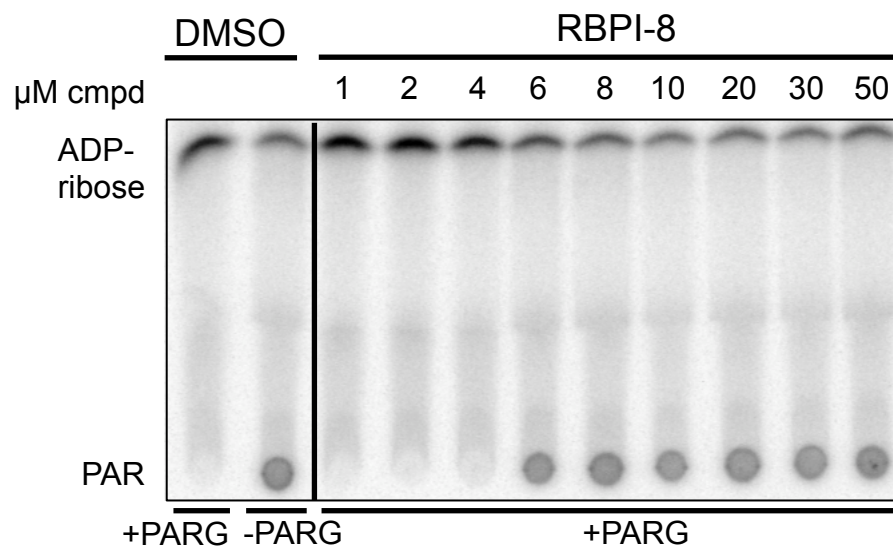
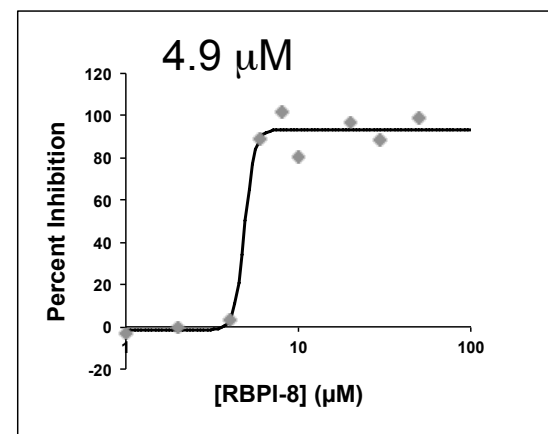
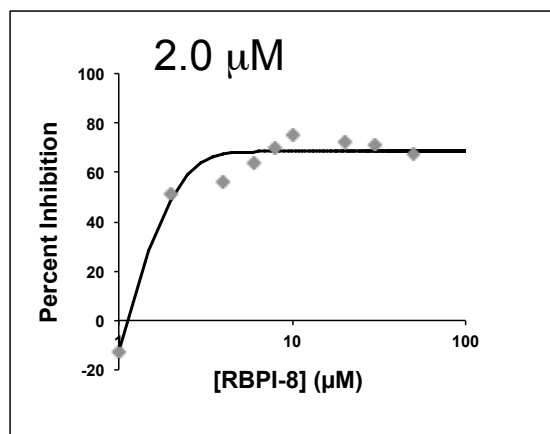
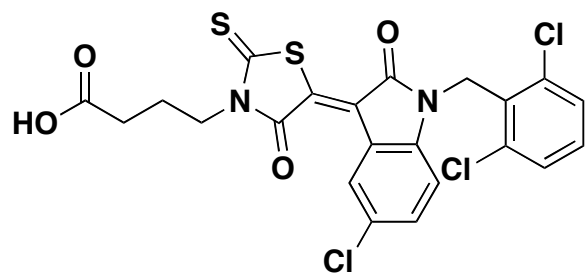


Figure S7 continued

RBPI-9

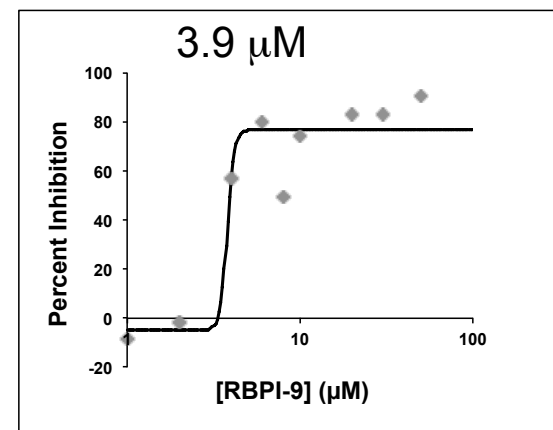
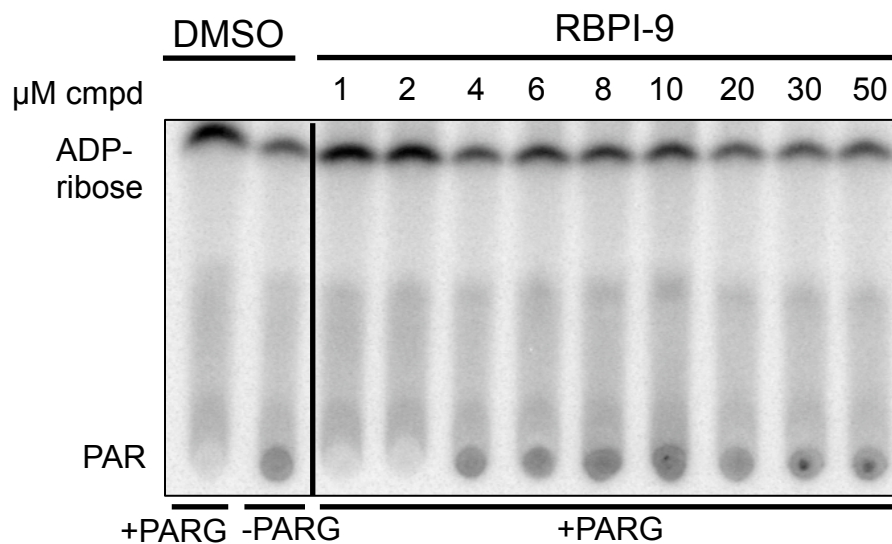
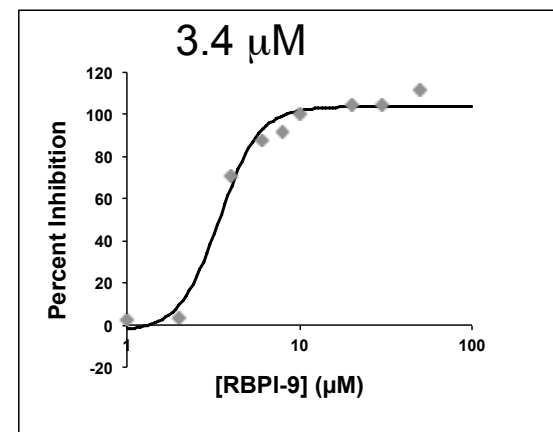
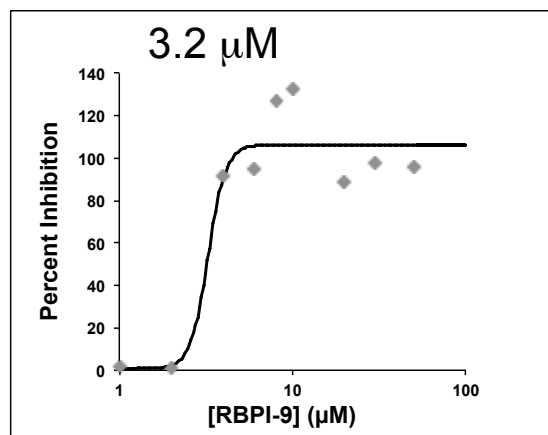
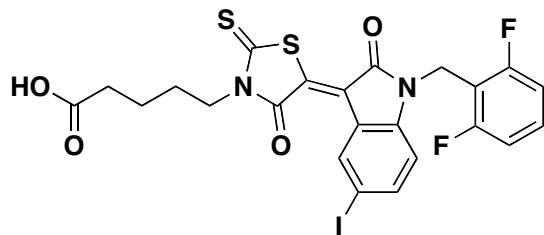


Figure S7 continued

RBPI-10

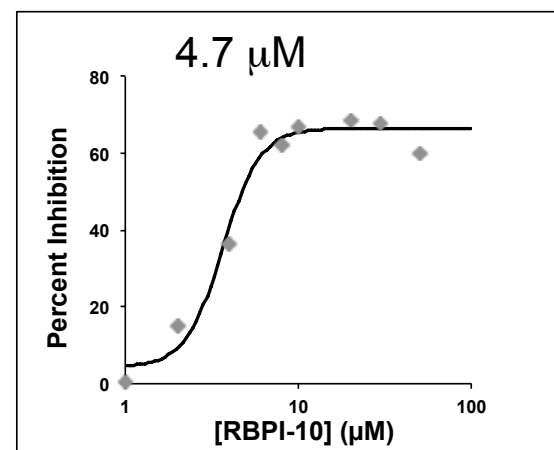
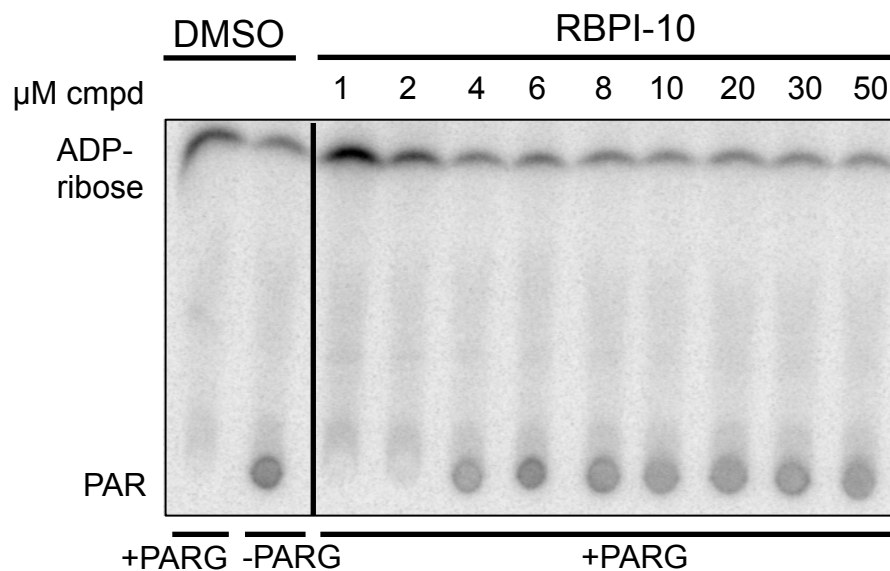
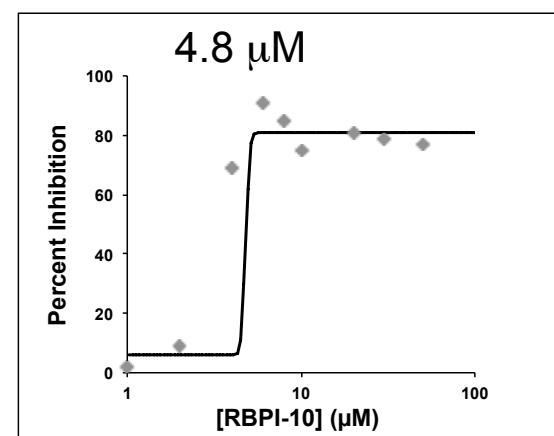
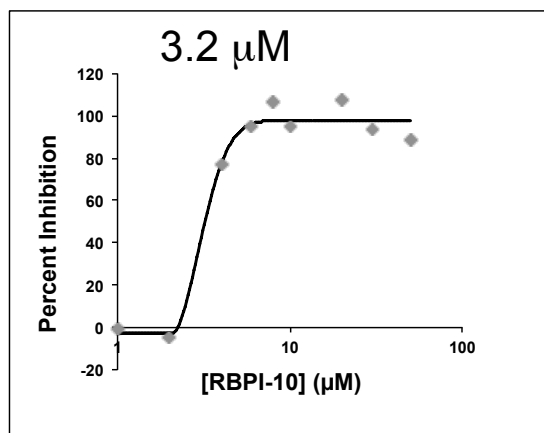
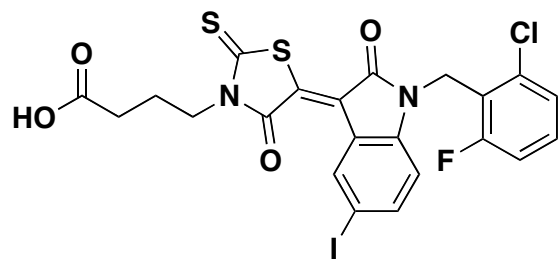


Figure S7 continued

RBPI-11

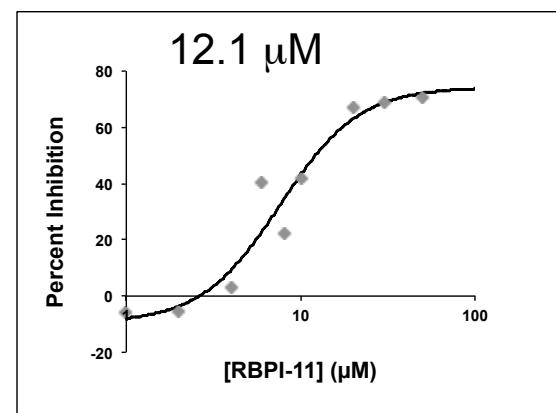
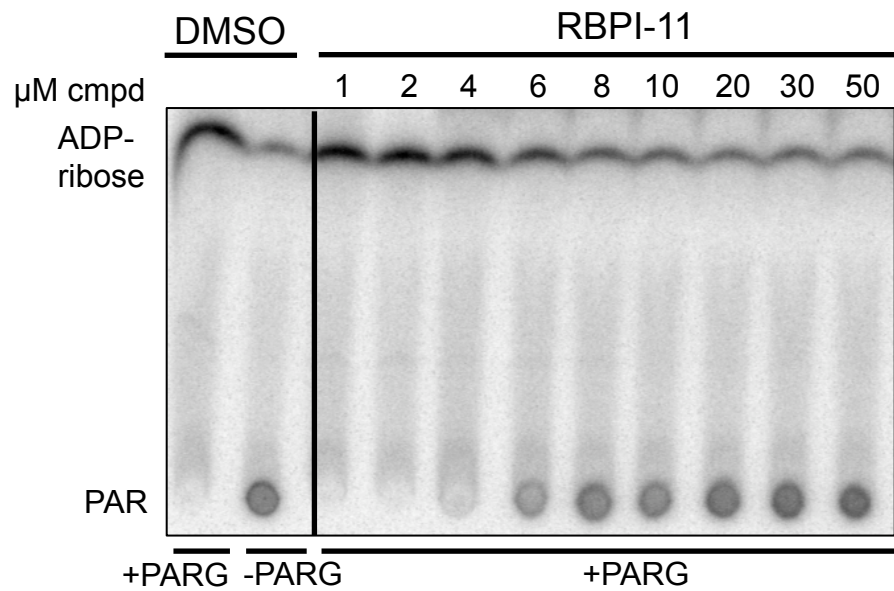
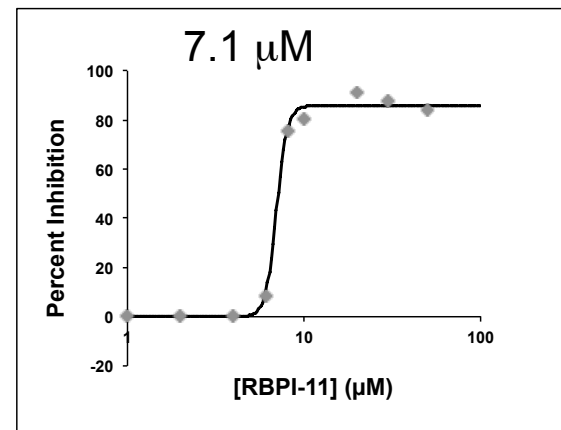
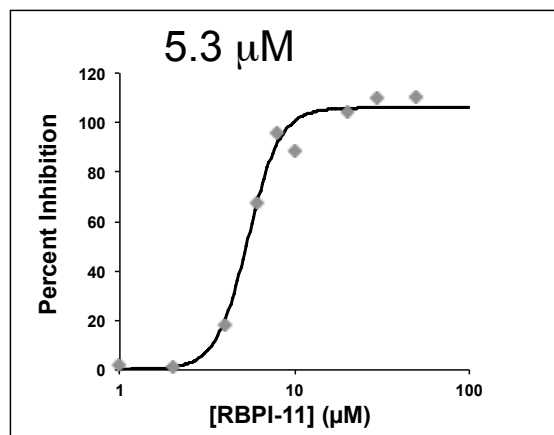
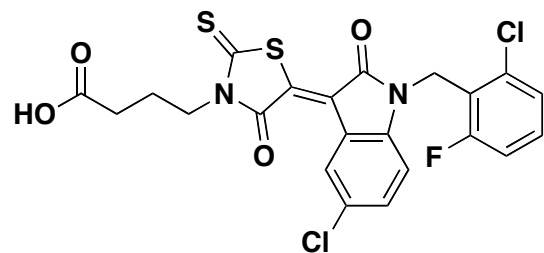


Figure S7 continued

RBPI-12

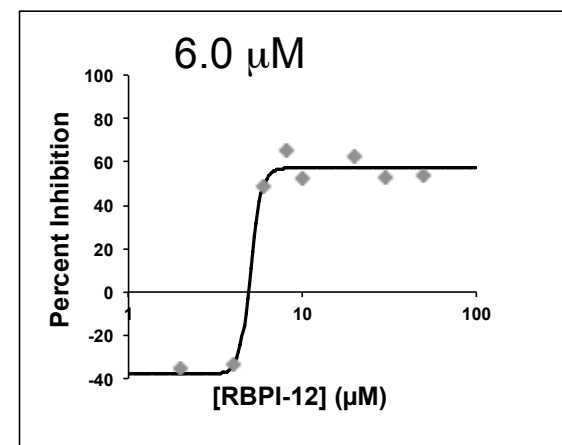
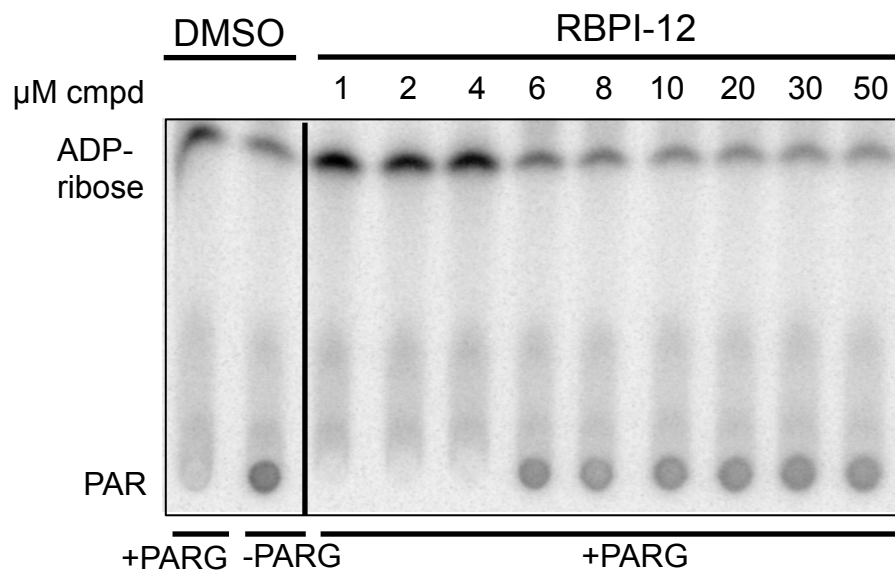
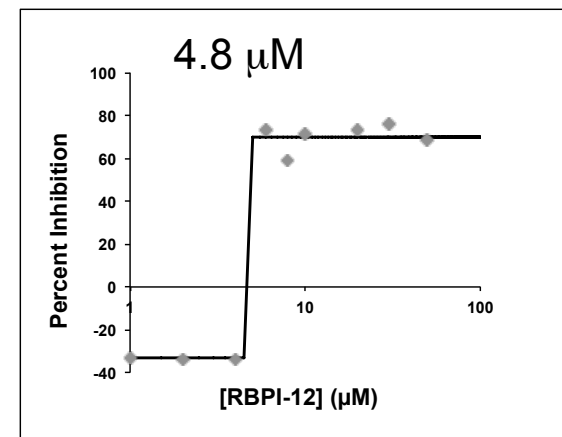
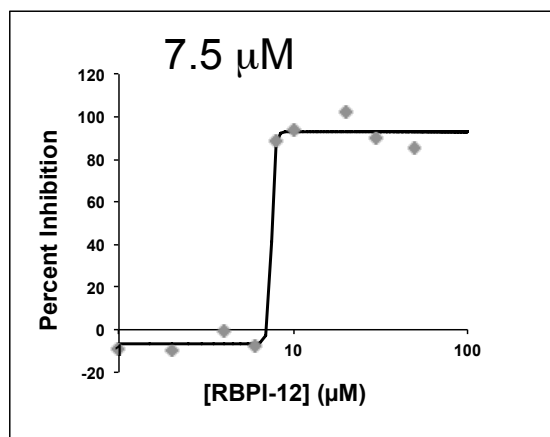
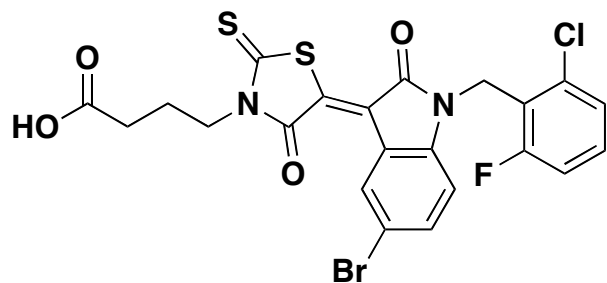


Figure S8. Inactive compounds assessed up to 100 μM in *in vitro* ^{32}P -PAR degradation assay

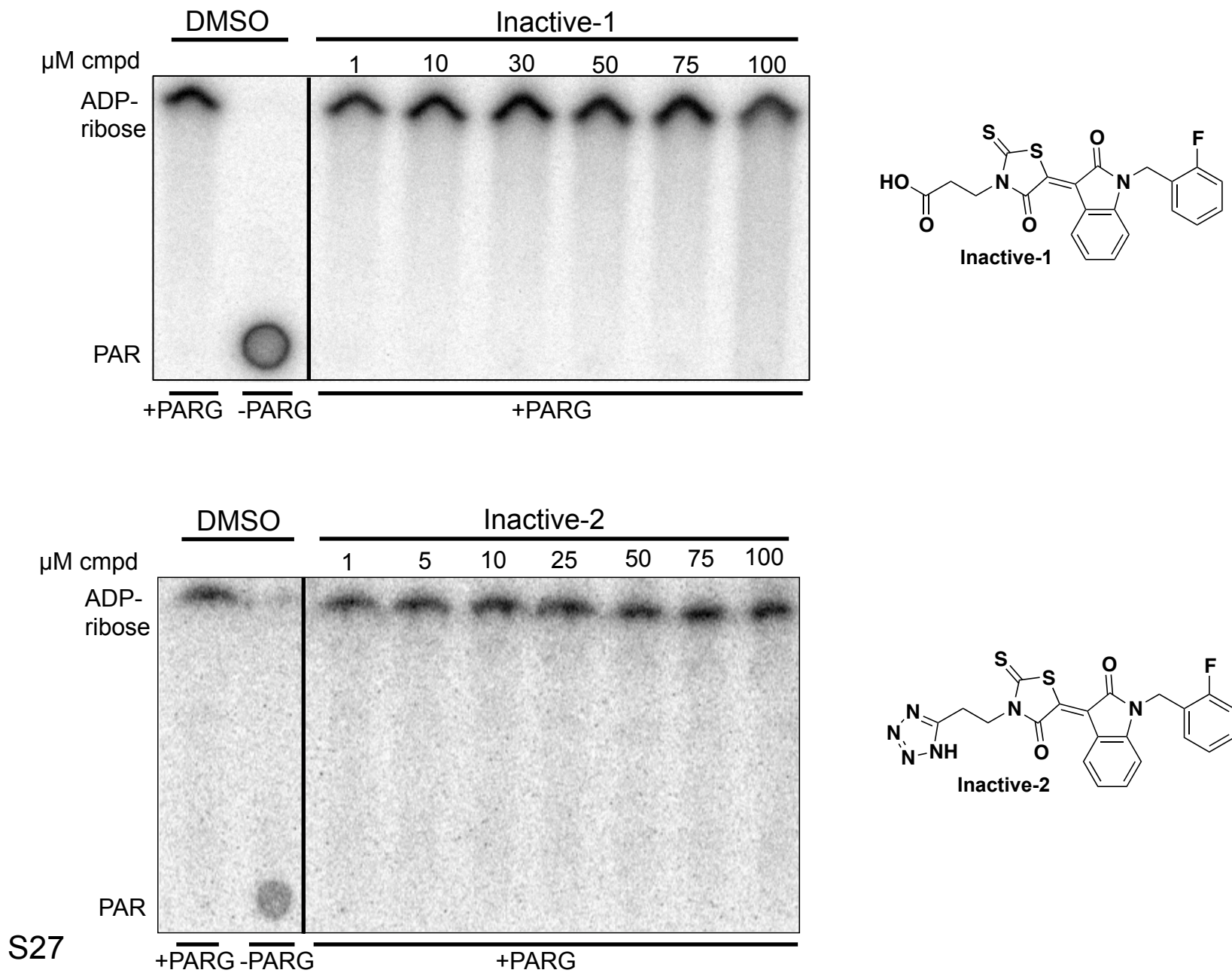


Figure S9. Addition of BSA to *in vitro* assay for PARG activity.
Final concentration of **RBPI-4** is 50 μ M.

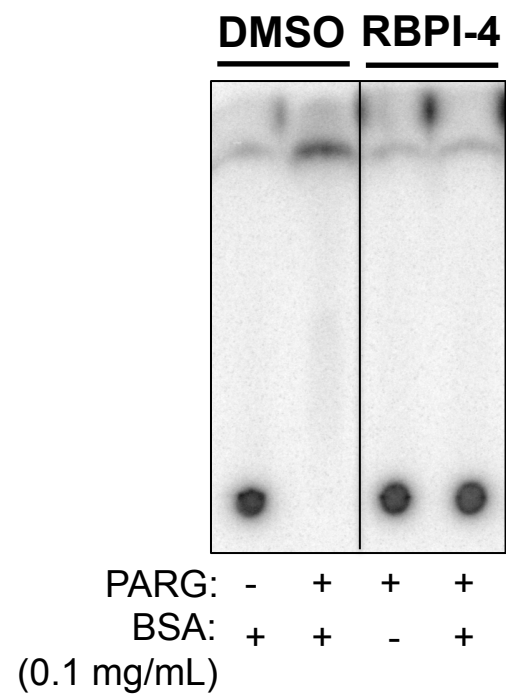


Figure S10. Triplicate IC_{50} curves of ADP-HPD against ARH3 obtained using ^{32}P -PAR degradation assay. Representative TLC plate is shown in upper left.

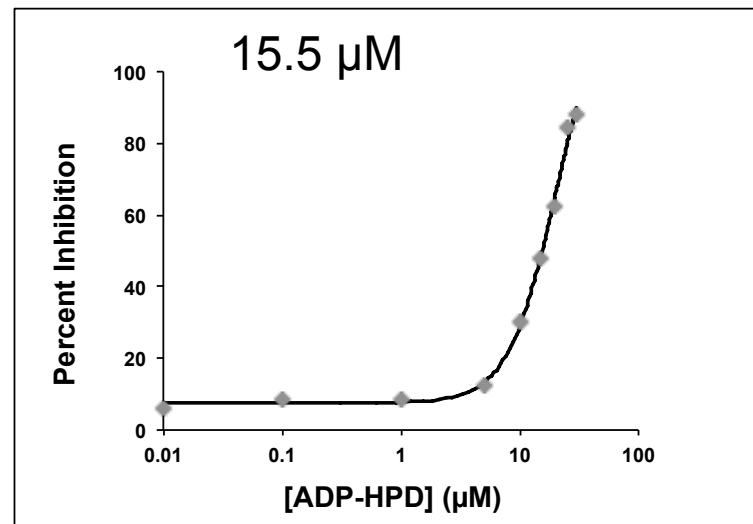
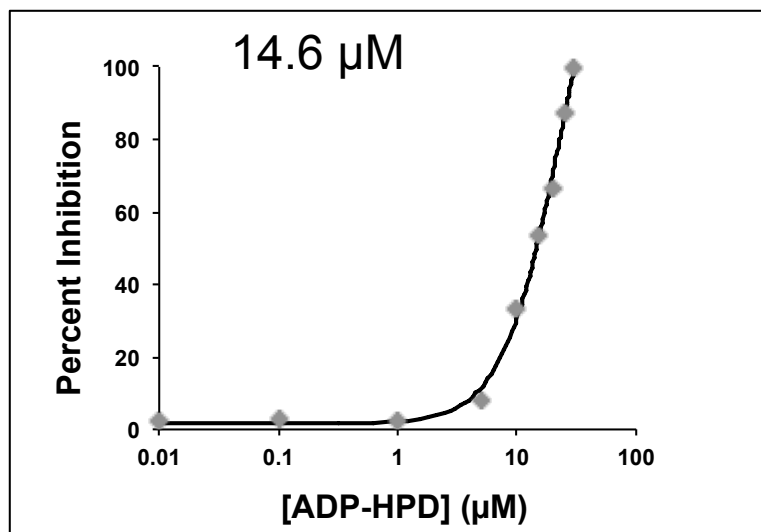
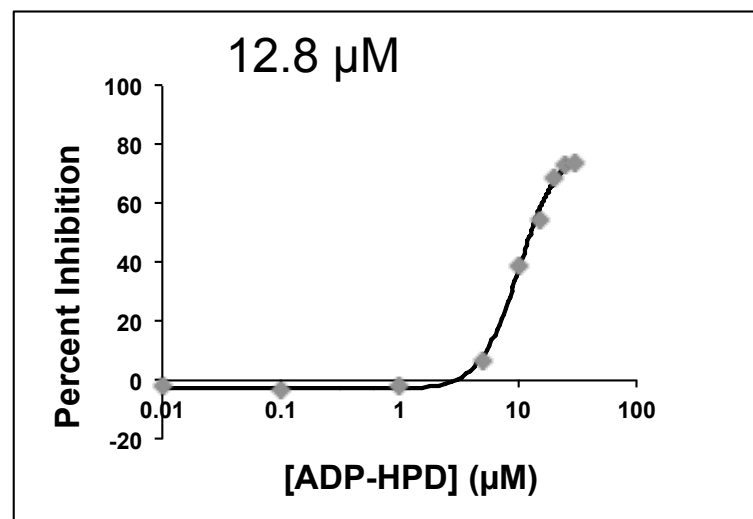
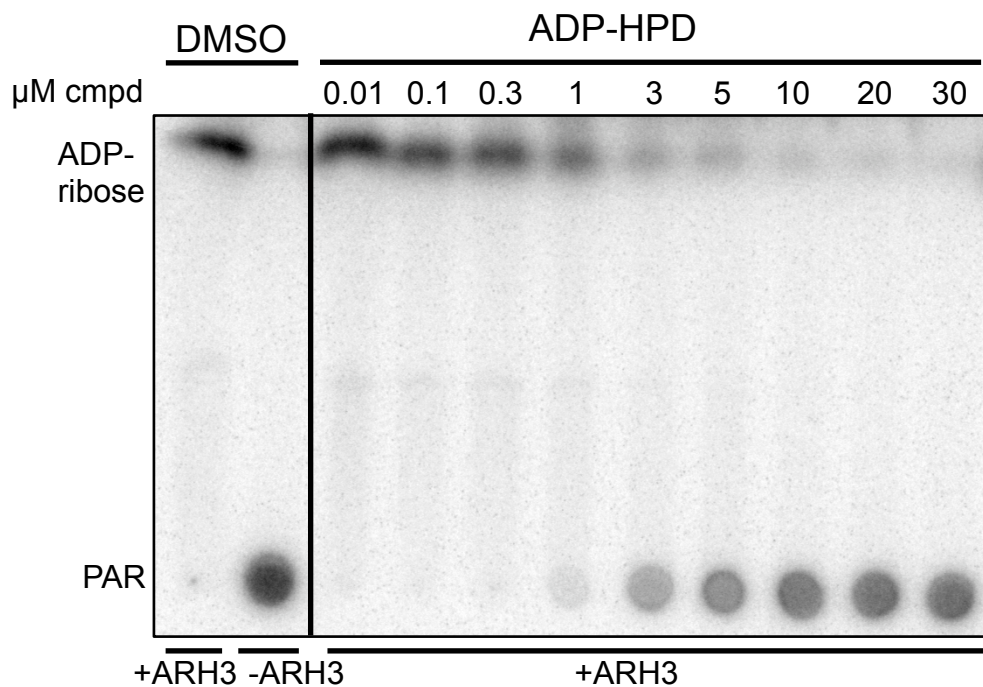
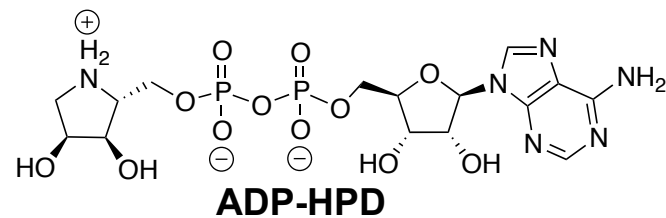


Figure S11. Representative results from ^{32}P -NAD $^{+}$ PARP inhibition assay with 25 μM RBPI-6 and PJ34. Additionally, RBPI-6 does not inhibit PARP up to 100 μM (data not shown).

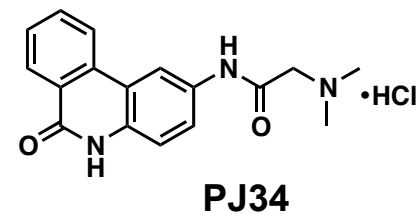
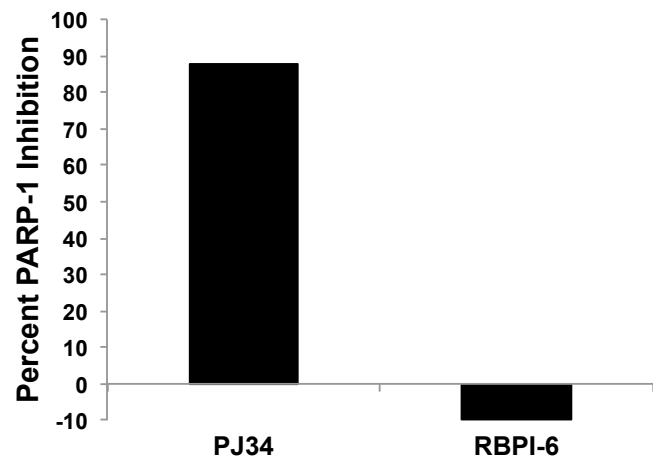


Figure S12. Salicylanilide **6a**, ADP-HPD, and **RBPI-4** under standard 2h *in vitro* assay conditions. Top – Percent inhibition of PARG, n = 3, error bars indicate standard error of the mean. Representative TLC plate shown at bottom.

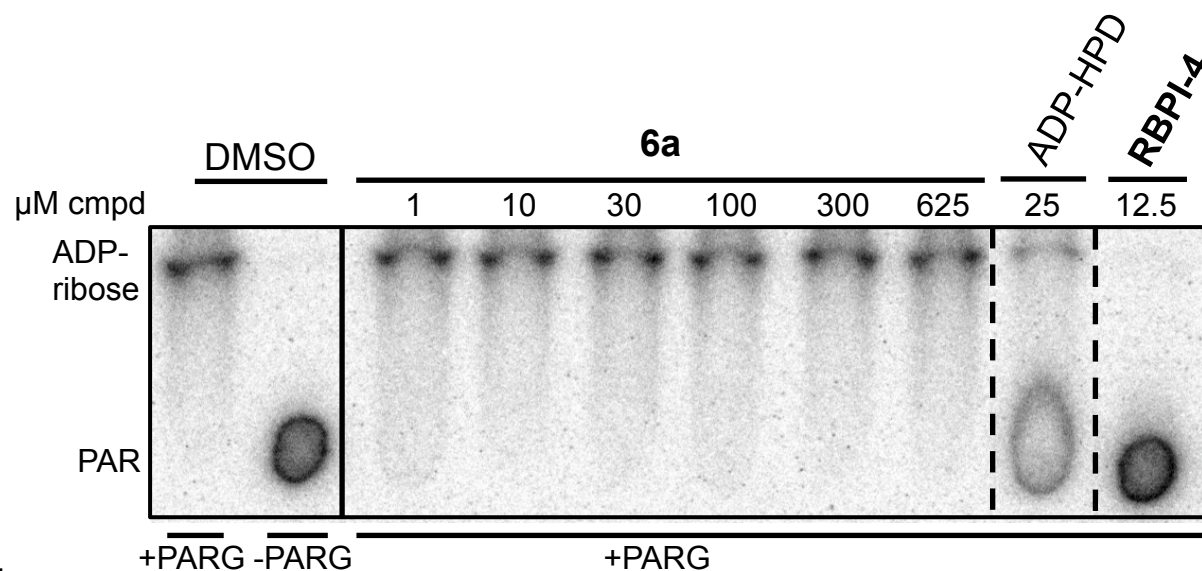
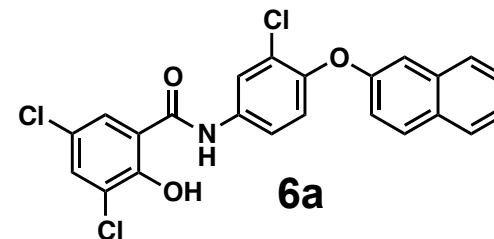
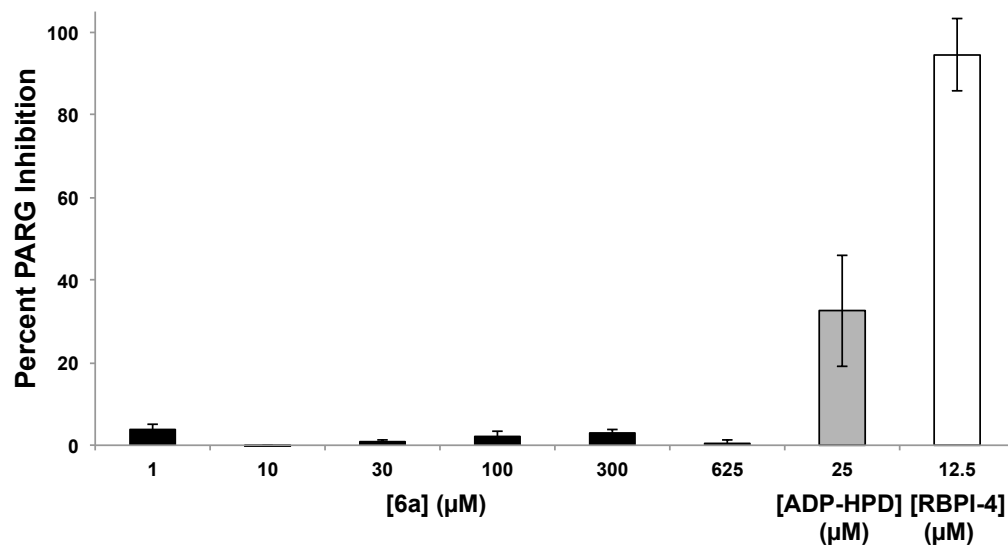
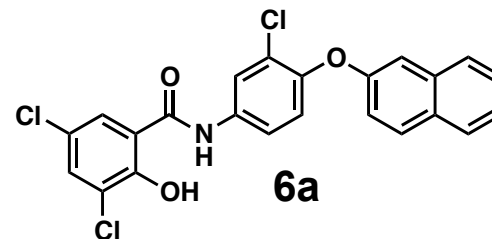
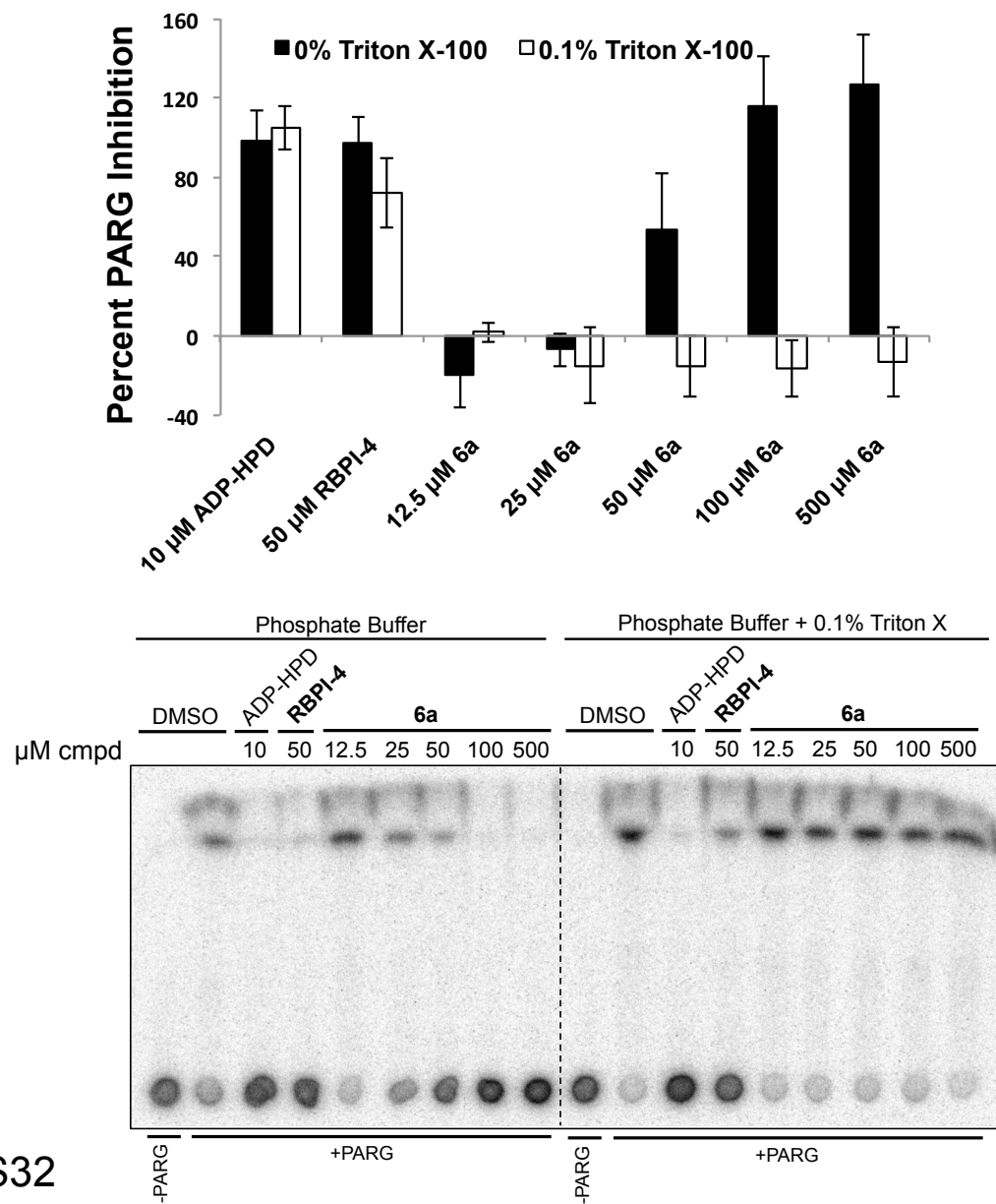


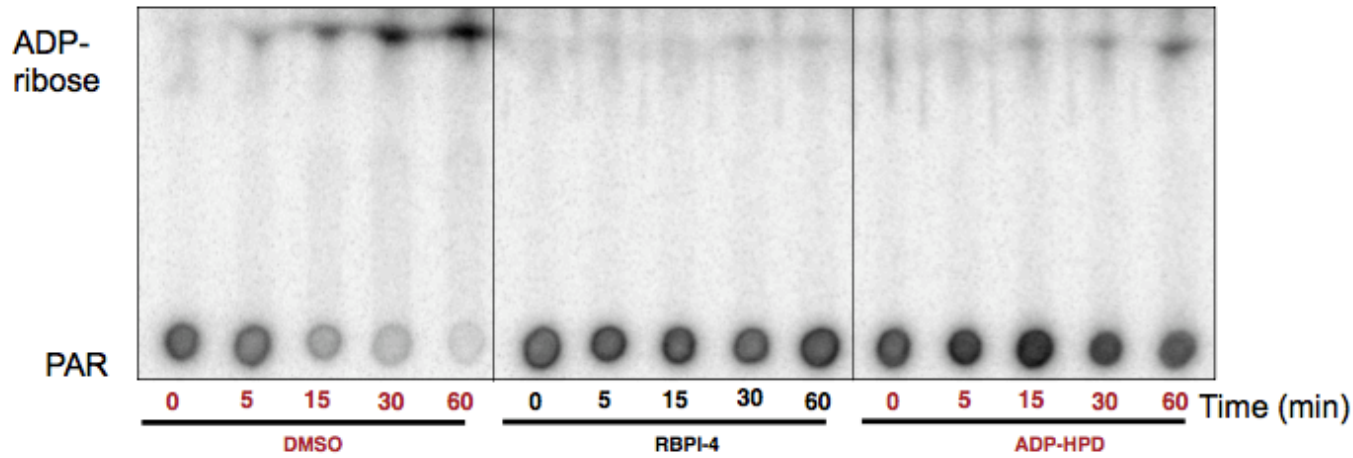
Figure S13. Salicylanilide **6a**, ADP-HPD, and **RBPI-4** under 5 min assay conditions. Top – percent PARG inhibition, $n = 3$, error bars indicate standard error of the mean, representative TLC plate is shown below.



Figures S14 through S21. ^{32}P -PAR Degradation in Cell Lysate – Triplicate Data

All compounds were used at a final concentration of 25 μM . For each cell line tested, one representative TLC plate is shown, along with graphs of normalized densitometry values for all three replicates

Figure S14. MEF lysate with RBPI-4



*See Figure 6 for first replicate of this experiment

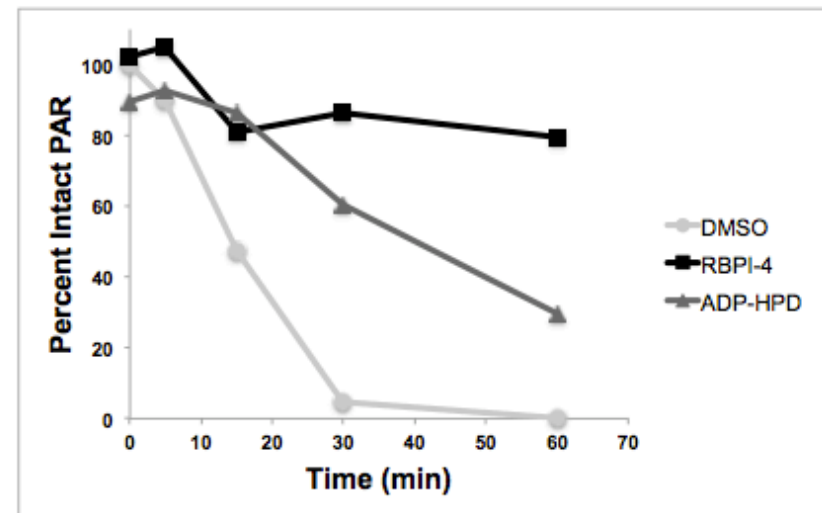
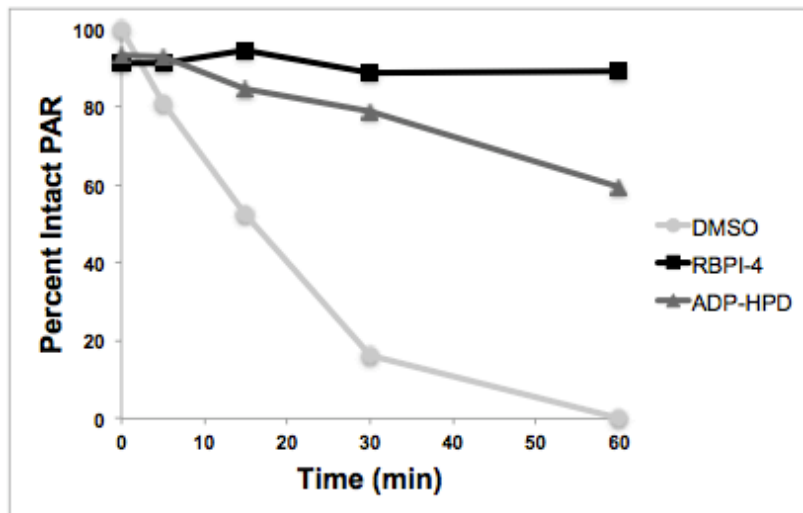


Figure S15. MEF lysate with RBPI-3, -5, and -6 (25 μ M)

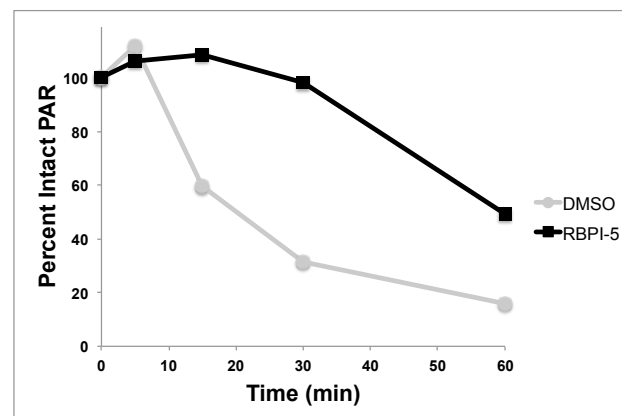
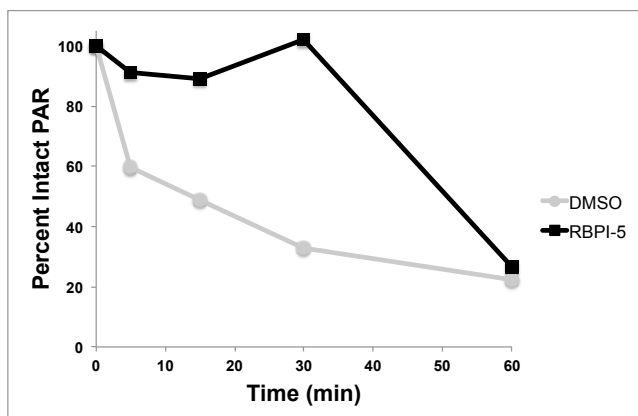
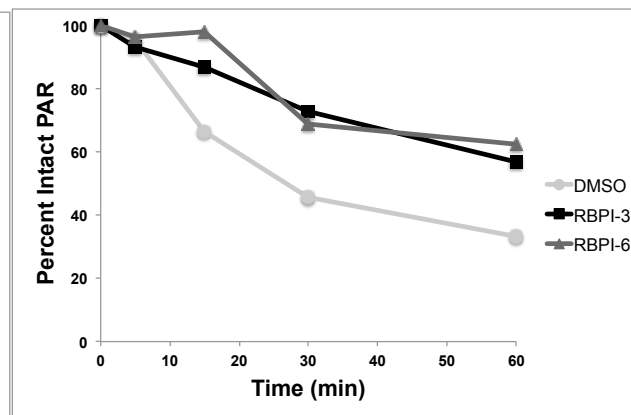
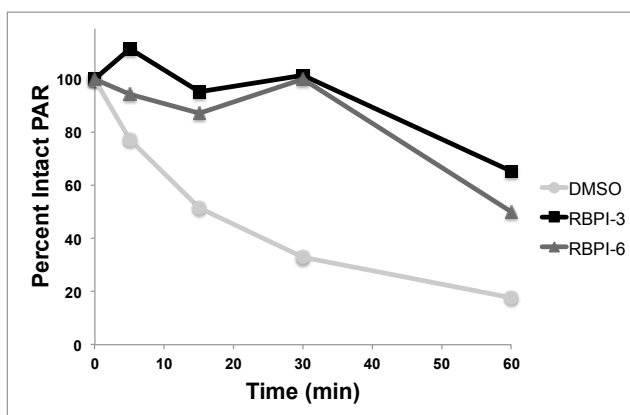
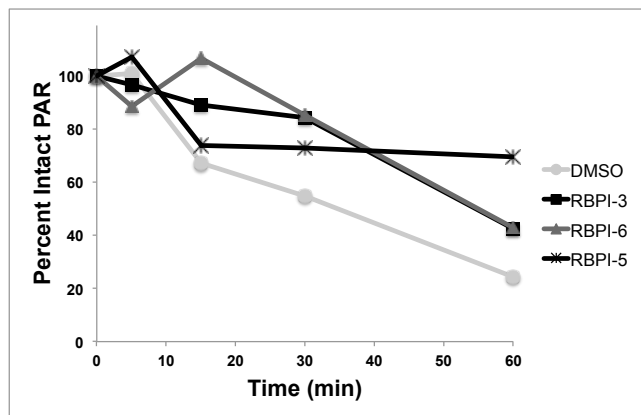
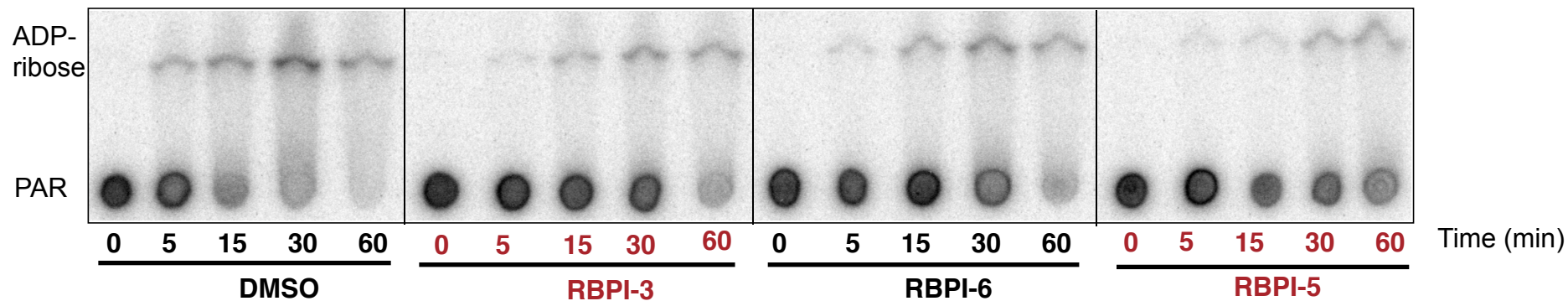


Figure S16. MEF lysate with Inactive-1

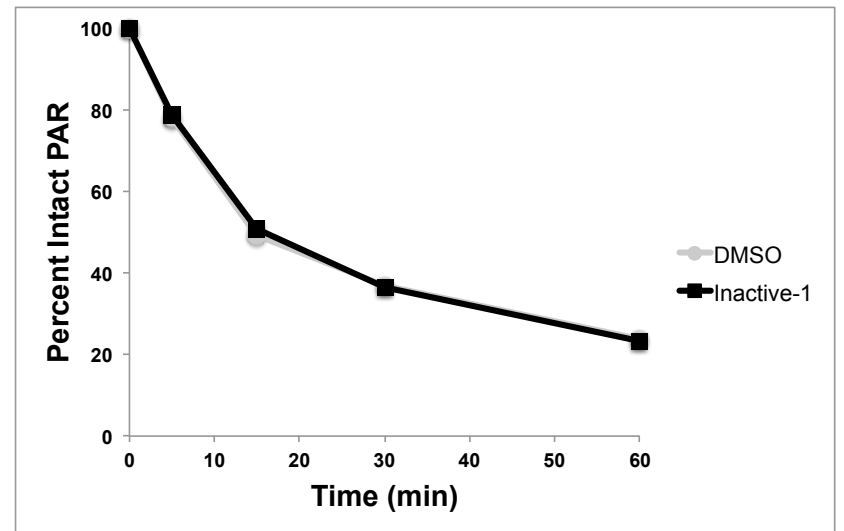
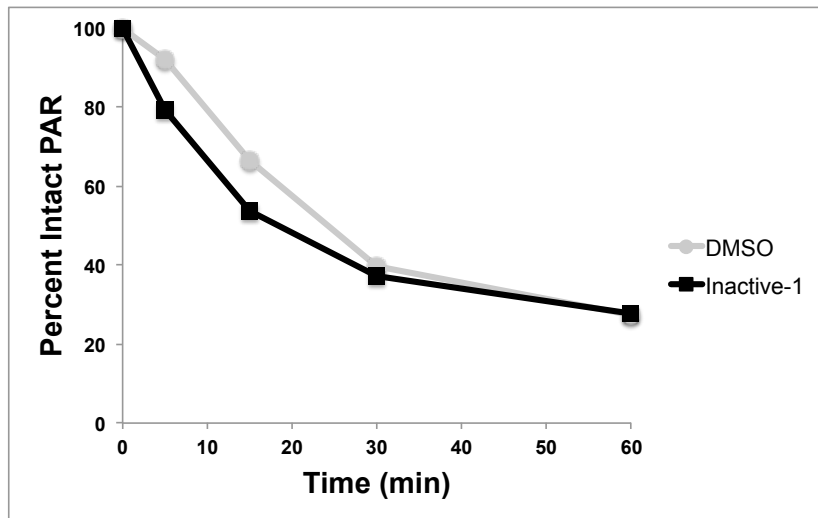
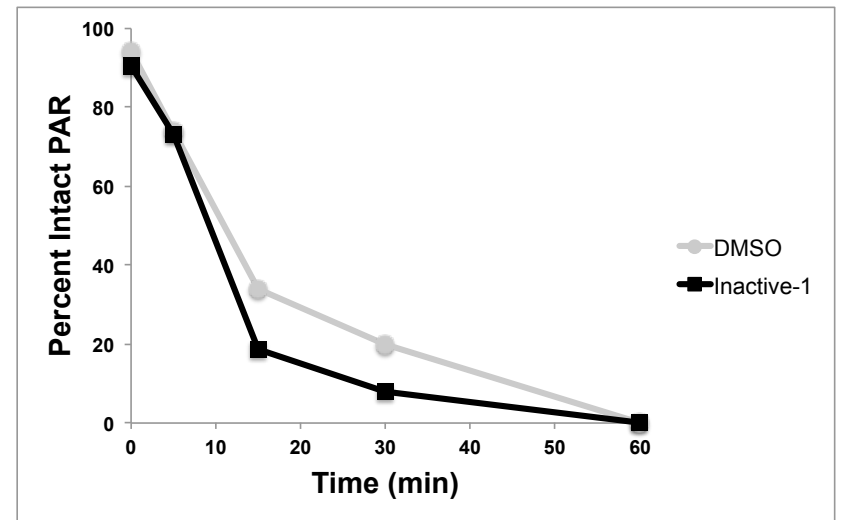
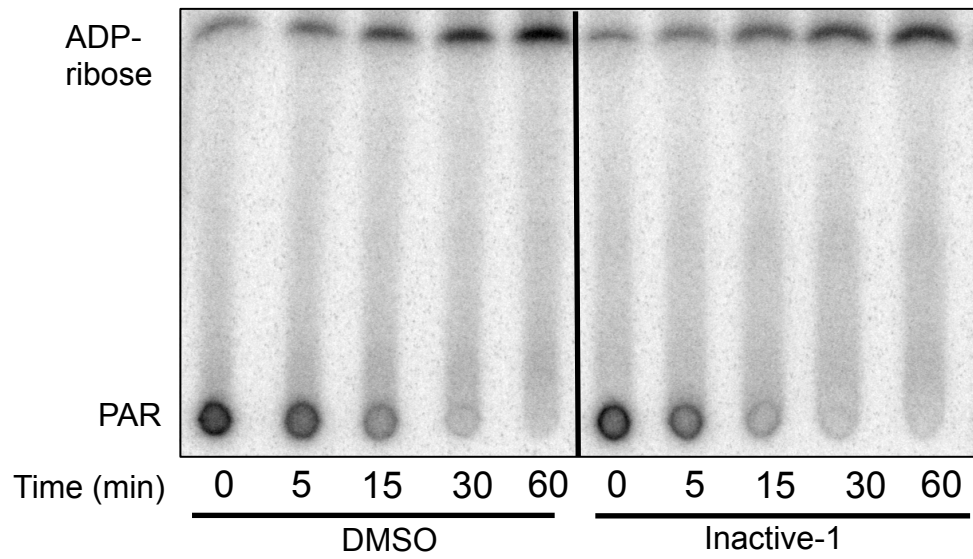


Figure S17. HeLa lysate with RBPI-4

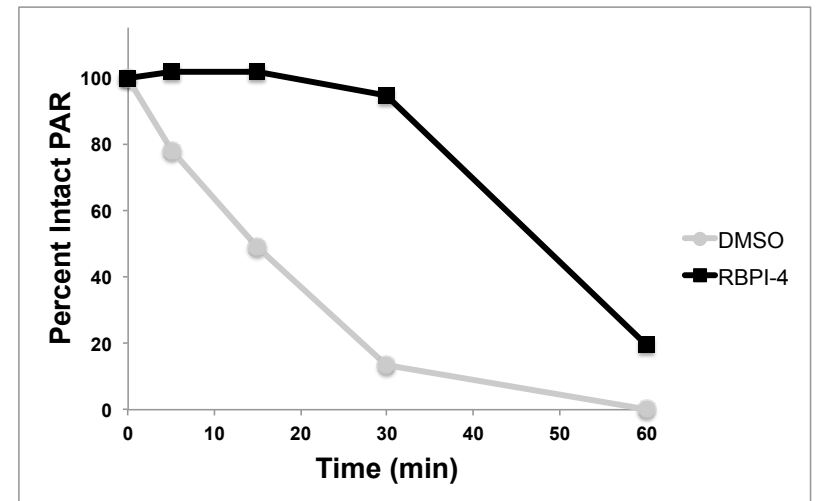
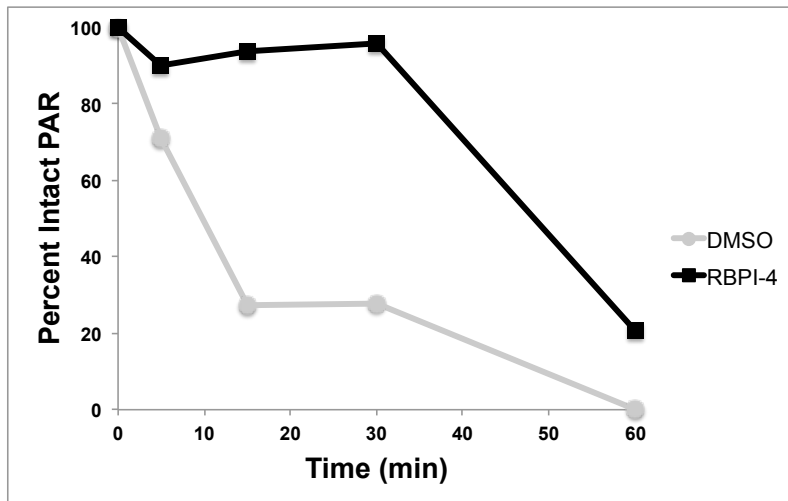
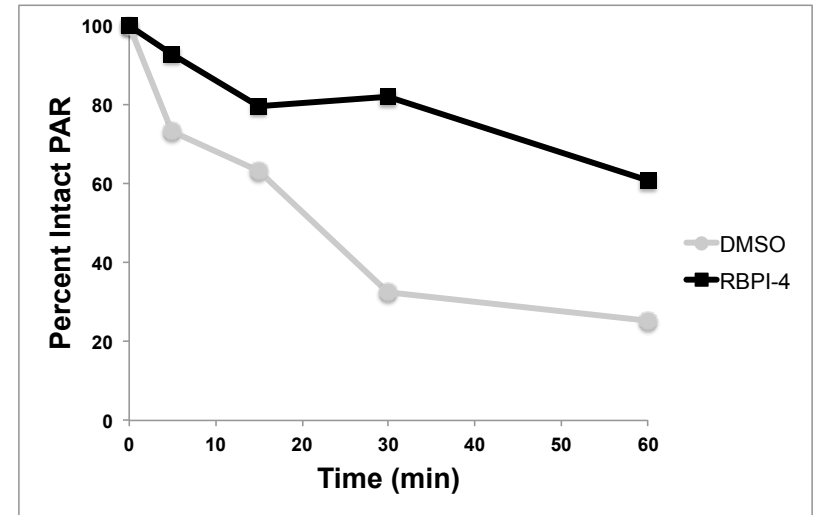
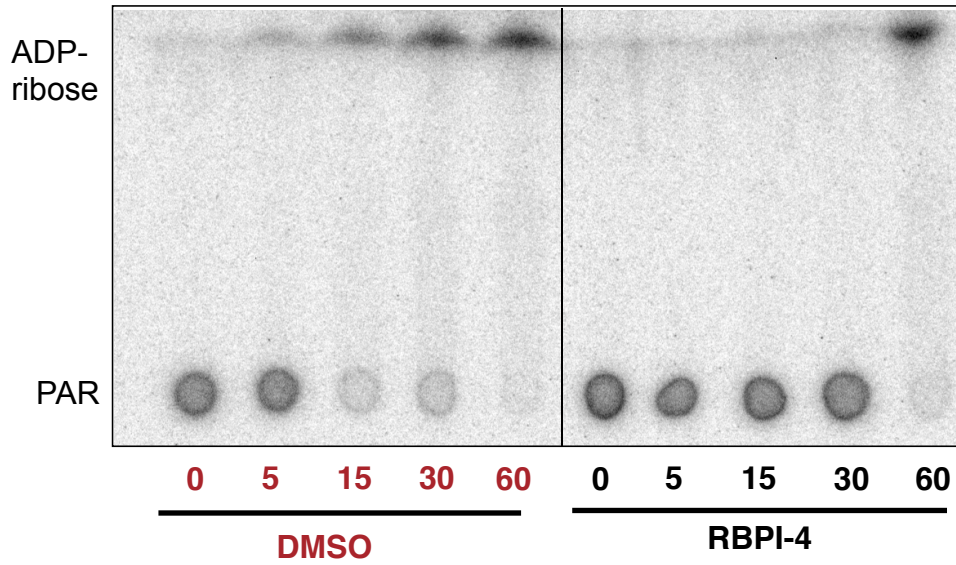
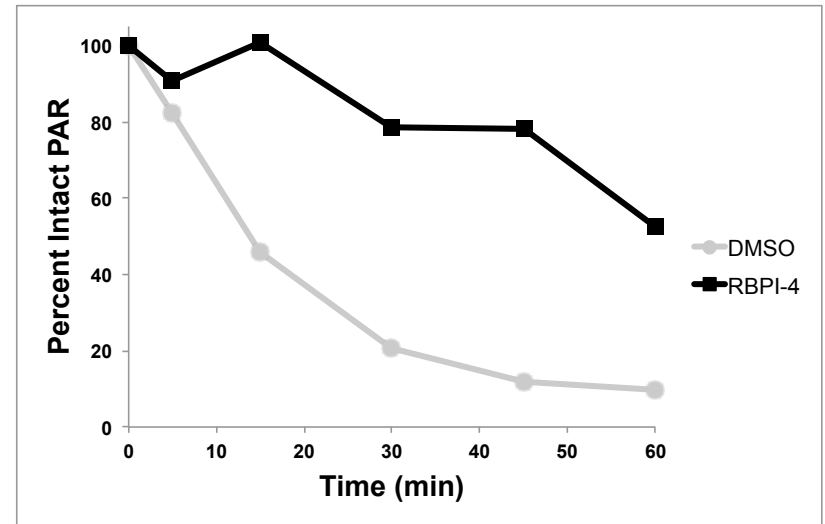
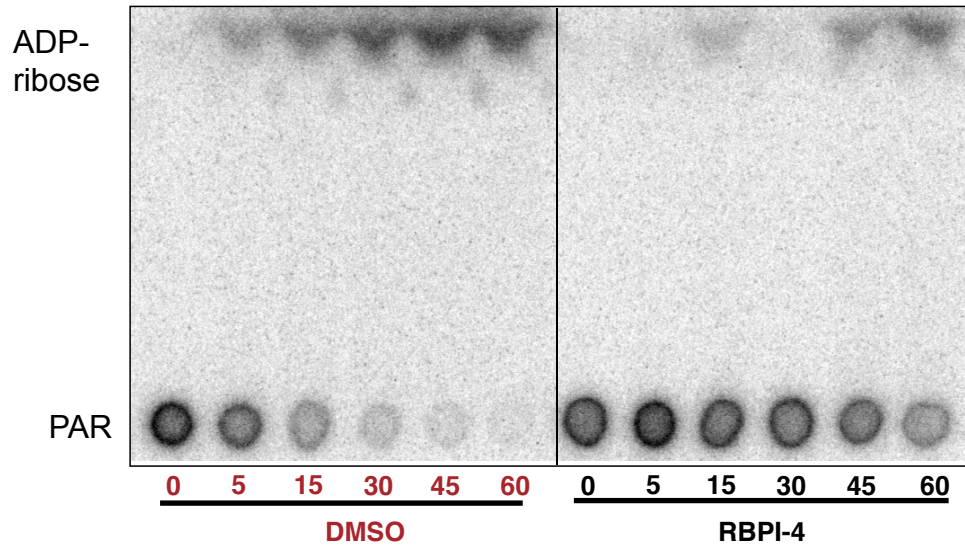


Figure S18. A549 lysate with RBPI-4



Time (min)

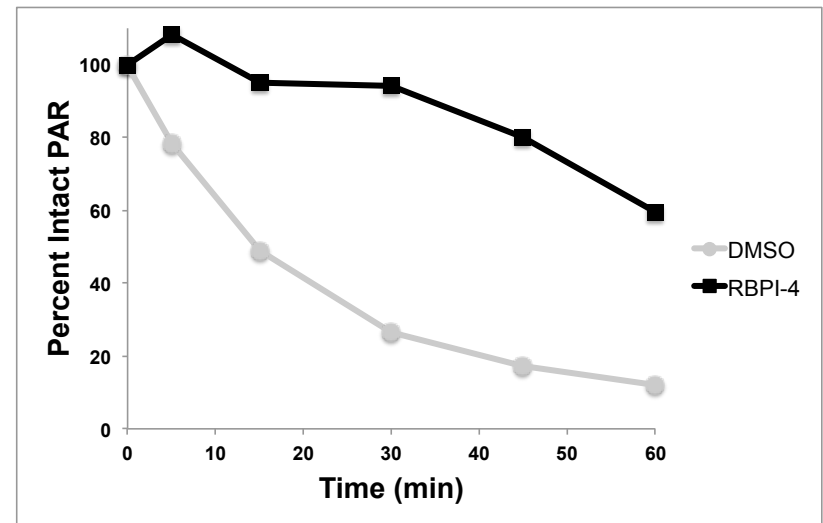
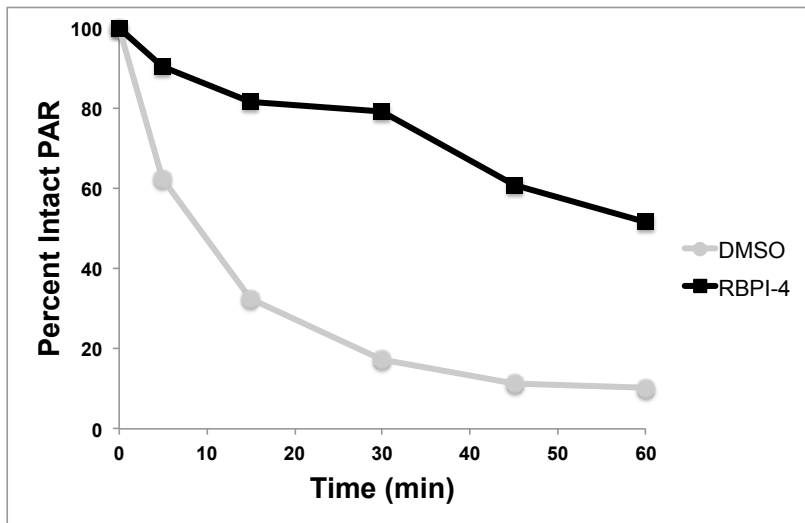
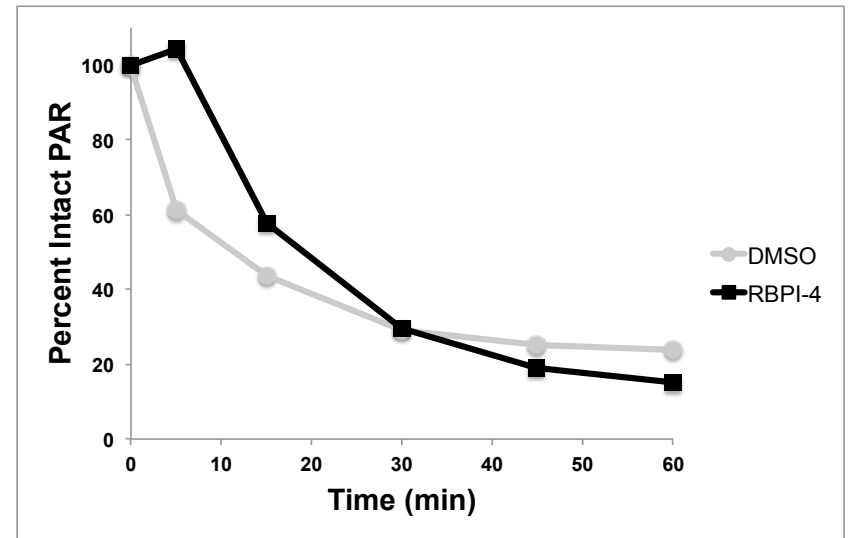
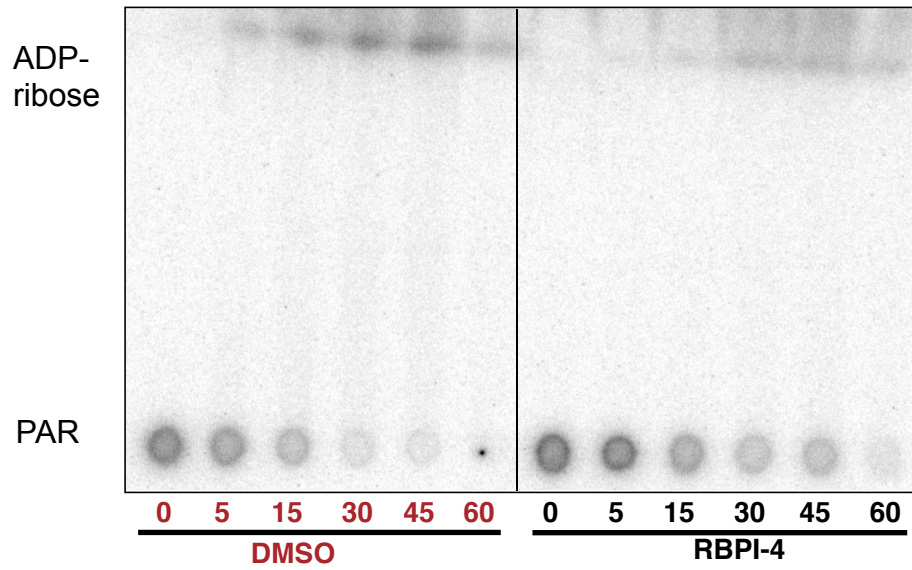


Figure S19. B16F10 lysate with **RBPI-4**



Time (min)

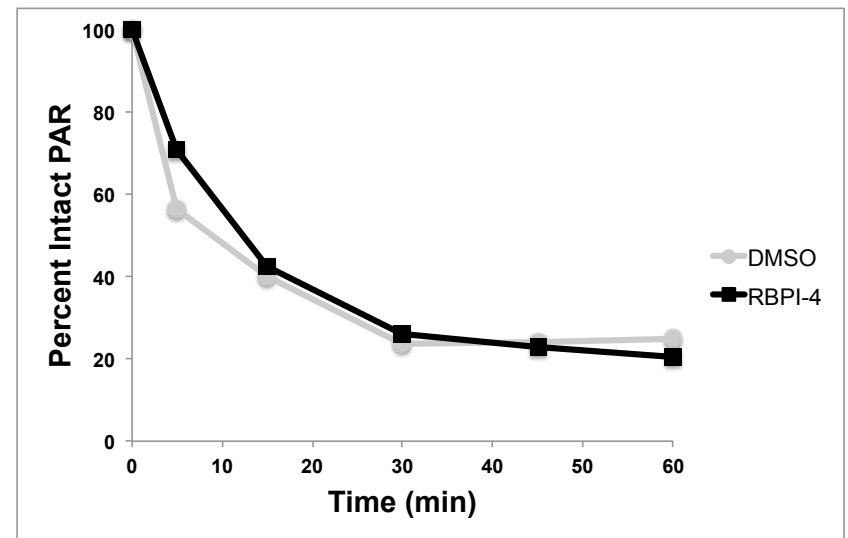
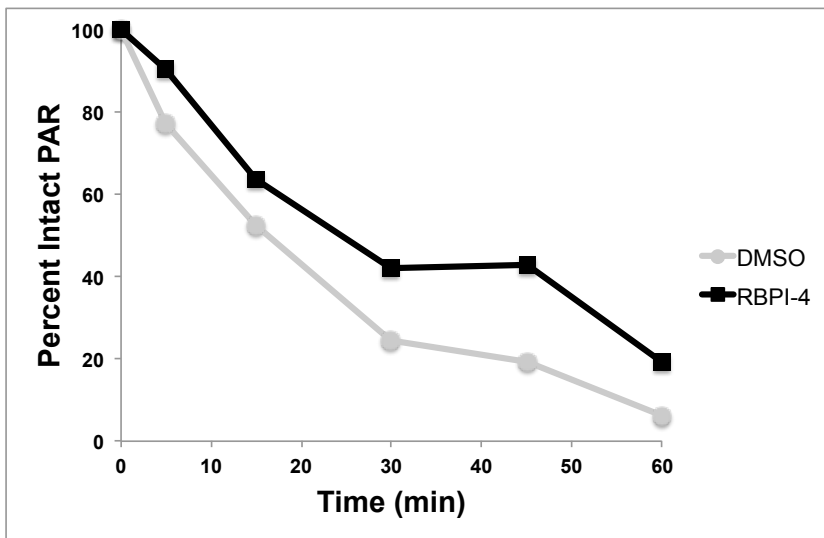
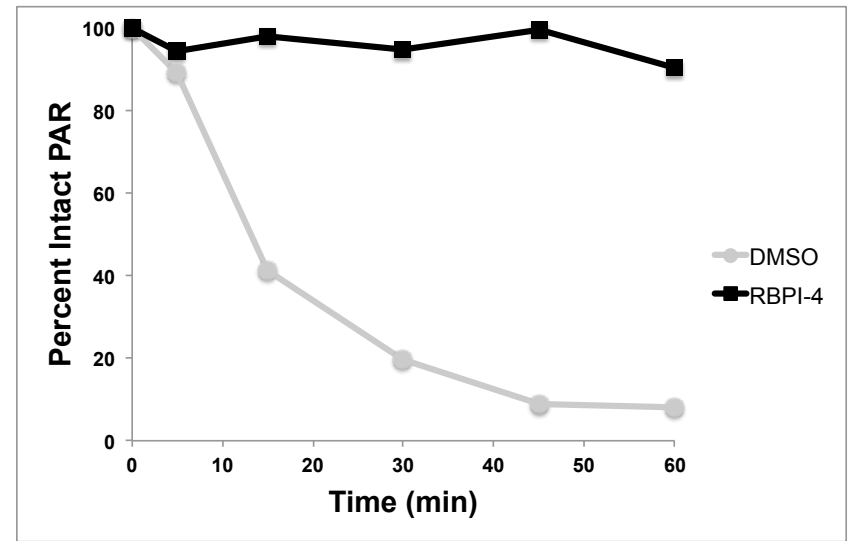
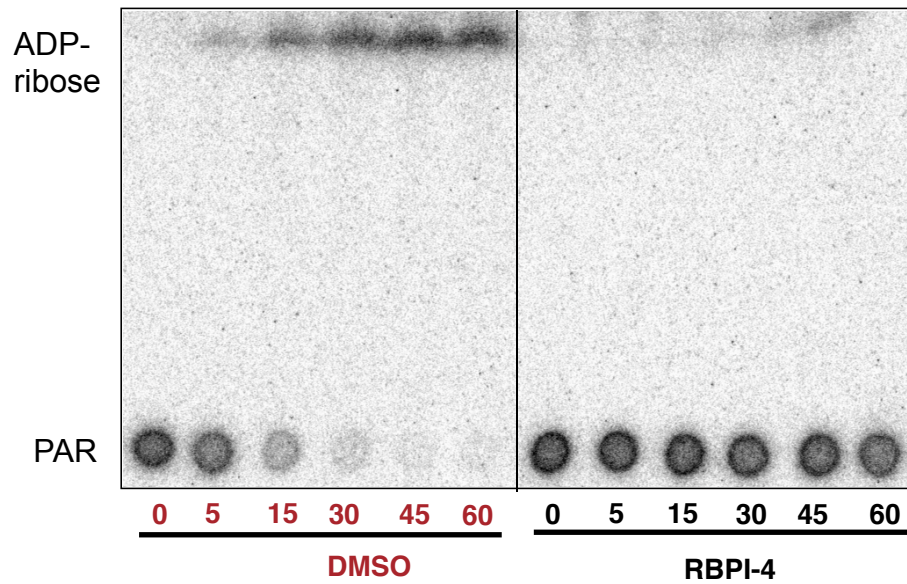


Figure S20. MCF-7 lysate with RBPI-4



Time (min)

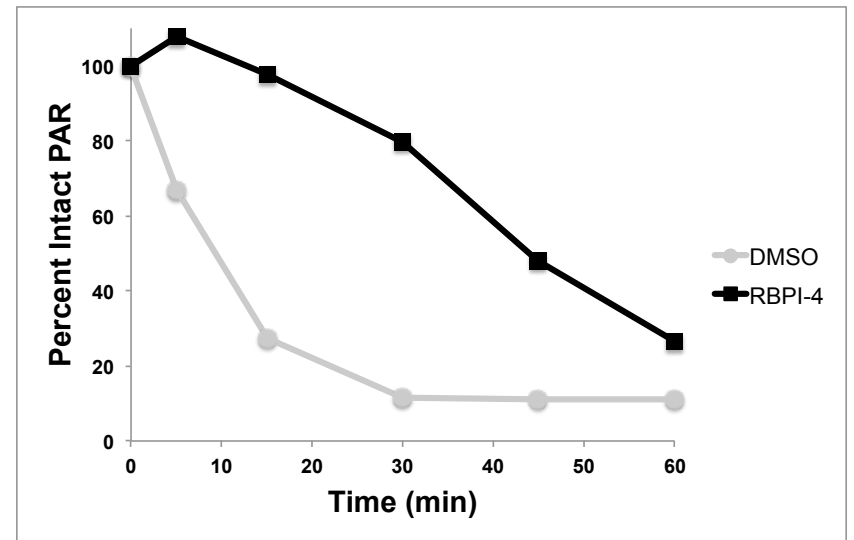
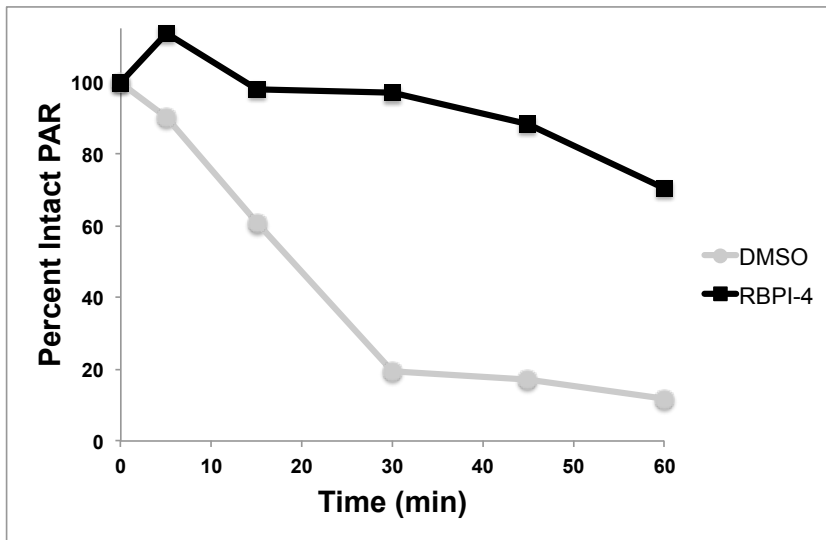
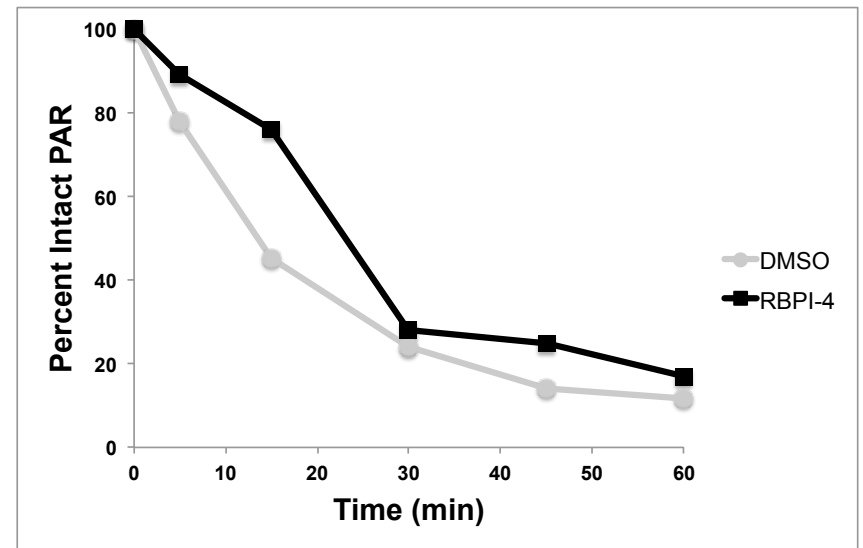
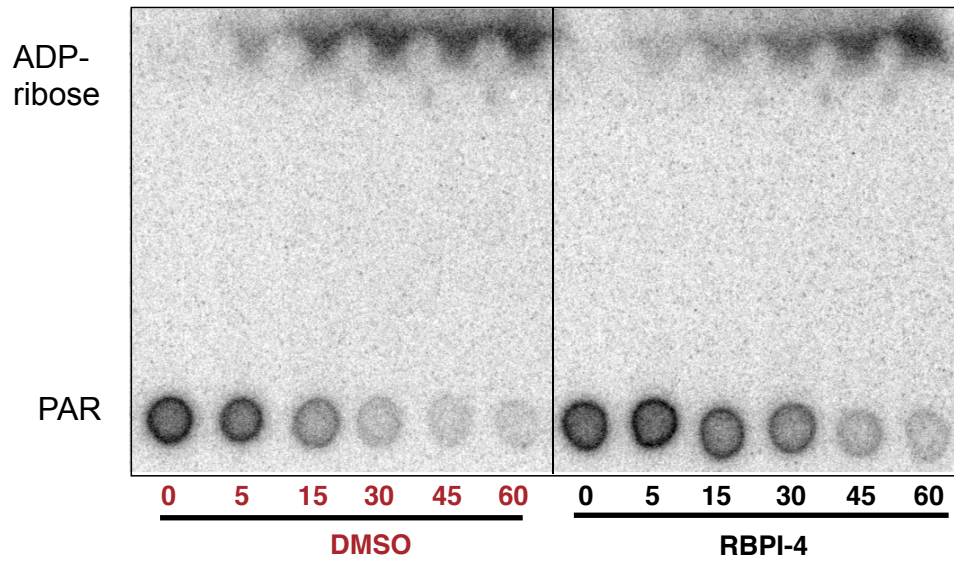
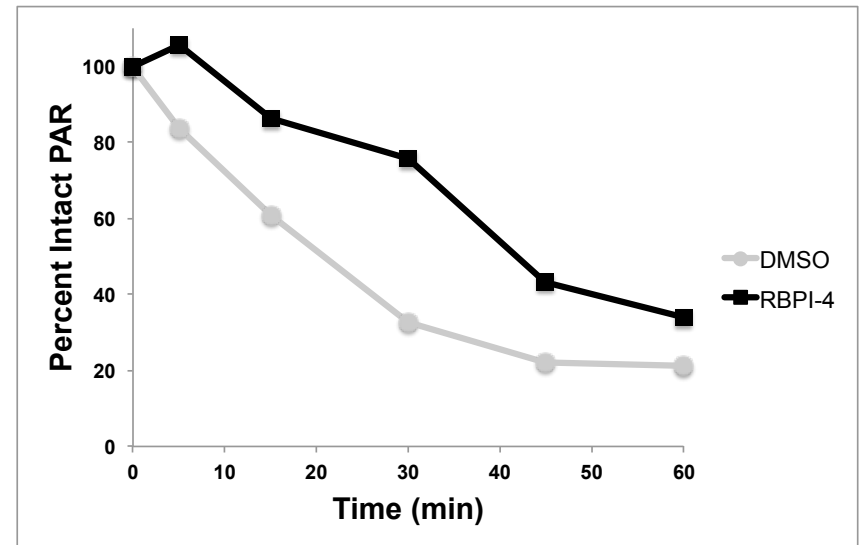
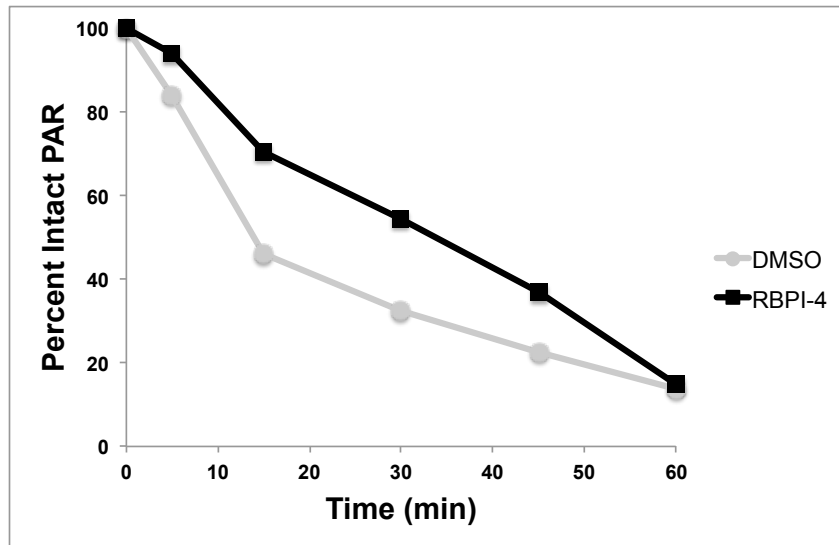


Figure S21. U937 lysate with RBPI-4



Time (min)



General Materials

Acetonitrile (Fisher, HPLC grade), and methanol (Fisher, low water) were dried by percolation through two columns packed with neutral alumina under a positive pressure of nitrogen. All other solvents were obtained from Fisher Scientific and were used without further purification. All H₂O used was either deionized or purified through a MilliQ purification system.

Silica gel for chromatography was performed on EMD Biosciences silica gel 60 (230-400 mesh). Thin-layer chromatography plates (Merck, 245 nm fluorescent indicator) were visualized by UV and stained with potassium permanganate (KMnO₄), iodine (I₂), or ninhydrin.

All NMR experiments were acquired in the Varian-Oxford Instrument Center for Excellence in NMR Spectroscopy (VOICE) laboratory at the University of Illinois at Urbana-Champaign. NMR experiments were recorded in CDCl₃, CD₃OD, or DMSO-*d*₆ on Varian Unity 500 MHz spectrometers. Chemical shift, δ (ppm); coupling constant, *J* (Hz); multiplicity (s = singlet, d = doublet, t = triplet, q = quartet, quin = quintet, m = multiplet); and integration are reported. High-resolution mass spectral data were recorded on a Micromass Q-T of Ultima hybrid quadrupole/time-of-flight ESI mass spectrometer at the University of Illinois at Urbana-Champaign Mass Spectrometry Laboratory.

³²P- β -NAD⁺ (ARP 0141, 800 Ci/mmol. 5 mCi/mL) was purchased from American Radiolabeled Chemicals, Inc. and stored at -20 °C. Calf thymus activated DNA (D4522, CAS 91080-16-9) was purchased from Sigma-Aldrich, diluted in H₂O, the concentration was determined per manufacturer's instructions and stored at -20 °C. PARG buffer (10, 4680-096-02), PARG (bovine, 4680-096-01) and PARP (human, 4668-100-01) were purchased from Trevigen and stored at -80°C or 4°C (or according to manufacturer's recommendation). Congo Red was purchased from Sigma-Aldrich (CAS 573-58-0). ADP-HPD was purchased from Calbiochem (118415) and stored as a 1 mM solution in H₂O at -20 °C.

Mouse embryonic fibroblasts (MEFs) and B16F10 (mouse melanoma cells) were cultured in Dulbecco's modified Eagle medium (DMEM) containing 4.5 g/L glucose and supplemented with 10% (v/v) fetal bovine serum (Gemini Bio-Products, West Sacramento, CA), 1mM sodium pyruvate, 100 U/ml penicillin (Cellgro, Manassas, VA), and 100 μ g/mL streptomycin (Cellgro, Manassas, VA). HeLa (human cervical carcinoma cells), MCF-7 (human breast cancer cells), U937 (human lymphoma cells), and A549 (human lung cancer cells) were grown in RPMI 1640 supplemented with 10% (v/v) fetal bovine serum (Gemini Bio-Products, West Sacramento, CA), 100 U/ml penicillin (Cellgro, Manassas, VA), and 100 μ g/mL streptomycin (Cellgro, Manassas, VA). All cells were maintained in a humidified atmosphere with 95% air and 5% CO₂.

Synthesis of ³²P-PAR

In a 2.0-mL tube, PAR synthesis buffer (final concentrations 100 mM Tris-HCl (pH 8.0), 10 mM MgCl₂, 8 mM DTT, 10% v/v glycerol, 1 mM unlabeled β -NAD⁺, 23 μ g of calf thymus activated DNA) was prepared from concentrated stocks. To the solution was added 75 μ Ci of ³²P β -NAD⁺, and water to a final volume of 900 μ L. Lastly, 100% ethanol (90 μ L) was added dropwise, and the solution heated at 30 °C for 5 min. 20 U of PARP-1 was added, and was incubated at 30 °C for 30 min. Upon completion, the reaction was quenched and 100 μ L of 3 M sodium acetate (pH 5.2) and 700 μ L of isopropanol were added. The sample was incubated at 0 °C for 30 min, and

then PAR was pelleted by centrifugation at 14,100xg at 4 °C for 10 min. The pellet was washed twice with cold 80% (v/v) ethanol in H₂O with centrifugation between each wash (14,000xg at 4 °C for 10 min). The pellet was re-suspended in 800 µL of H₂O and stored at -20 °C.

Radiometric PARG TLC Assay

Compounds were diluted from 10 mM stock solutions in DMSO (or 1 mM stocks in H₂O for ADP-HPD) to the specified concentrations. First, 10X PARG buffer was diluted to 2X concentration. Next, PARG was diluted to 0.025 ng/µL (from a 1 µg/mL solution of PARG) in 2X PARG buffer. To 4.5 µL of this diluted PARG was added 0.5 µL of compound (16X). Control samples were prepared with DMSO in the presence and absence of PARG. The solution was incubated at room temperature for 10 min. Next, ³²P-PAR (3 µL) was added to each solution with mixing and the samples were incubated at 37 °C for 2 h. Samples were quenched either by heating at 90 °C for 2 min or by the addition of 1 µL 1% SDS. Then 1.3 µL of each sample was spotted twice on a TLC plate. The plate was developed twice in 70:30 ¹PrOH:0.2% NH₄OH (aq), allowing for the TLC plate to dry completely between each run. Once dry, the TLC plate was wrapped in clear plastic wrap, and placed in Storage Phosphor Screen (Amersham Biosciences, Sunnydale, CA) overnight, and the screen was imaged on a Storm Imager (GE Life Sciences, Piscataway, NJ). Intact ³²P-PAR was analyzed by densitometry using ImageJ (NIH, Bethesda, MD), and the mean intensity of each spot was used to calculate percent PARG inhibition as compared to the control lacking PARG enzyme.

IC₅₀ curves: Increasing concentrations of compound were tested. The data were plotted as compound concentration versus percent PARG inhibition, and fitted to a logistic-dose response curve using Table Curve (SYSTAT Software, Richmond, CA). The data were generated in triplicate, and IC₅₀ values are reported as the average of three separate experiments along with standard deviation. Fitted graphs from each of the triplicate experiments are shown for each compound.

Addition of detergent or BSA: ³²P-PAR degradation was assessed as described above except using phosphate buffer (final concentrations of 50 mM KHPO₄, 50 mM KCl, 10 mM β-mercaptoethanol, pH = 7.5) supplemented with a final concentration of 100 µg/mL bovine serum albumin or 0.1% Triton X-100 as appropriate.

ARH3 Activity: See below for ARH3 expression and purification. ³²P-PAR degradation was assessed in Trevigen PARG buffer as described above except with a final concentration of 10 µg/mL ARH3 and 4 mM MgCl₂. When directly comparing PARG and ARH3 activity and inhibition (as in Figure 5), PARG activity was assessed in the presence of a final concentration of 4 mM MgCl₂.

Activity in cellular lysate: Generation of cellular lysate – Cells were lysed at 0 °C in 1X Trevigen PARG buffer and centrifuged at 4 °C to remove cell debris. Protein content was determined by BCA assay (Pierce, Rockford, IL). Lysate was diluted in 1X Trevigen PARG buffer to the desired concentration (final lysate concentrations: MEF – 1.5 µg; HeLa – 1.5 µg; U937 – 2.5 µg; MCF7 – 1.5 µg; B16F10 – 3.0 µg; A549 – 1.5 µg) and treated with either vehicle or compound. Then 3.0 µL ³²P-PAR was added with mixing and the samples were incubated at 37 °C for various amounts of time (0 – 60 min). The reaction was quenched by the addition of 1.0 µL 1% SDS with mixing, then the samples were applied to a TLC plate, eluted and analyzed as described above. Graphed as percent intact PAR by normalizing the 0 min time-point as 100% intact PAR.

PARG assay for comparison with salicylanilide 6a: Assay was performed as reported (1)

with the following minor modifications: Total volume was reduced to 10 μL (final concentration of all components was unchanged) and used 10 ng/mL PARG with 4.0 μL ^{32}P -PAR. After 5 min incubation at 37 $^{\circ}\text{C}$, quenched by addition of 1.0 μL 1% SDS. Samples were applied to a TLC plate, eluted and analyzed as described above.

Radiometric PARP-1 Inhibition Assay

Compounds were diluted from 10 mM stock solutions in DMSO to the specified concentrations. Control samples were prepared with DMSO in the presence and absence of PARG. To 90 μL of Trevigen PARG buffer containing compound, calf thymus activated DNA (5 μg), NAD^+ (500 μM), ^{32}P - NAD^+ (1 μCi), and DTT (200 μM), 10 μL containing PARP-1 enzyme (1 U) was added with mixing (all amounts are final concentrations). The solution was incubated at room temperature for 30 min. Next, 175 μL $^i\text{PrOH}$ and 25 μL 3 M NaOAc was added and the samples were incubated at 0 $^{\circ}\text{C}$ for 30 min. After centrifugation at 4 $^{\circ}\text{C}$ (10 min, 14.1 g), the liquid was removed and 100 μL of 80% EtOH was added. After an additional centrifugation at 4 $^{\circ}\text{C}$, the liquid was removed again. The pellet was suspended in 5 μL of Trevigen PARG buffer. Next 1.5 μL of each sample was spotted twice on a cellulose PEI TLC plate. The plate was developed in 100% MeOH, allowed to dry, then developed in 0.9 M AcOH 0.3 M LiCl (aq). Once dry, the lower spots were cut out, the solid phase was removed from the backing and placed in 2 mL of scintillation fluid. Intact ^{32}P -PAR was quantified by scintillation counting (Beckman LS6500) and the mean cpm for each sample was used to calculate percent PARP inhibition as compared to the control lacking PARP enzyme.

ARH3 protein expression

The ARH3 plasmid containing an N-terminal His₆-tag (a generous gift from Hening Lin, Cornell University, Cornell, NY) was transformed into chemically competent Rosetta™ 2 (DE3) cells (Novagen, San Diego, CA) according to the manufacturer's protocols. Cells from a single overnight colony were seeded (1:100) in Luria Bertani broth containing 100 $\mu\text{g}/\text{mL}$ ampicillin and 20 $\mu\text{g}/\text{mL}$ chloramphenicol. After growing at 37 $^{\circ}\text{C}$ to $\text{OD}_{600}=0.5$, cells were cooled to 18 $^{\circ}\text{C}$ and protein expression was induced with a final concentration of 0.1 mM IPTG for 18 hrs. The cells were collected by centrifugation, suspended in lysis buffer (20 mM Tris, pH 7.4, 500 mM NaCl, 10 mM MgCl₂, 30 mM imidazole), and lysed by sonication in the presence of 1 mM PMSF, 2 $\mu\text{g}/\text{mL}$ aprotinin, 1 $\mu\text{g}/\text{mL}$ leupeptin, and 1 $\mu\text{g}/\text{mL}$ pepstatin A. After clarifying the lysate (35,000g for 30 min), the supernatant was batch purified with 1.5 mL of Ni-NTA slurry (Qiagen, Valencia, CA). The protein was eluted by gravity flow with increasing concentrations of imidazole, where the 50 mM to 200 mM fractions were pooled, exchanged into storage buffer (20mM Tris, pH 7.4, 500mM NaCl, 10% glycerol), and assessed for protein concentration by the BCA assay (Pierce, Rockford, IL).

General Procedure for Rhodanine-Containing Compound Synthesis:

Alkylation of Isatin

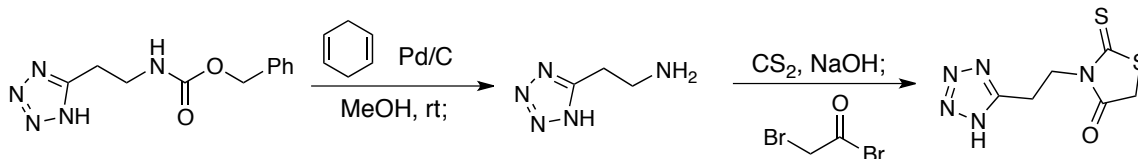
In a 25 mL round-bottomed flask, a solution of isatin (1 mmol) and potassium carbonate (2 mmol) were stirred in acetonitrile (10 mL) at room temperature for 30 min. In a second 25 mL round-bottomed flask, a solution of benzylhalide (1 mmol) and potassium iodide (0.1 mmol) were stirred in acetonitrile (10 mL) at room temperature for 10 min. Upon completion, the solution of benzylhalide/potassium iodide was added dropwise to the stirring solution of

isatin/potassium carbonate over 10 min. The solution continued to stir at room temperature overnight. Upon completion (12 h), the solution was concentrated *in vacuo*. The resulting solids were resuspended in 100 mL of dichloromethane, and filtered to remove any insoluble particulates. The solution was concentrated *in vacuo* to obtain a solid, which was purified through trituration by sonication with MeOH (2 mL x 3). Any residual MeOH was concentrated to dryness to afford the desired alkylated isatin in 35-78% yield.

Condensation of Rhodanine and Isatin

In a 20 mL reflux condenser vial, a solution of alkylated isatin (1 mmol), *N*-acetic or *N*-propionic acid rhodanine (1 mmol), and sodium acetate (10 mmol) were stirred in acetic acid (4 mL) under reflux overnight. Upon completion, the solids were filtered, washed with H₂O (30 mL), and dried under high vacuum to afford the isatin functionalized rhodanine without any further purification in 56-85% yield.

3-(2-(1H-tetrazol-5-yl)ethyl)-2-thioxothiazolidin-4-one



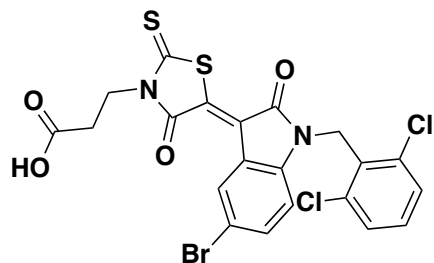
A 25 mL round-bottom flask under nitrogen was charged with Pd/C (400 mg, equal weight to **57**) and **57** (400.0 mg, 1.62 mmol, 1 equiv.). Neat 1,4-cyclohexadiene (0.92 mL, 97 mmol, 6.0 equiv.) was added via syringe, followed by methanol (6.5 mL, 0.25M). The reaction was stirred at ambient temperature for 24 hours, after which the stir bar was removed and the reaction solution was filtered through Celite, rinsing with methanol. Solvent was removed from the filtrate *in vacuo* to yield a white crystalline solid (183 mg, 1.62 mmol, quant.) whose ¹H-NMR spectrum matched the reported values. This intermediate was used within 1 day and was not purified further. **65** (457.0 mg, 4.04 mmol, 1.0 equiv.) was dissolved in deionized water (20 mL, 0.2 M) and NaOH (484.8 mg, 12.12 mmol, 3.0 equiv.) was added. The mixture was stirred until all solids were dissolved. Carbon disulfide (384 μ L, 6.06 mmol, 1.5 equiv.) was added dropwise followed by tetrahydrofuran (8 mL, 0.5 M) in one portion. The flask was capped and the reaction was stirred at ambient temperature for 18 hours. The mixture was subjected to rotary evaporation to remove all volatile components – a bleach mixture was placed in the trap to reduce the smell from carbon disulfide vapors. To the resulting aqueous solution was added a solution of bromoacetyl bromide (532 μ L, 6.06 mmol, 1.5 equiv.) in dichloromethane (5 mL, 0.8 M). The reaction was allowed to stir at ambient temperature for 2.5 hours, at which time large amounts of white precipitate was observed. The precipitate was filtered off and the filtrate was returned to the flask and stirred for an additional 14 hours. The reaction mixture was filtered again, yielding more white precipitate. The solids were dried *in vacuo* yielding a white powder (721.4 mg, 3.15 mmol, 78%).

¹H NMR (DMSO-*d*₆): δ 4.19 (s, 2H), 4.17 (t, 2H, J = 7.5 Hz), 3.20 (t, 2H, J = 7.5 Hz),

¹³C NMR (DMSO-*d*₆): δ 203.9, 174.9, 153.7, 42.4, 36.7, 21.2.

HRMS (ESI) calcd (M+H)⁺: 230.0170, found: 230.0176.

(E)-3-(5-(5-bromo-1-(2,6-dichlorobenzyl)-2-oxoindolin-3-ylidene)-4-oxo-2-thioxothiazolidin-3-yl)propanoic acid, RBPI-2



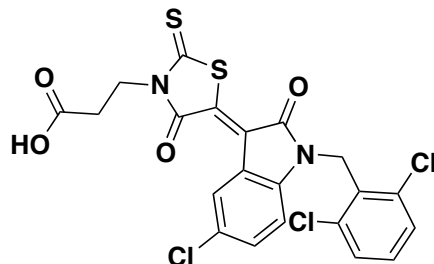
¹H NMR (DMSO-*d*₆): δ 9.03 (s, 1H), 7.65 (br s, 1H), 7.51 (d, 2H, *J* = 8 Hz), 7.40 (t, 1H, *J* = 8.5 Hz), 6.92 (d, 1H, *J* = 9 Hz), 5.23 (s, 2H), 4.24 (t, 2H, *J* = 7.5 Hz), 2.63 (t, 2H, *J* = 7.5 Hz)

¹³C NMR (DMSO-*d*₆): δ 197.3, 172.4, 167.2, 166.7, 144.2, 136.0, 135.5, 135.2, 131.5, 130.4, 130.3, 129.8, 122.5, 121.7, 115.2, 112.4, 41.3, 39.7, 31.5,

HRMS (ESI) calcd (M+H)⁺ for C₂₁H₁₄BrCl₂N₂O₄S₂

570.8955; found 570.8956

(E)-3-(5-(5-chloro-1-(2,6-dichlorobenzyl)-2-oxoindolin-3-ylidene)-4-oxo-2-thioxothiazolidin-3-yl)propanoic acid, RBPI-3



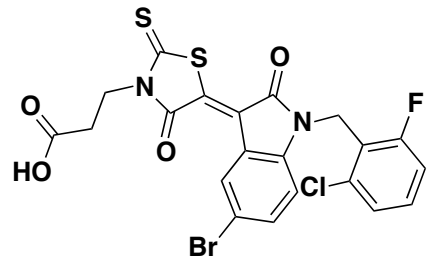
¹H NMR (DMSO-*d*₆): δ 8.92 (s, 1H), 7.56 (m, 3H), 7.42 (t, 1H, *J* = 7.5 Hz), 7.00 (d, 1H, *J* = 8.5 Hz), 5.26 (s, 2H), 4.26 (d, 2H, *J* = 8 Hz), 2.64 (t, 2H, *J* = 8 Hz)

¹³C NMR (DMSO-*d*₆): δ 197.3, 172.5, 167.2, 166.8, 143.8, 136.0, 135.2, 132.7, 131.5, 130.4, 127.6, 127.5, 122.6, 121.3, 111.9, 41.3, 40.9, 31.4

HRMS (ESI) calcd (M+H)⁺ for C₂₁H₁₄Cl₃N₂O₄S₂ 526.9461;

found 526.9470

(E)-3-(5-(5-bromo-1-(2-chloro-6-fluorobenzyl)-2-oxoindolin-3-ylidene)-4-oxo-2-thioxothiazolidin-3-yl)propanoic acid, RBPI-4

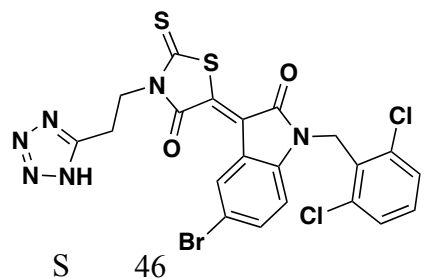


¹H NMR (DMSO-*d*₆): δ 9.00 (d, 1H, *J* = 2.0 Hz), 7.66 (dd, 1H, *J* = 2.1 Hz, *J* = 8.5 Hz), 7.41 (dt, 1H, *J* = 6.0 Hz, *J* = 8.1 Hz), 7.36 (d, 1H, *J* = 7.7 Hz), 7.24 (t, 1H, *J* = 8.6 Hz), 6.98 (d, 1H, *J* = 8.5 Hz), 5.13 (s, 2H), 4.24 (t, 2H, *J* = 7.8 Hz), 2.62 (t, 2H, *J* = 7.8 Hz)

¹³C NMR (DMSO-*d*₆): δ 196.5, 171.7, 166.5, 165.9, 161.3 (d, *J* = 249.6), 143.4, 134.9, 134.5, 134.2 (d, *J* = 5.3), 131.0 (d, *J* = 9.9), 129.7, 125.9 (d, *J* = 3.0), 121.8, 120.9, 120.4 (d, *J* = 16.3), 114.9 (d, *J* = 22.4), 114.5, 111.5, 40.1, 40.0, 39.9, 39.8, 39.8, 39.7, 39.6, 39.5, 39.3, 39.2, 39.0, 36.5 (d, *J* = 3.0), 30.76

HRMS (ESI) calcd (M+H)⁺ for C₂₁H₁₄BrClF₂N₂O₄S₂ 554.9251; found 554.9227

(E)-3-(2-(1H-tetrazol-5-yl)ethyl)-5-(5-bromo-1-(2,6-dichlorobenzyl)-2-oxoindolin-3-ylidene)-2-thioxothiazolidin-4-one, RBPI-5



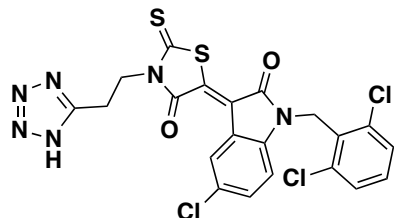
¹H NMR (DMSO-*d*₆): δ 9.01 (d, 1H, *J* = 2.5 Hz), 7.68 (dd, 1H, *J* = 8.5, 2 Hz), 7.53 (d, 2H, *J* = 8 Hz), 7.42 (t, 1H, *J* = 8.5 Hz), 6.95 (d, 1H, *J* = 8.5 Hz), 6.95 (d, 1H, *J* = 8.5 Hz), 5.26 (s,

2H), 4.37 (t, 2H, $J = 7.5$ Hz), 3.27 (t, 2H, $J = 7.5$ Hz).

^{13}C NMR (DMSO- d_6): δ 197.3, 167.3, 166.7, 156.2, 144.2, 136.0, 135.5, 135.3, 131.5, 130.4, 130.3, 129.8, 122.4, 121.8, 115.2, 112.2, 43.6, 41.3, 22.7.

HRMS (ESI) calcd (M+H) $^+$: 596.9211, found: 592.9200.

(E)-3-(2-(1H-tetrazol-5-yl)ethyl)-5-(5-chloro-1-(2,6-dichlorobenzyl)-2-oxoindolin-3-ylidene)-2-thioxothiazolidin-4-one, RBPI-6

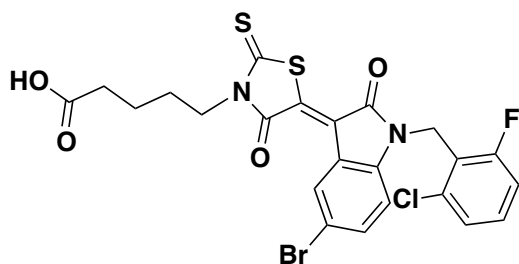


^1H NMR (DMSO- d_6): δ 8.87 (d, 1H, $J = 2$ Hz), 7.56 (m, 3H), 7.42 (t, 1H, $J = 7.5$ Hz), 7.01 (d, 1H, $J = 8.5$ Hz), 5.27 (s, 2H), 4.40 (t, 2H, $J = 7.5$ Hz), 3.27 (t, 2H, $J = 7.5$ Hz).

^{13}C NMR (DMSO- d_6): δ 197.4, 167.3, 166.8, 155.0, 143.9, 136.0, 135.2, 132.7, 131.5, 130.4, 129.8, 127.6, 127.5, 122.7, 121.3, 111.9, 43.1, 41.3, 22.0.

HRMS (ESI) calcd (M+H) $^+$ for $\text{C}_{21}\text{H}_{13}\text{Cl}_3\text{N}_6\text{O}_2\text{S}_2$, 550.9685; found, 550.9683.

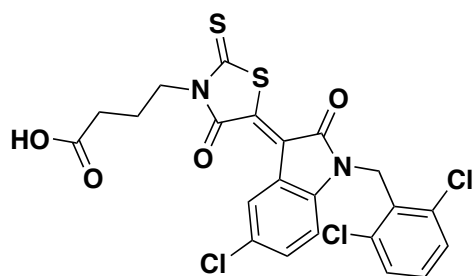
(E)-5-(5-(5-bromo-1-(2-chloro-6-fluorobenzyl)-2-oxoindolin-3-ylidene)-4-oxo-2-thioxothiazolidin-3-yl)pentanoic acid, RBPI-7



^1H NMR (DMSO- d_6): δ 9.04 (s, 1H), 7.68 (d, 1H, $J = 8.4$ Hz), 7.41 (dd, 1H, $J = 7.9$ Hz, $J = 14.2$ Hz), 7.36 (d, 1H, $J = 7.9$ Hz), 7.24 (t, 1H, $J = 9.0$ Hz), 7.00 (d, 1H, $J = 8.4$ Hz), 5.14 (s, 2H), 4.03 (t, 2H, $J = 7.1$ Hz), 2.24 (t, 2H, $J = 7.1$ Hz), 1.66 (td, 2H, $J = 7.4$ Hz, $J = 14.4$ Hz), 1.54 (td, 2H, $J = 7.0$ Hz, $J = 14.2$ Hz)

HRMS (ESI) calcd (M+H) $^+$ for $\text{C}_{23}\text{H}_{18}\text{BrClFN}_2\text{O}_4\text{S}_2$ 582.0564; found 582.9570

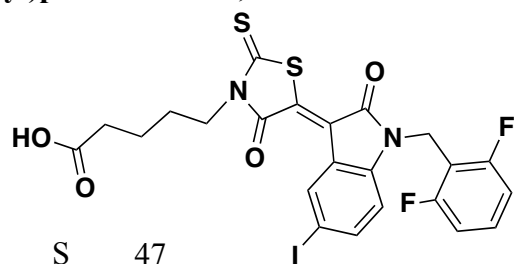
(E)-4-(5-(5-chloro-1-(2,6-dichlorobenzyl)-2-oxoindolin-3-ylidene)-4-oxo-2-thioxothiazolidin-3-yl)butanoic acid, RBPI-8



^1H NMR (DMSO- d_6): δ 8.89 (s, 1H), 7.51 (d, 3H, $J = 8.1$ Hz), 7.39 (t, 1H, $J = 8.1$ Hz), 6.97 (s, 1H), 5.23 (s, 2H), 4.08 (t, 2H, $J = 7.0$ Hz), 2.32 (t, 2H, $J = 7.5$ Hz), 1.88 (m, 2H)

HRMS (ESI) calcd (M+H) $^+$ for $\text{C}_{22}\text{H}_{16}\text{Cl}_3\text{N}_2\text{O}_4\text{S}_2$ 540.9617; found 540.9608

(E)-5-(5-(1-(2,6-difluorobenzyl)-5-iodo-2-oxoindolin-3-ylidene)-4-oxo-2-thioxothiazolidin-3-yl)pentanoic acid, RBPI-9



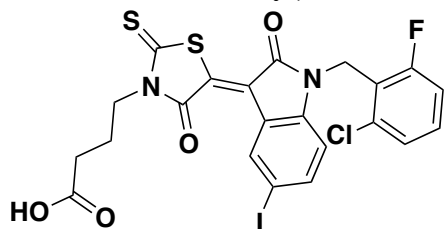
^1H NMR (DMSO- d_6): δ 12.03 (s, 1H), 9.23 (d, 1H, $J = 1.5$ Hz), 7.85 (dd, 1H, $J = 8.5$, 1.5 Hz), 7.44 (quin, 1H, $J = 6.5$ Hz), 7.12 (t, 1H, $J = 8$ Hz), 6.96 (d, 1H, $J = 8.5$ Hz), 5.09 (s, 2H), 4.06 (t, 2H, $J = 7$ Hz), 2.26 (t, 2H, J

= 7 Hz), 1.68 (quin, 2H, $J = 6.5$ Hz), 1.56 (quin, 2H, $J = 7$ Hz)

^{13}C NMR (DMSO- d_6): δ 197.6, 174.9, 167.5, 166.4, 161.6 (dd, $J = 247$, 6 Hz), 144.3, 141.3, 136.1, 134.9, 131.6 (t, $J = 11$ Hz), 122.4, 122.1, 112.7, 112.5 (t, $J = 6$ Hz), 111.4 (t, $J = 18$ Hz), 86.7, 44.6, 33.9, 33.2, 26.7, 22.4

HRMS (ESI) calcd (M+H) $^+$ for $\text{C}_{23}\text{H}_{18}\text{IF}_2\text{N}_2\text{O}_4\text{S}_2$ 614.9721; found 614.9719

(E)-4-(5-(1-(2-chloro-6-fluorobenzyl)-5-iodo-2-oxoindolin-3-ylidene)-4-oxo-2-thioxothiazolidin-3-yl)butanoic acid, RBPI-10

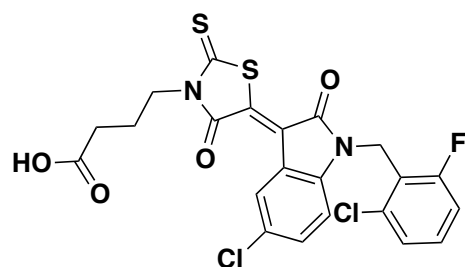


^1H NMR (DMSO- d_6): δ 9.18 (s, 1H), 7.79 (s, 1H), 7.41 (dt, 1H, $J = 6.1$ Hz, $J = 8.1$ Hz), 7.35 (d, 1H, $J = 8.0$ Hz), 7.24 (t, 1H, $J = 9.2$ Hz), 6.86 (d, 1H, $J = 8.3$ Hz), 5.12 (s, 1H), 4.09 (t, 2H, $J = 6.9$ Hz), 2.32 (t, 2H, $J = 7.3$ Hz), 1.88 (quin, 2H, $J = 7.1$ Hz)

^{13}C NMR (DMSO- d_6): δ 197.0, 173.8, 166.9, 166.0, 161.3 (d, $J = 249.7$), 142.9, 134.8, 134.3 (d, $J = 5.3$), 131.9, 131.0 (d, $J = 10.0$), 126.9, 126.8, 126.0 (d, $J = 2.8$), 121.7, 120.6, 120.4 (d, $J = 16.3$), 114.9 (d, $J = 22.4$), 110.9, 43.6, 40.0, 39.8, 39.8, 39.7, 39.5, 39.3, 39.2, 39.0, 36.5 (d, $J = 1.8$, 1H), 30.9, 22.02

HRMS (ESI) calcd (M+H) $^+$ for $\text{C}_{22}\text{H}_{16}\text{IClFN}_2\text{O}_4\text{S}_2$ 616.9269; found 616.9256

(E)-4-(5-(5-chloro-1-(2-chloro-6-fluorobenzyl)-2-oxoindolin-3-ylidene)-4-oxo-2-thioxothiazolidin-3-yl)butanoic acid, RBPI-11

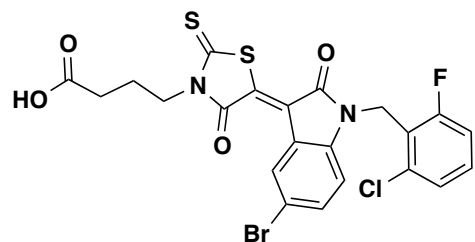


^1H NMR (DMSO- d_6): δ 8.89 (s, 1H), 7.55 (s, 1H), 7.41 (dt, 1H, $J = 6.1$ Hz, $J = 8.1$ Hz), 7.36 (d, 1H, $J = 7.9$ Hz), 7.24 (t, 1H, $J = 9.2$ Hz), 7.05 (s, 1H), 5.15 (s, 2H), 4.09 (t, 2H, $J = 6.9$ Hz), 2.32 (t, 2H, $J = 7.4$ Hz), 1.88 (quin, 2H, $J = 7.0$ Hz)

^{13}C NMR (DMSO- d_6): δ 197.0, 173.8, 166.9, 166.0, 161.3 (d, $J = 249.7$), 142.9, 134.8, 134.3 (d, $J = 5.3$), 131.9, 131.0 (d, $J = 10.0$), 126.9, 126.8, 126.0 (d, $J = 2.8$), 121.7, 120.6, 120.4 (d, $J = 16.3$), 114.9 (d, $J = 22.4$), 110.9, 43.6, 40.0, 39.8, 39.8, 39.7, 39.5, 39.3, 39.2, 39.0, 36.5 (d, $J = 1.8$, 1H), 30.9, 22.02

HRMS (ESI) calcd (M+H) $^+$ for $\text{C}_{22}\text{H}_{16}\text{Cl}_2\text{FN}_2\text{O}_4\text{S}_2$ 524.9913; found 524.9924

(E)-4-(5-(5-bromo-1-(2-chloro-6-fluorobenzyl)-2-oxoindolin-3-ylidene)-4-oxo-2-thioxothiazolidin-3-yl)butanoic acid, RBPI-12



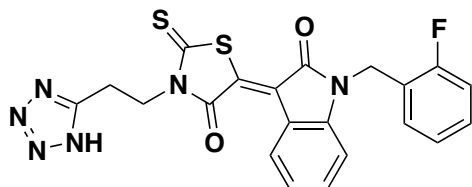
^1H NMR (DMSO- d_6): δ 12.12 (bs, 1H), 9.05 (s, 1H), 7.69 (d, 1H, $J = 8.5$ Hz), 7.42 (m, 1H), 7.37 (d, 1H, $J = 8$ Hz), 7.26 (t, 1H, $J = 9$ Hz), 7.02 (d, 1H, $J = 8.5$ Hz), 5.16 (s, 2H), 4.10 (t, 2H, $J = 7$ Hz), 2.34 (t, 2H, $J = 7.5$ Hz), 1.90 (m, 2H).

^{13}C NMR (DMSO- d_6): δ 197.7, 174.5, 167.6, 166.7, 162.0 (d, $J = 249$ Hz), 144.0, 135.4, 134.9 (d, $J = 5.5$ Hz), 131.6 (d, $J = 10.0$ Hz), 130.4, 126.6 (d, $J = 3.6$ Hz), 122.3, 121.7, 121.1 (d, $J = 16$ Hz), 155.6 (d, $J = 22$ Hz), 115.2, 112.1, 44.3, 37.2,

31.6, 22.7.

HRMS (ESI) calcd (M+H)⁺ for C₂₂H₁₆BrClFN₂O₄S₂, 568.9407; found, 568.9416.

(E)-3-(2-(1H-tetrazol-5-yl)ethyl)-5-(1-(2-fluorobenzyl)-2-oxindolin-3-ylidene)-2-thioxothiazolidin-4-one, Inactive-2



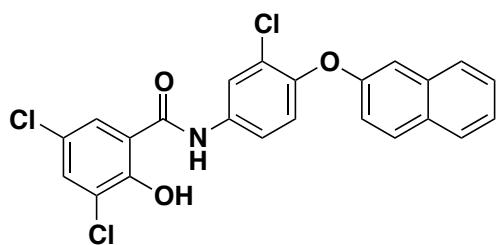
¹H NMR (DMSO-*d*₆): δ 8.80 (d, 1H, J = 8 Hz), 7.45 (t, 1H, J = 7.5 Hz), 7.34 (m, 1H), 7.27 (t, 1H, J = 7.5 Hz), 7.22 (t, 1H, J = 9 Hz), 7.15 (t, 2H, J = 7.5 Hz), 7.06 (d, 1H, J = 8 Hz), 5.07 (s, 2H), 4.40 (t, 2H, J = 7.5 Hz), 3.22 (t, 2H, J = 7 Hz).

¹³C NMR (DMSO-*d*₆): δ 197.8, 167.3, 167.2, 160.8 (d, J = 245 Hz), 145.1, 133.8, 132.9, 130.6 (d, J = 8 Hz), 130.1 (d, J = 5 Hz), 128.5, 125.5, 125.4, 124.6, 123.7, 123.1 (d, J = 15 Hz), 120.0, 116.3, 111.6, 42.5 (d, J = 4 Hz), 38.5, 21.4.

HRMS (ESI) calcd (M+H)⁺: 467.0760, found: 467.0754.

3,5-dichloro-N-(3-chloro-4-(naphthalen-2-yloxy)phenyl)-2-hydroxybenzamide, 6a

Prepared according to reported procedure (1).

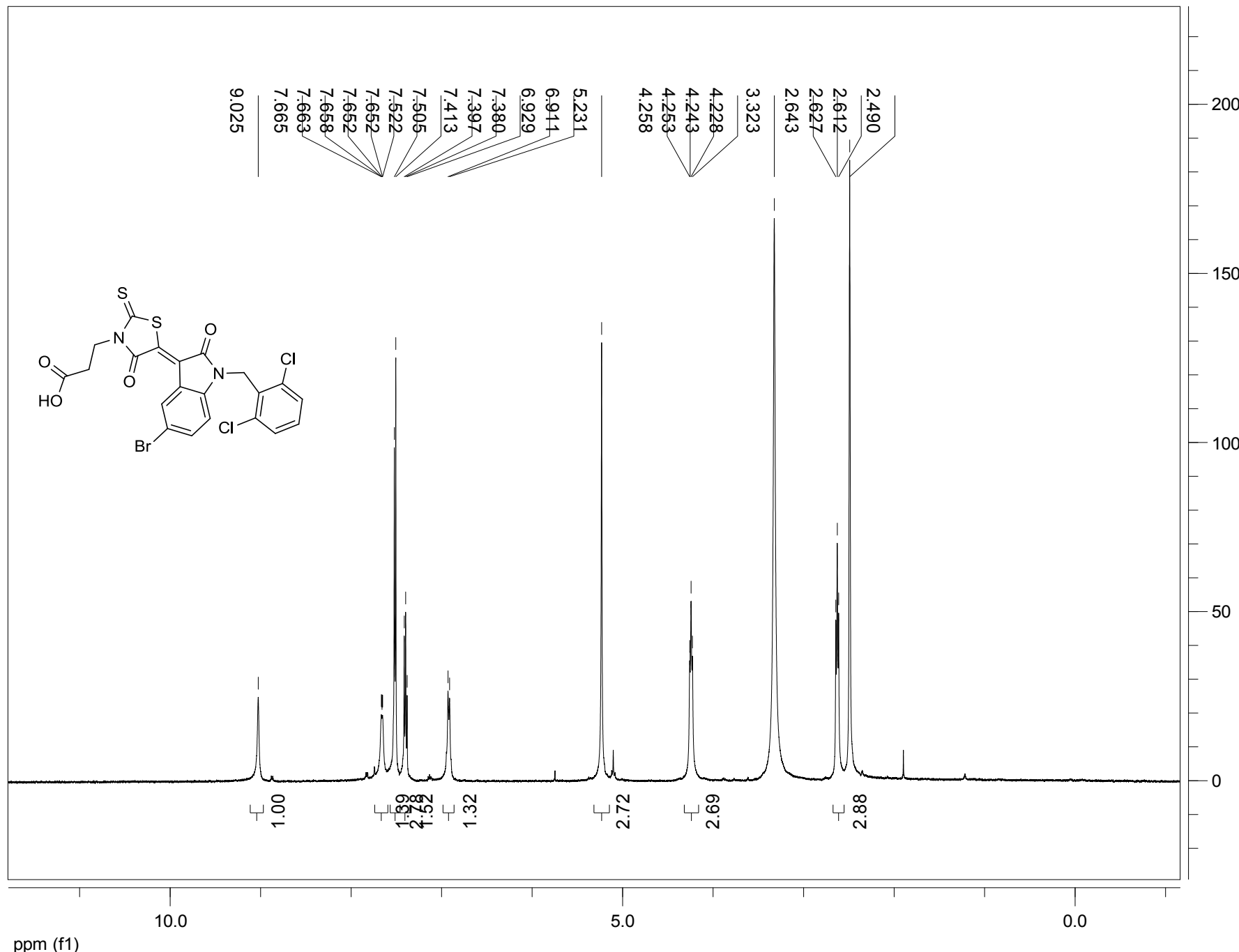


¹H NMR (DMSO-*d*₆): δ 12.42 (bs, 1H), 10.83 (bs, 1H), 8.07 (s, 2H), 7.99 (d, 1H, J = 9.0 Hz), 7.93 (d, 1H, J = 8.0 Hz), 7.83 (d, 1H, J = 11.5 Hz), 7.84 (s, 1H), 7.70 (dd, 1H, J = 9.0, 2.5 Hz), 7.50 (t, 1H, J = 7.5 Hz), 7.45 (t, 1H, J = 8.0 Hz), 7.33 (dd, 1H, J = 9.0, 2.0 Hz), 7.29 (d, 1H, J = 9.0 Hz), 7.26 (d, 1H, J = 2.0 Hz).

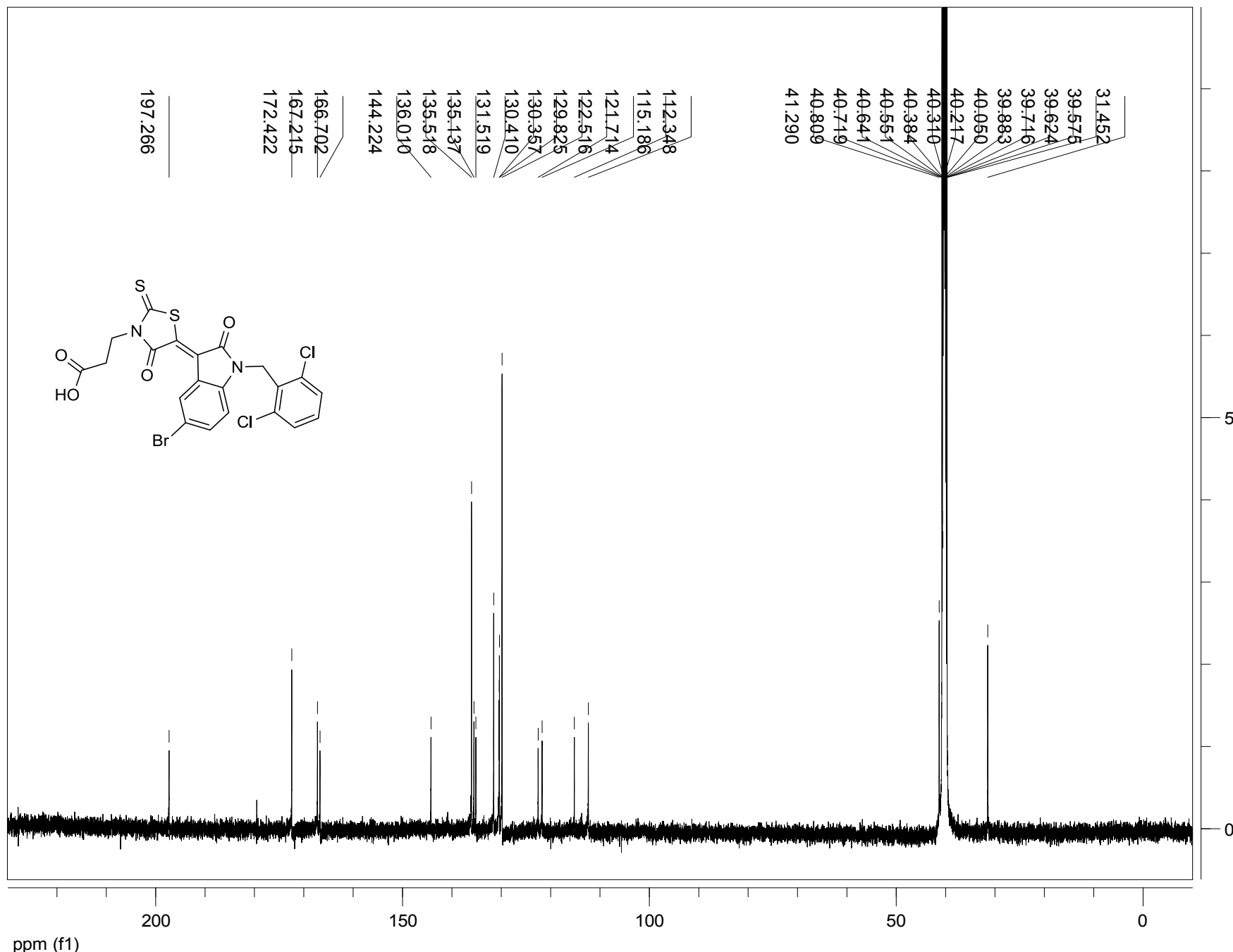
HRMS (ESI) calcd (M+H)⁺ for C₂₃H₁₄Cl₃NO₃, 458.0118; found, 458.0125.

1. Steffen JD, Coyle DL, Damodaran K, Beroza P, & Jacobson MK (2011) Discovery and Structure-Activity Relationships of Modified Salicylanilides as Cell Permeable Inhibitors of Poly(ADP-ribose) Glycohydrolase (PARG). *J Med Chem* 54:5403-5413.

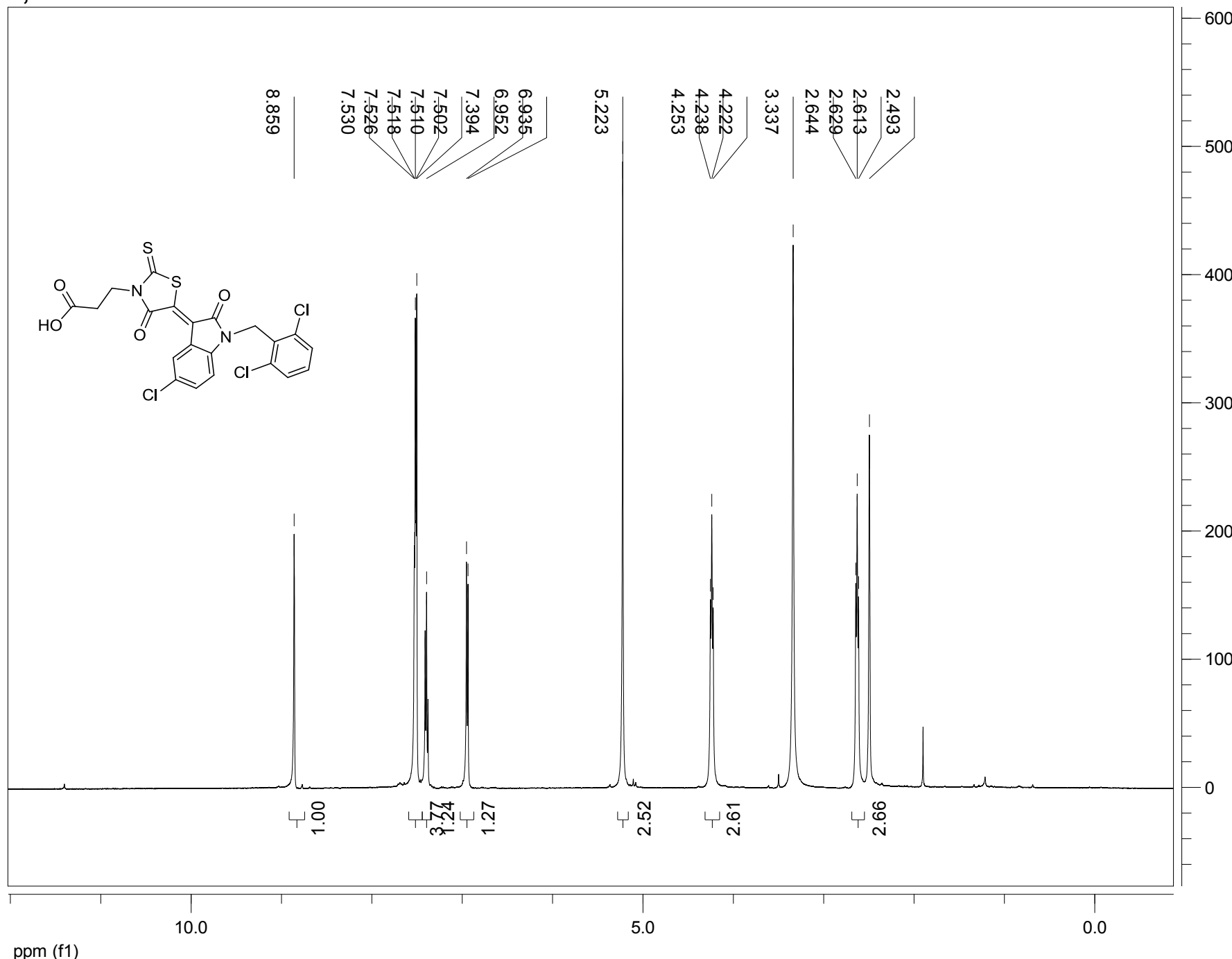
RBPI-2; 1H



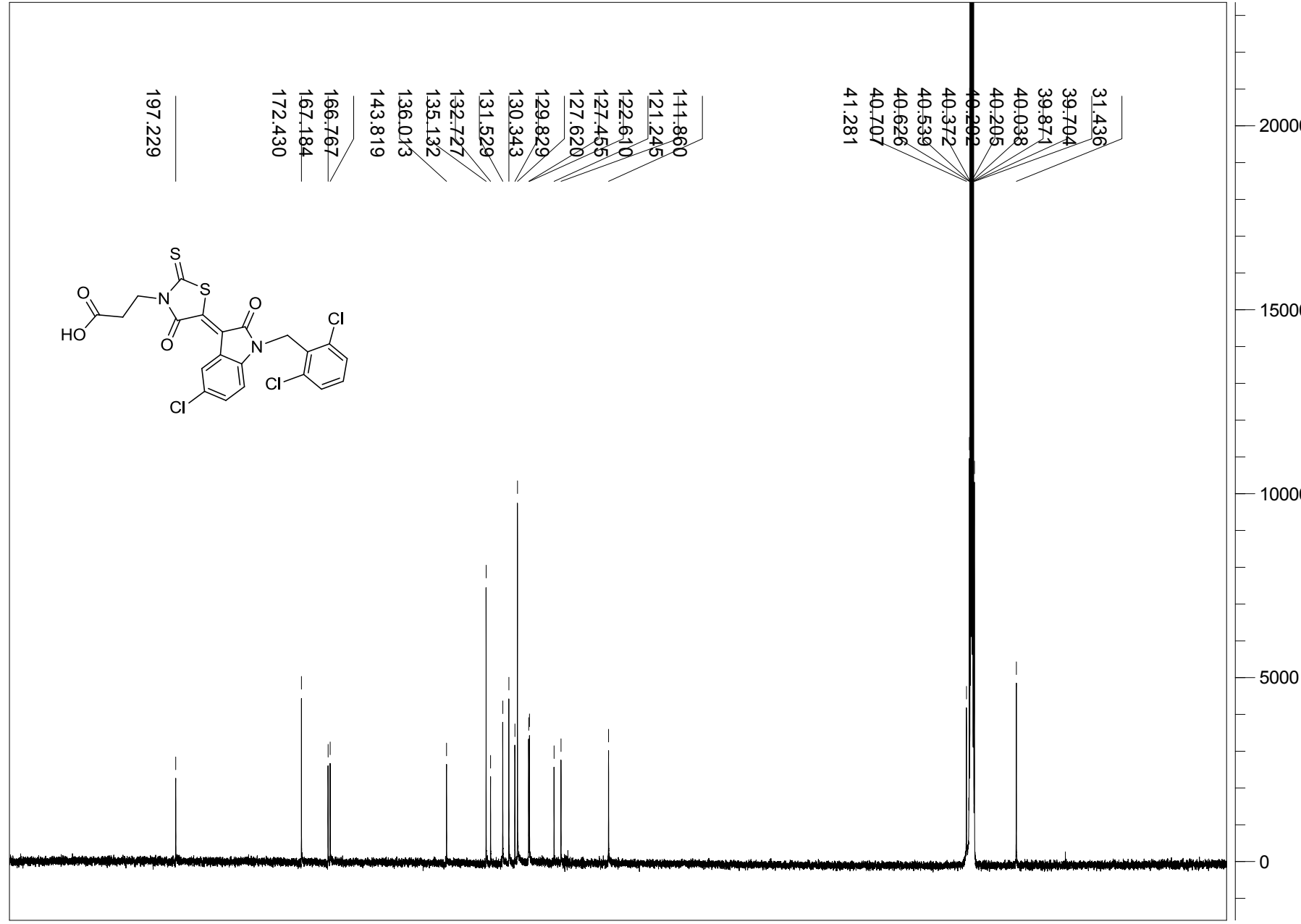
RBPI-2; 13C



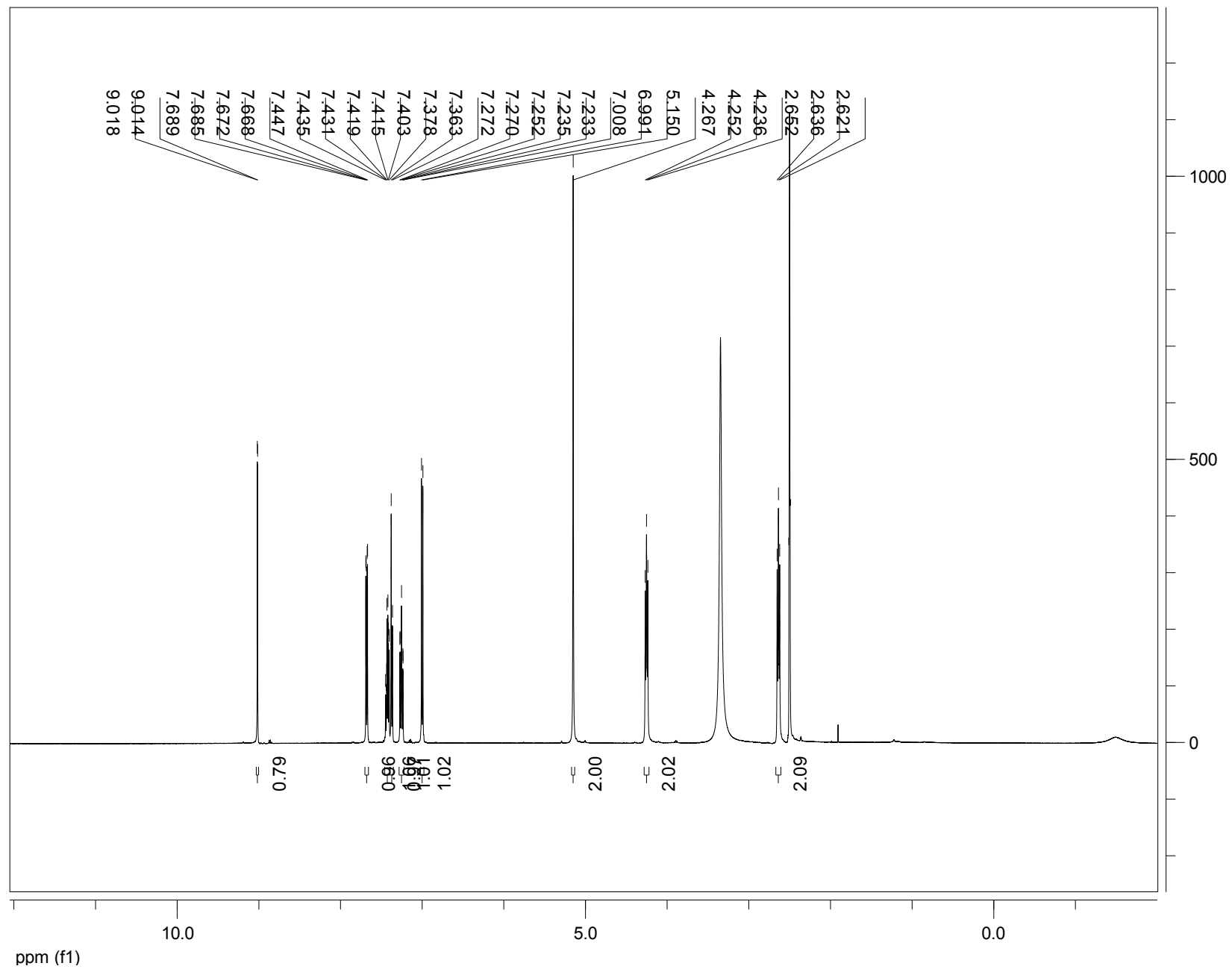
RBPI-3; 1H



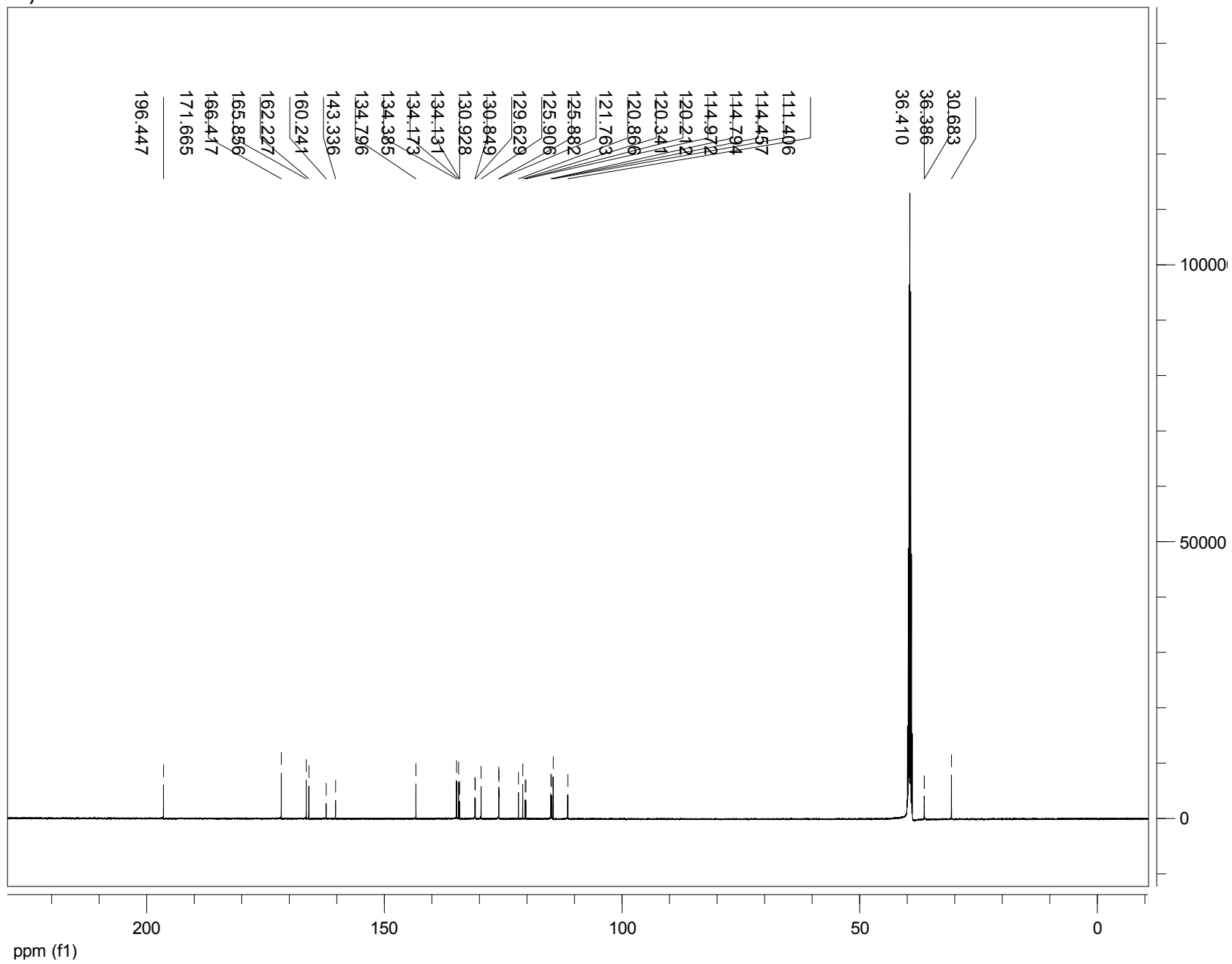
RBPI-3; 13C



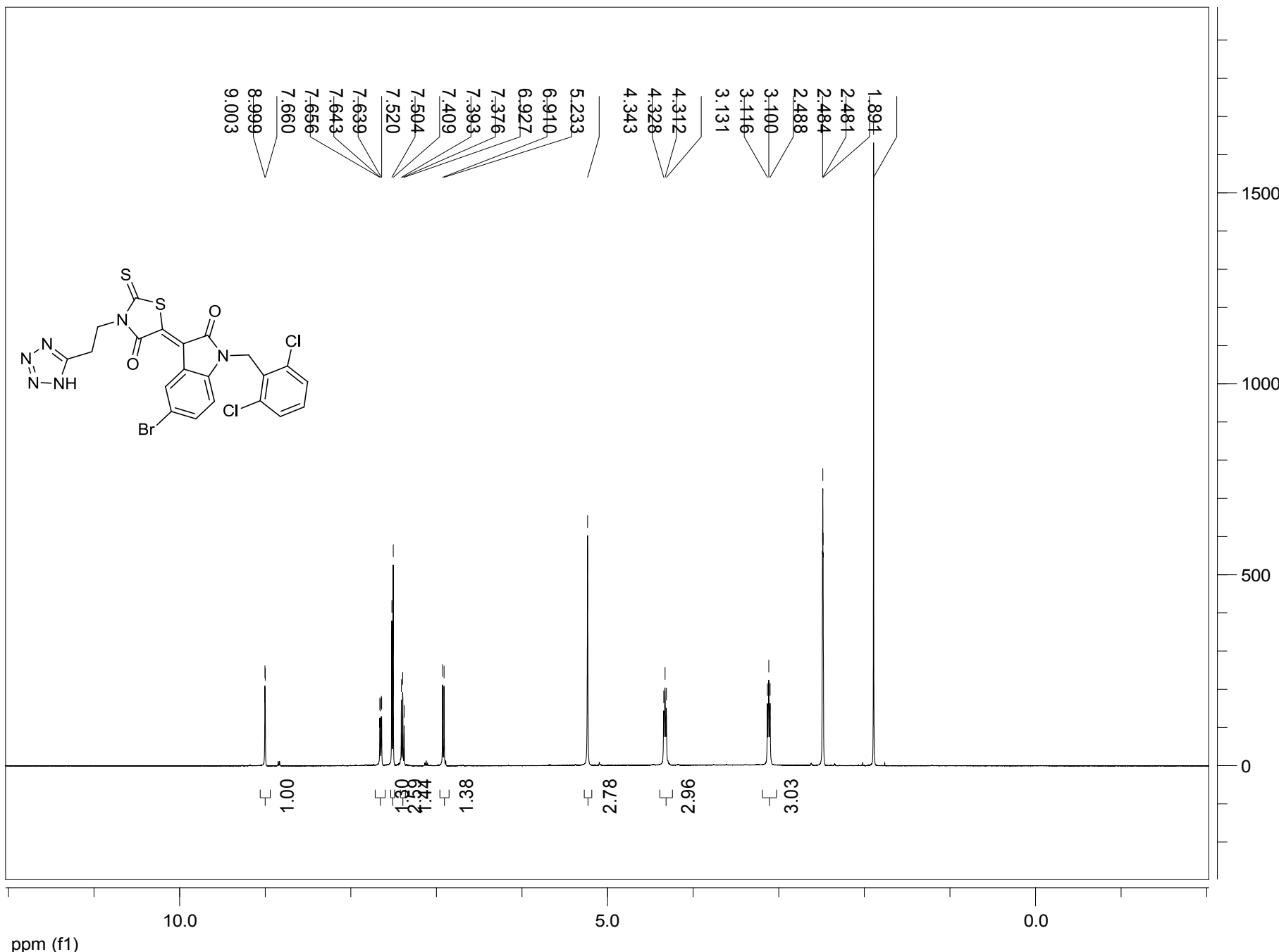
RBPI-4; 1H



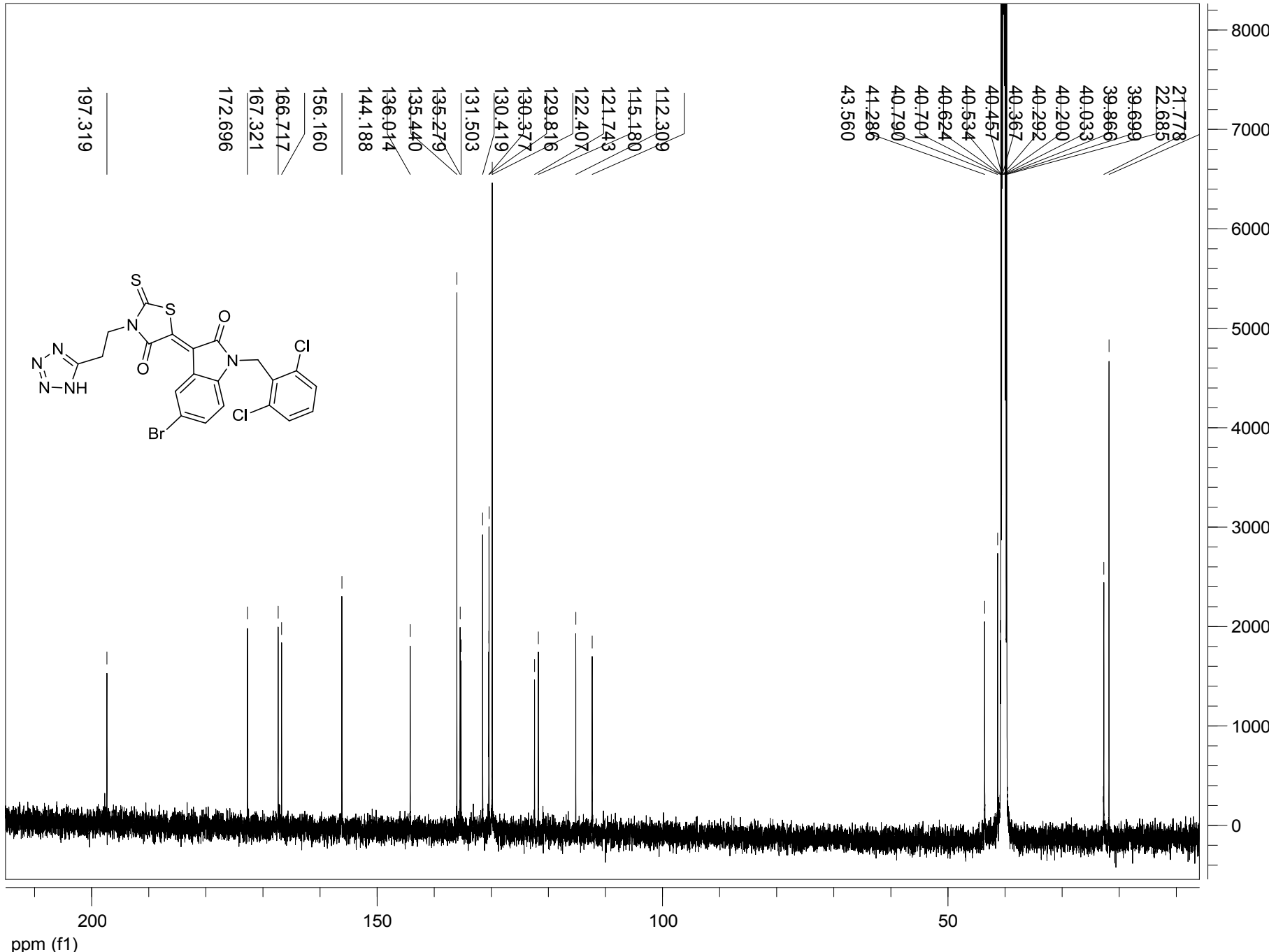
RBPI-4; 13C



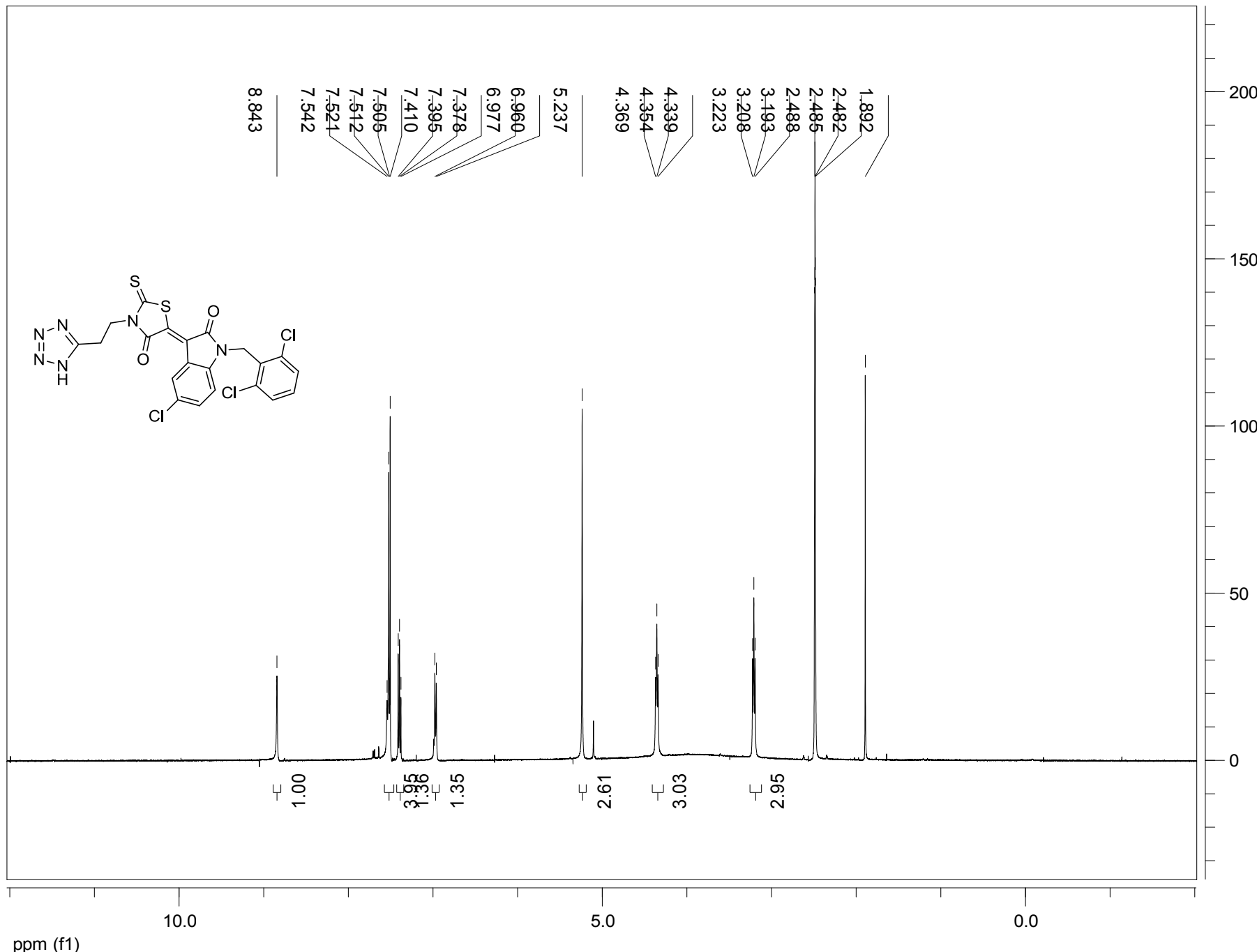
RBPI-5; 1H



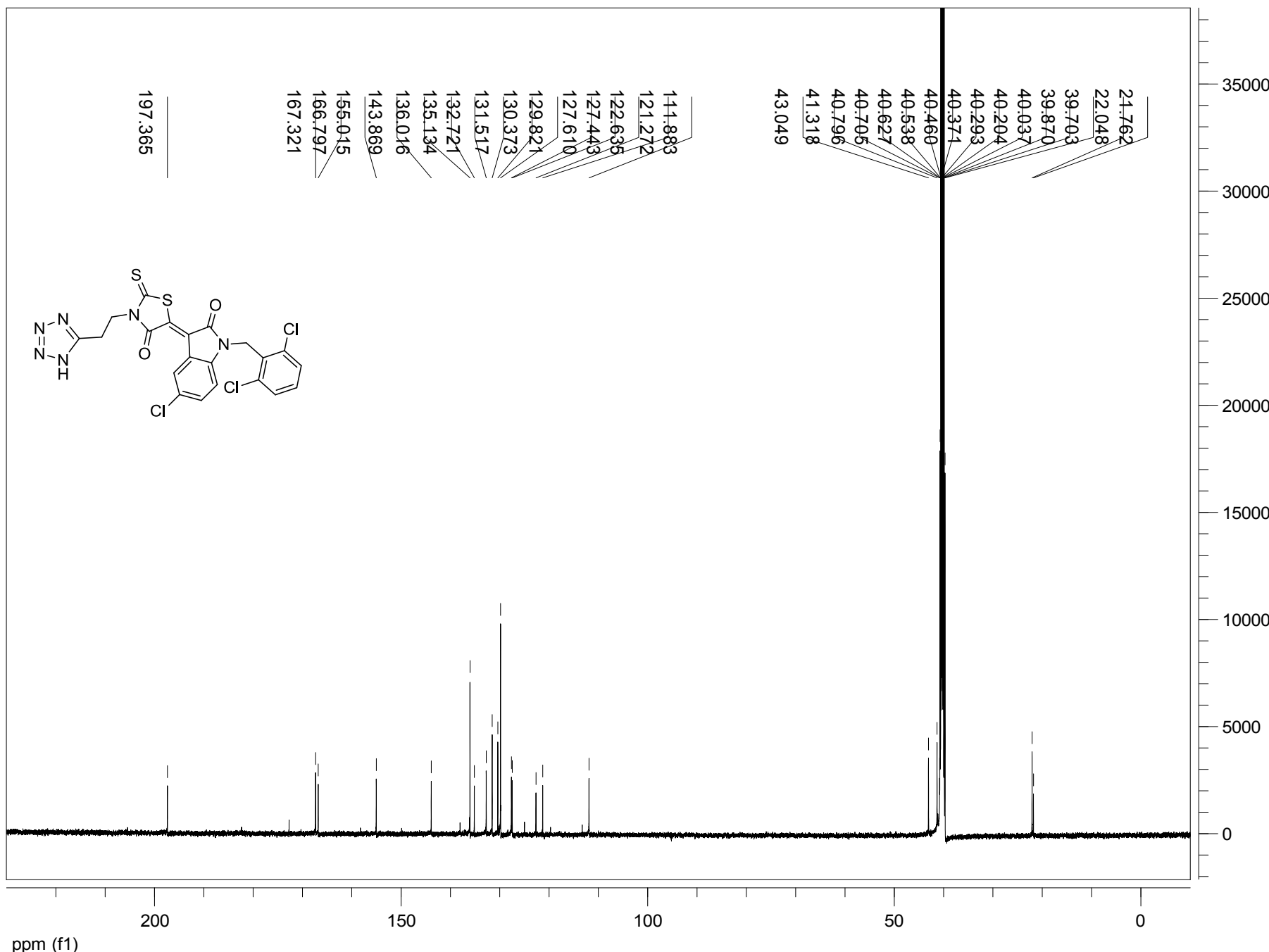
RBPI-5; 13C



RBPI-6; 1H



RBPI-6; 13C

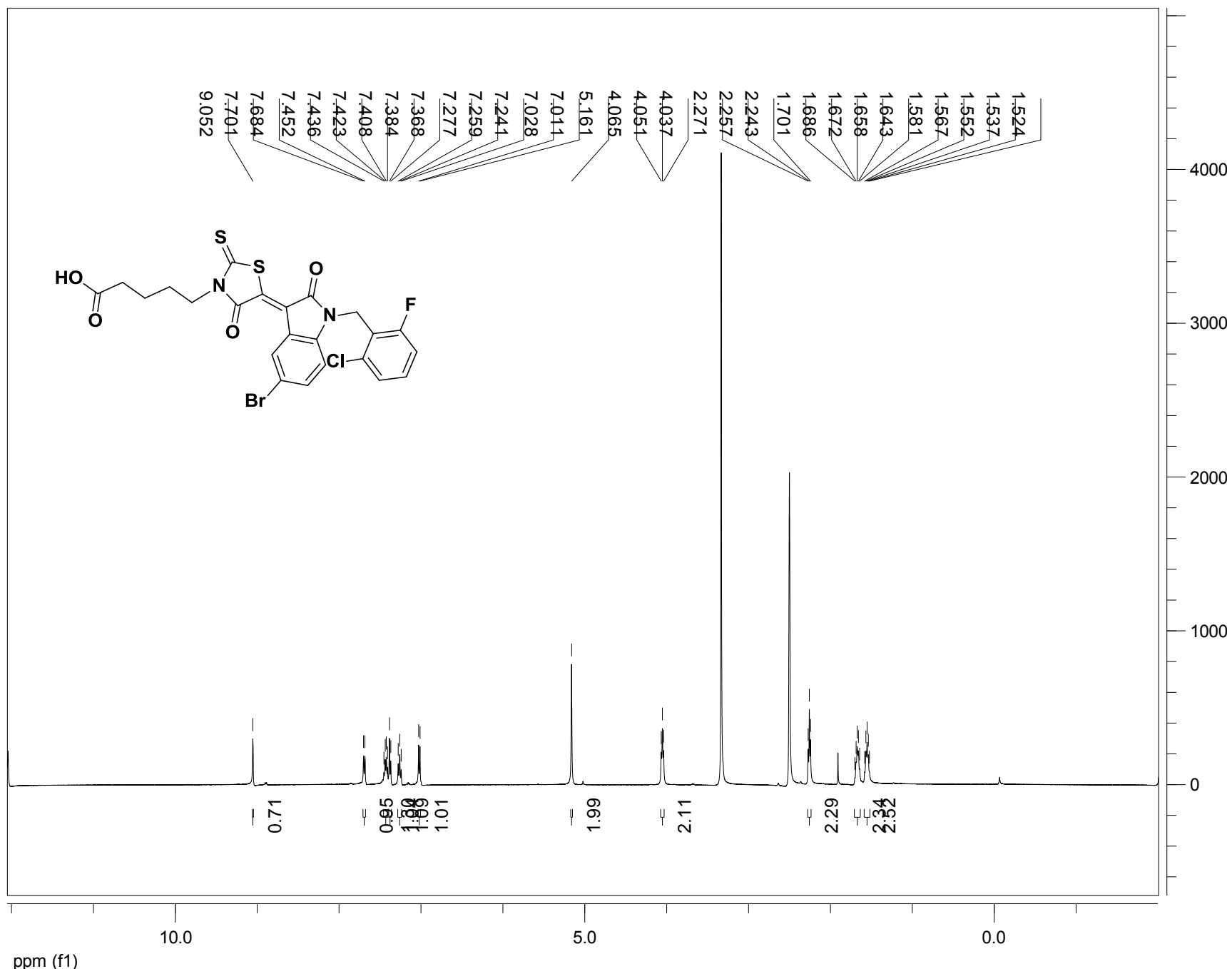


21.762
22.048
39.703
39.870
40.037
40.204
40.293
40.371
40.460
40.538
40.627
40.705
40.796
41.318
43.049

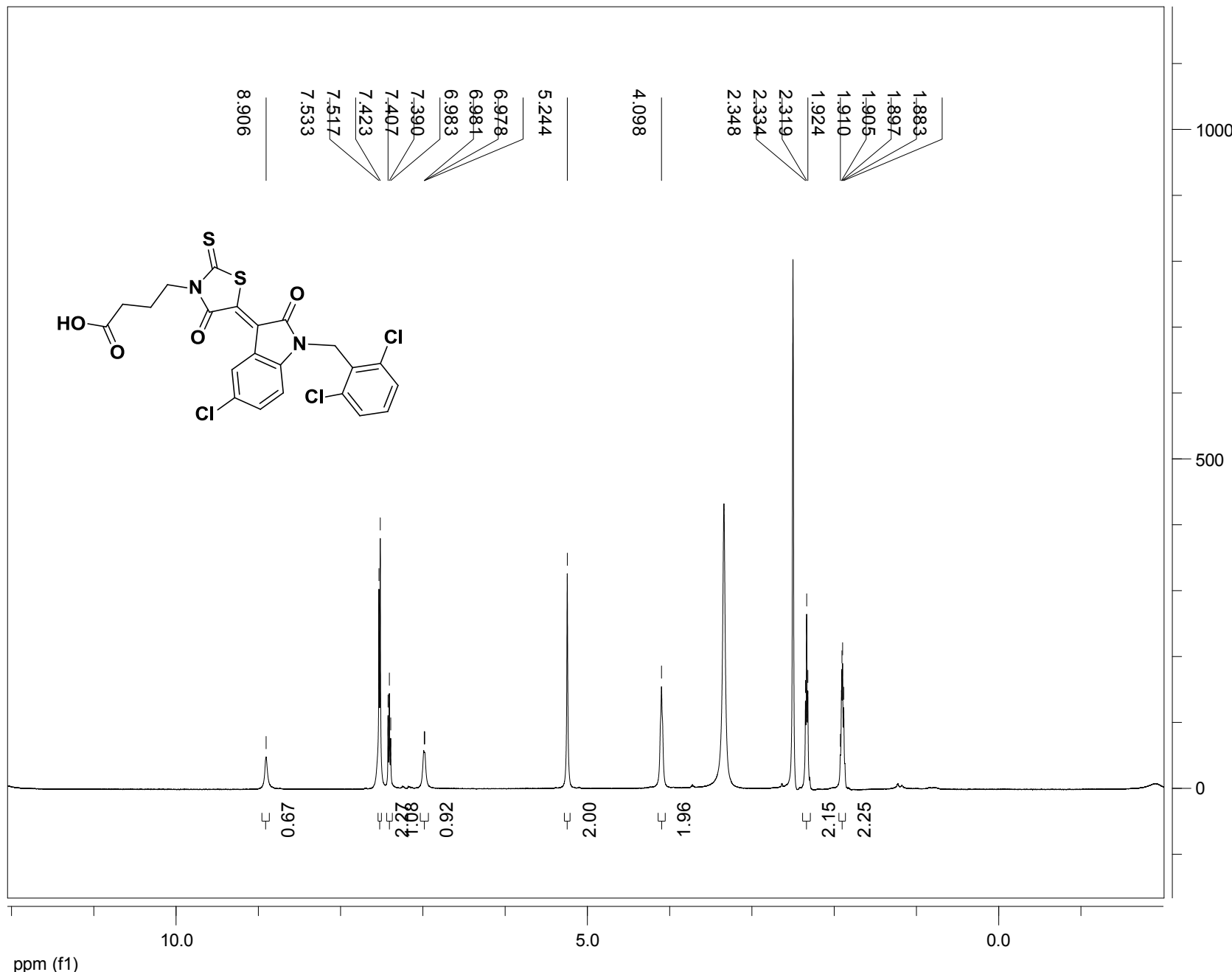
114.883
121.272
122.635
127.443
127.610
129.821
130.373
131.517
132.721
135.134
136.016
143.869
155.015
166.797
167.321

197.365

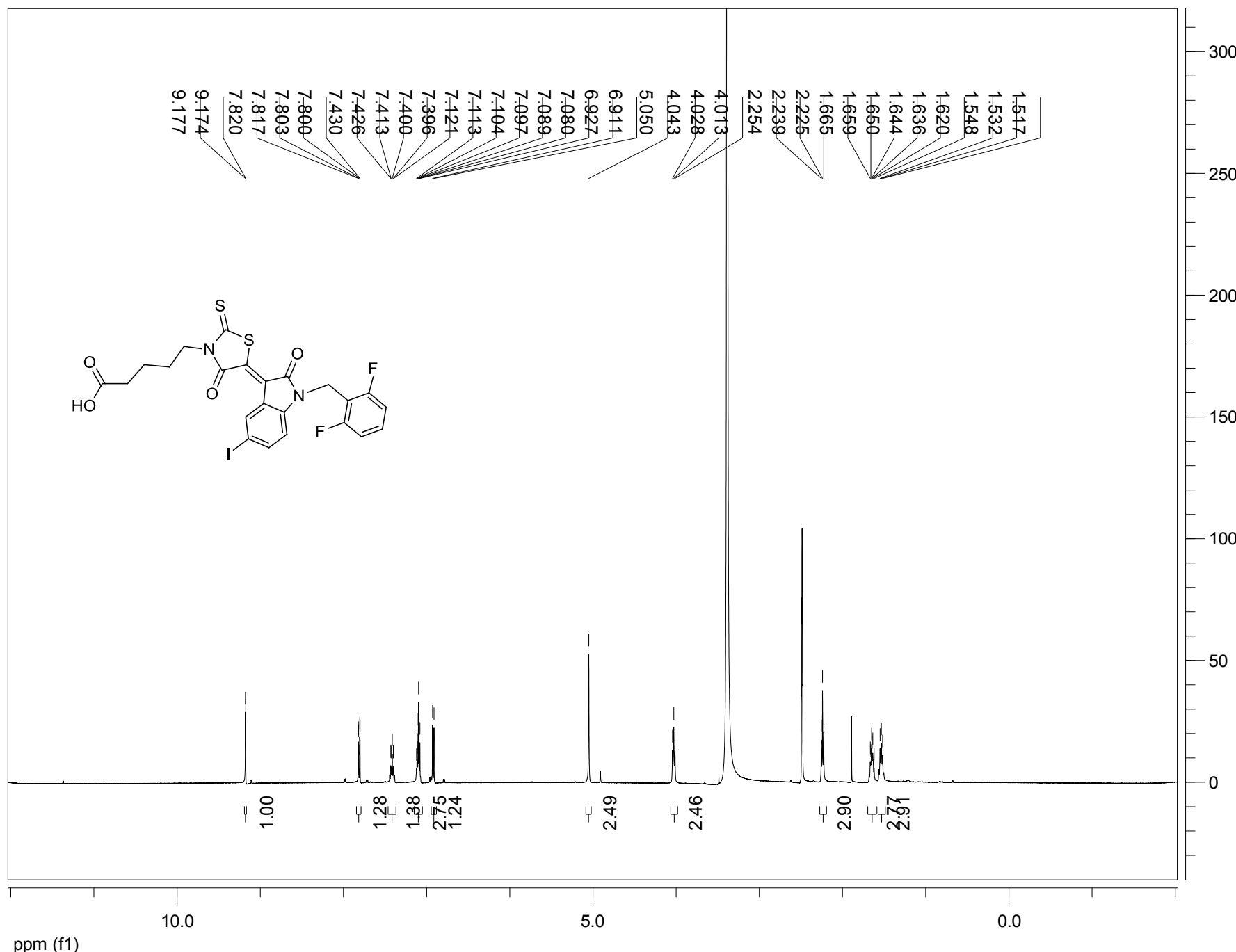
RBPI-7; 1H



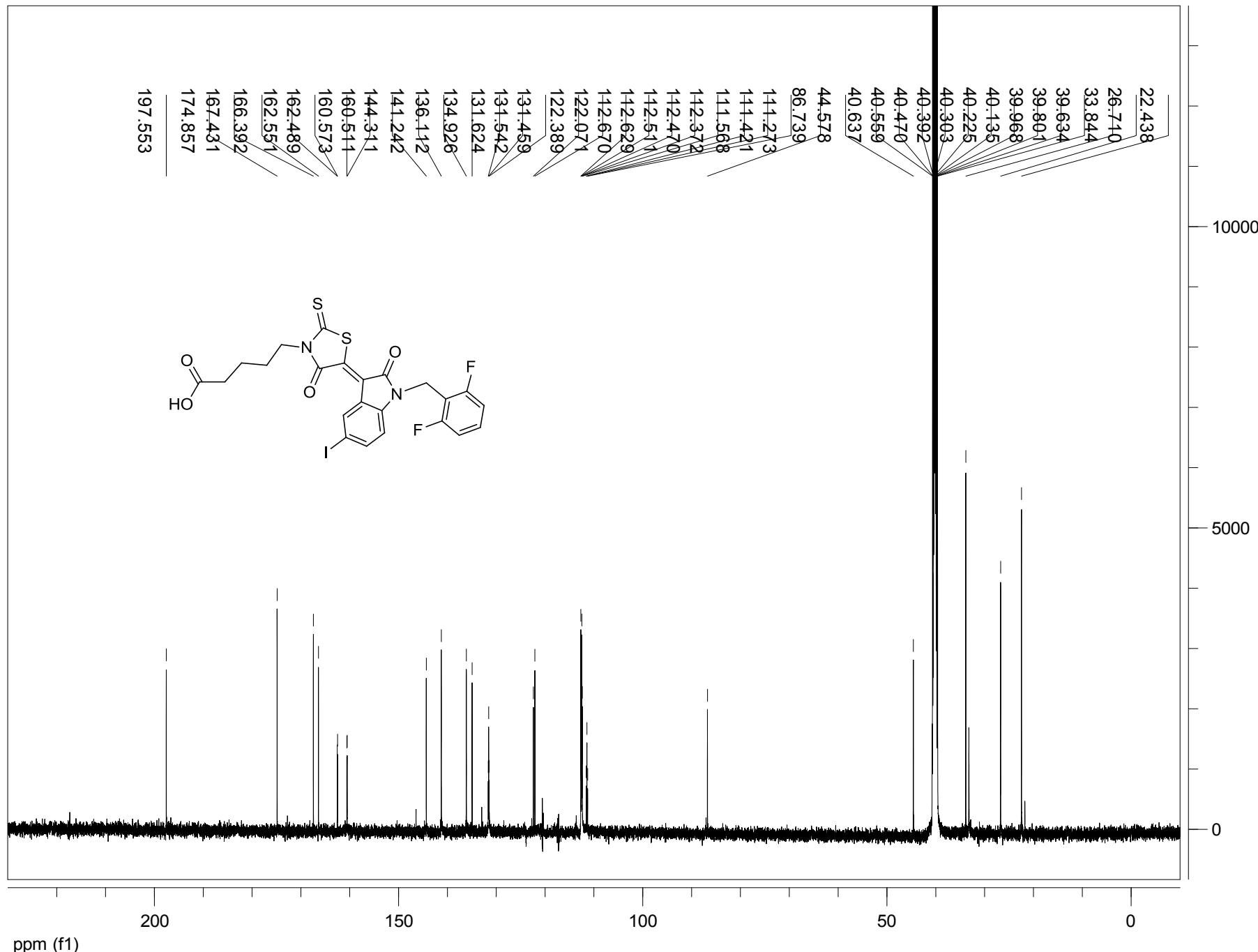
RBPI-8; 1H



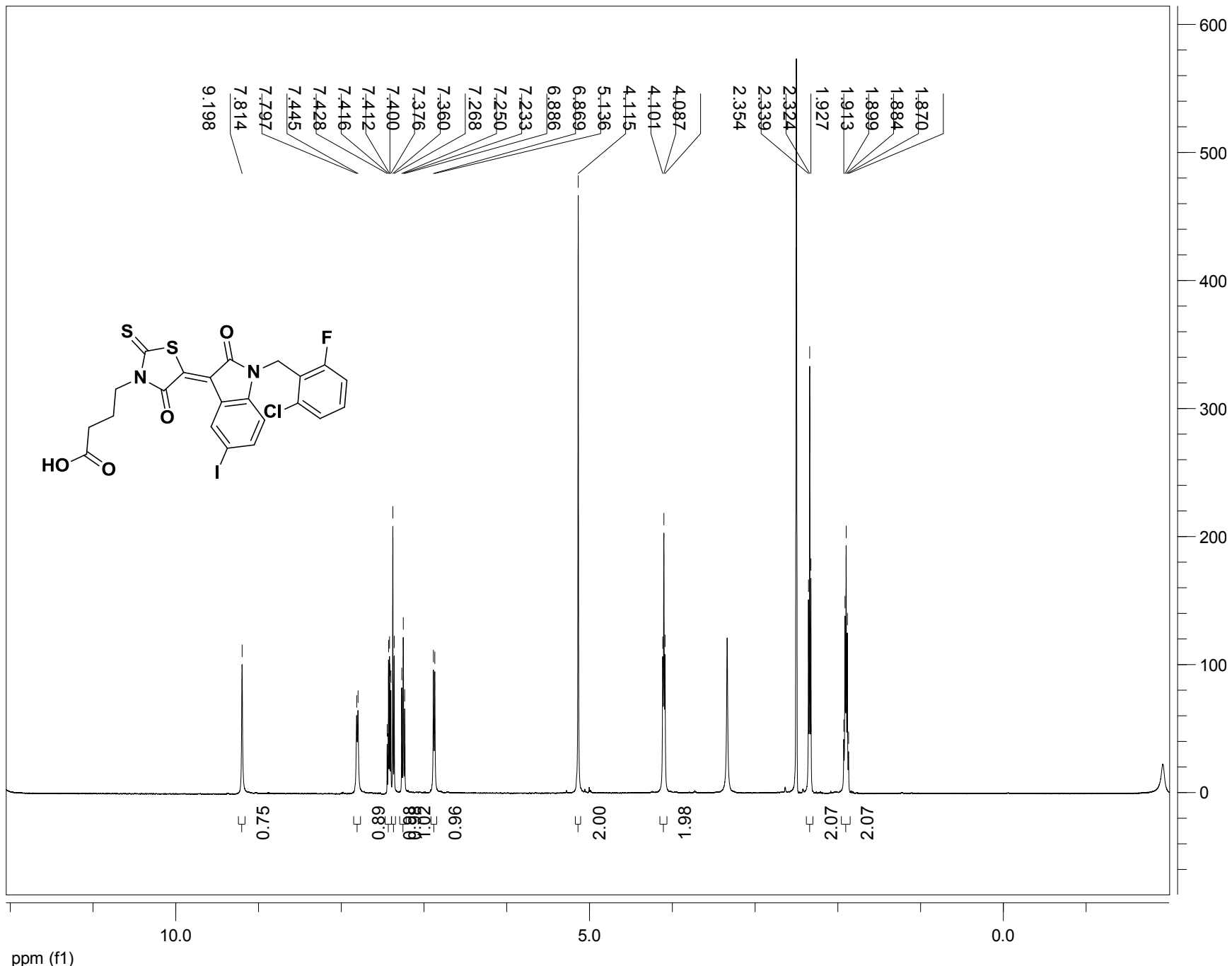
RBPI-9; 1H



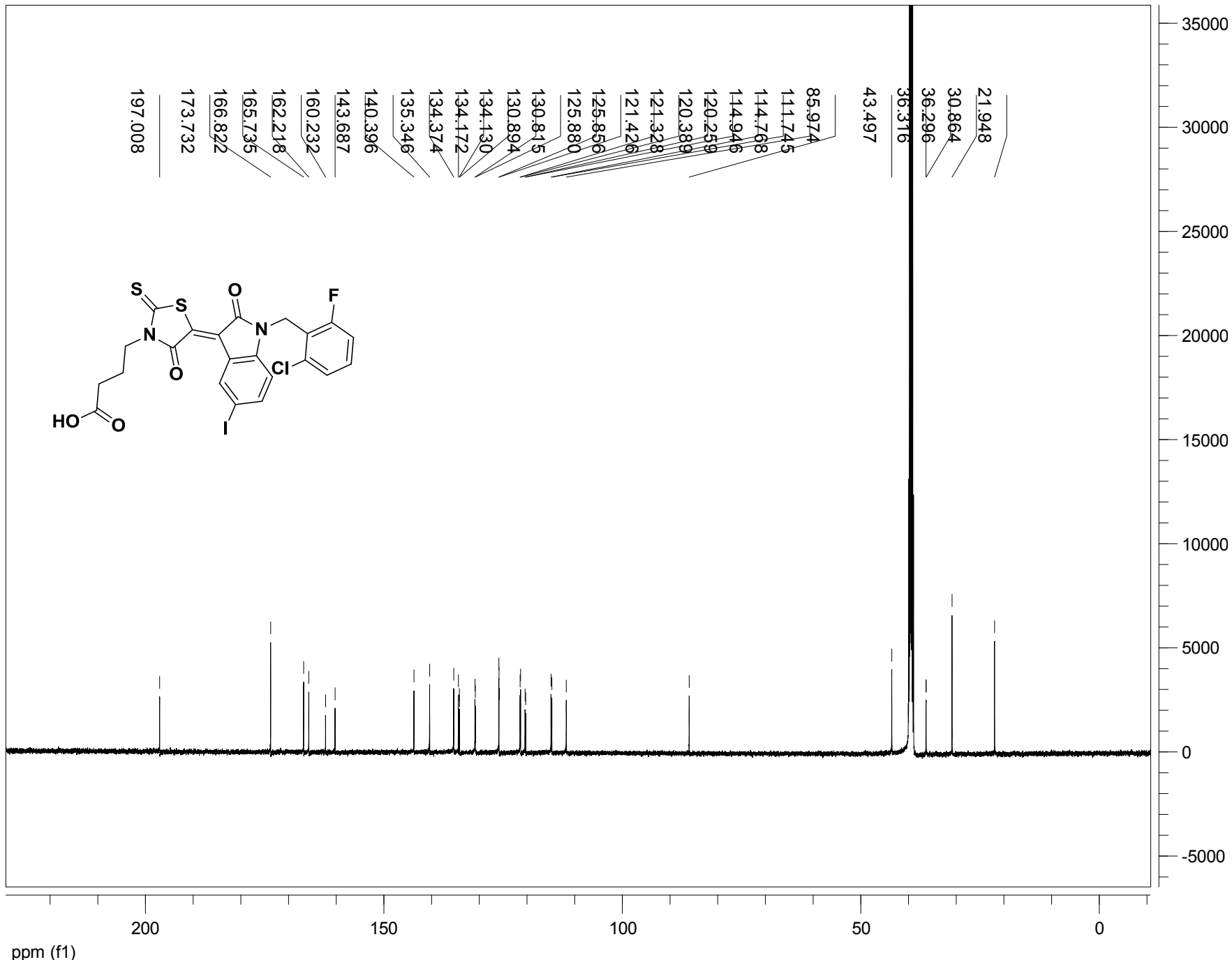
RBPI-9; 13C



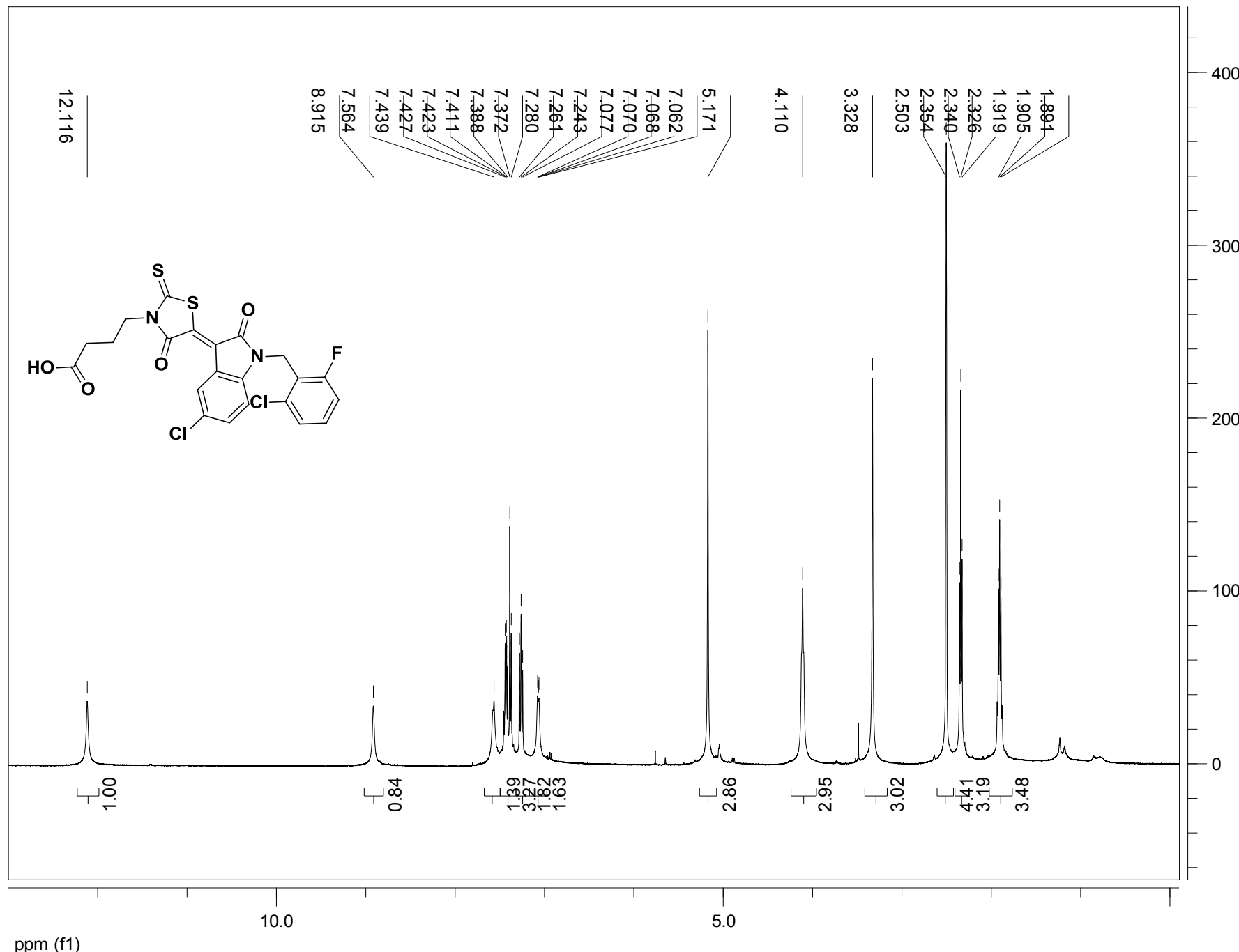
RBPI-10; 1H



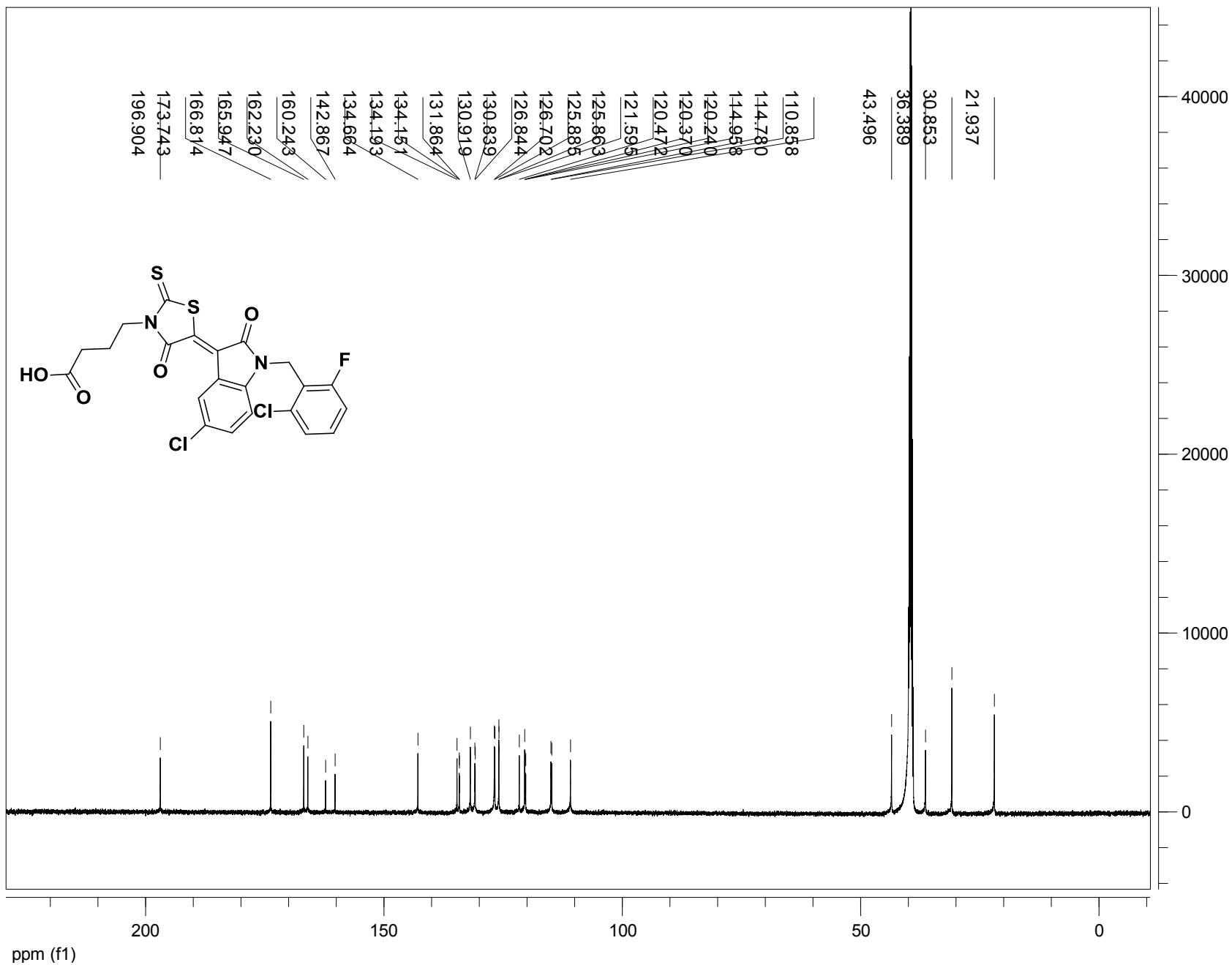
RBPI-10; 13C



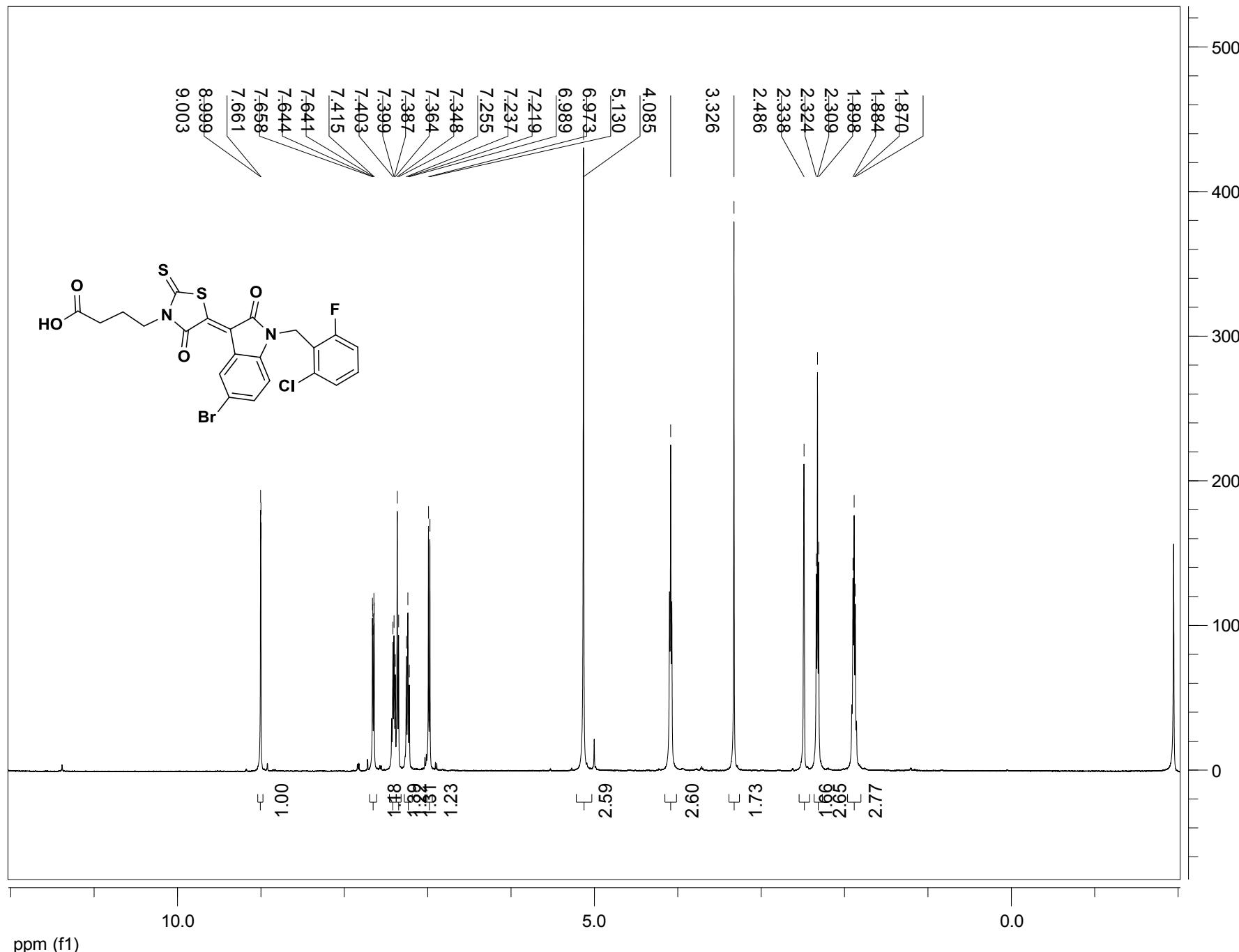
RBPI-11; 1H



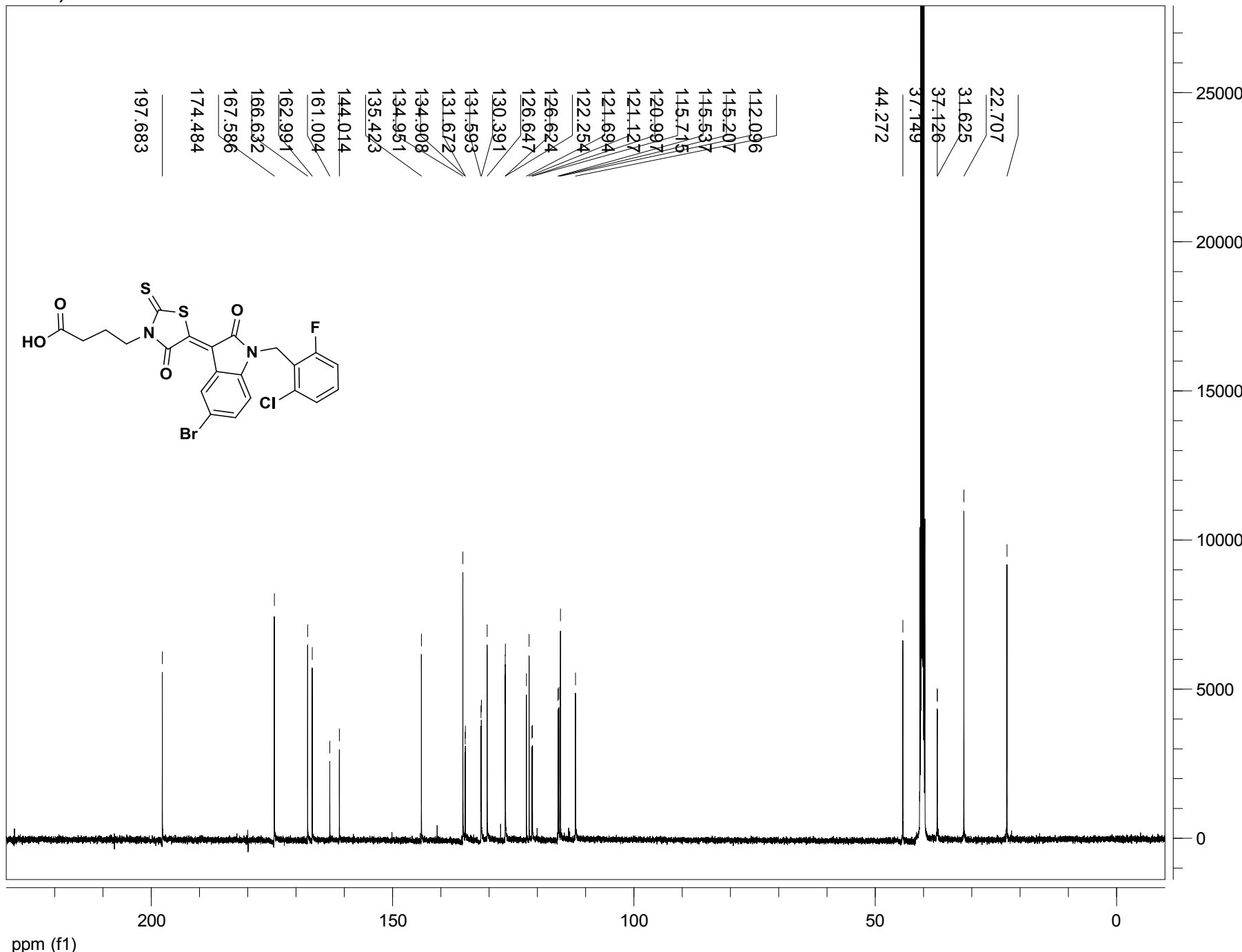
RBPI-11; 13C



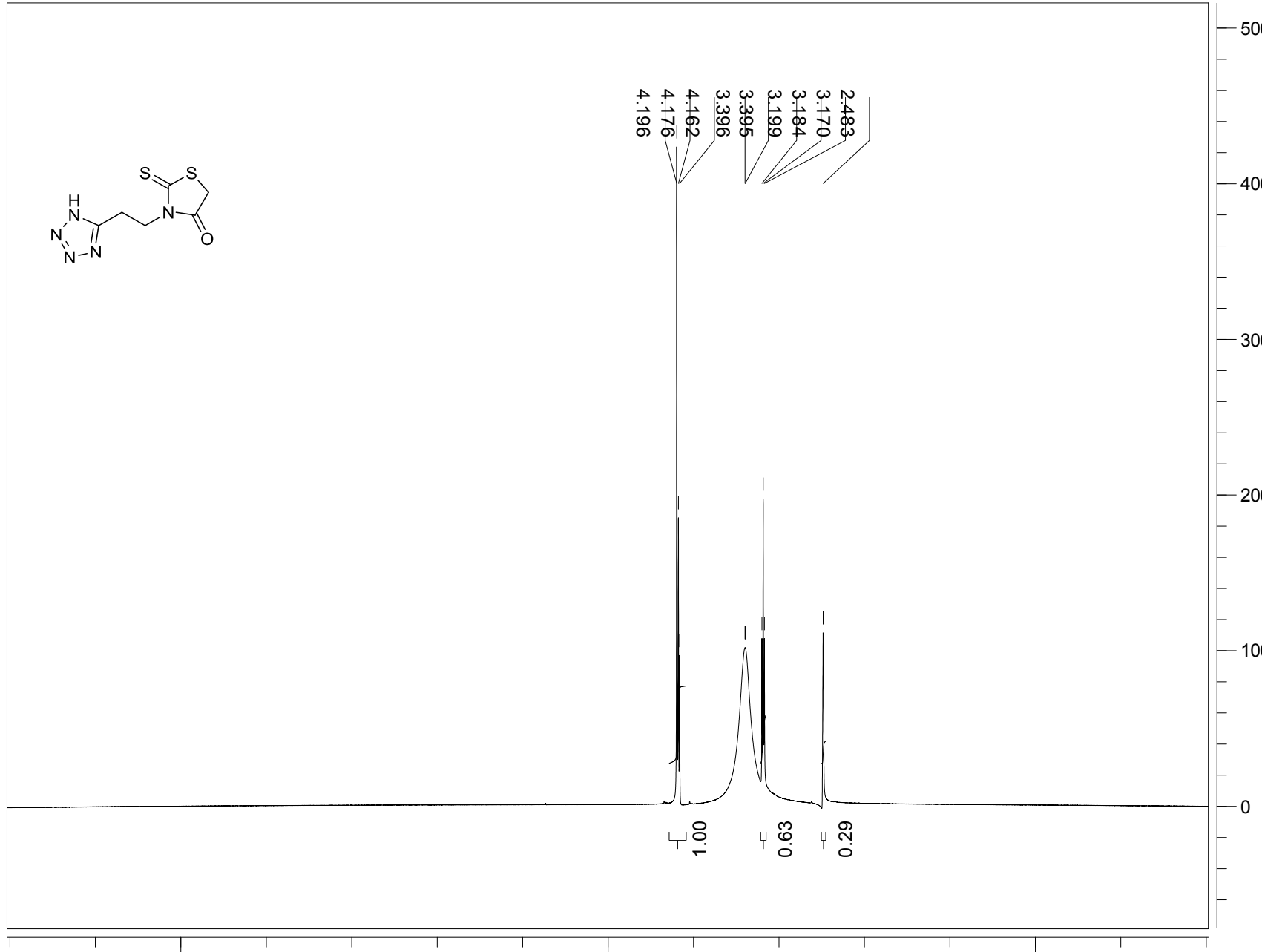
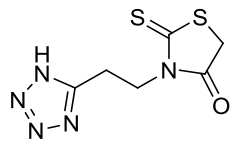
RBPI-12; 1H



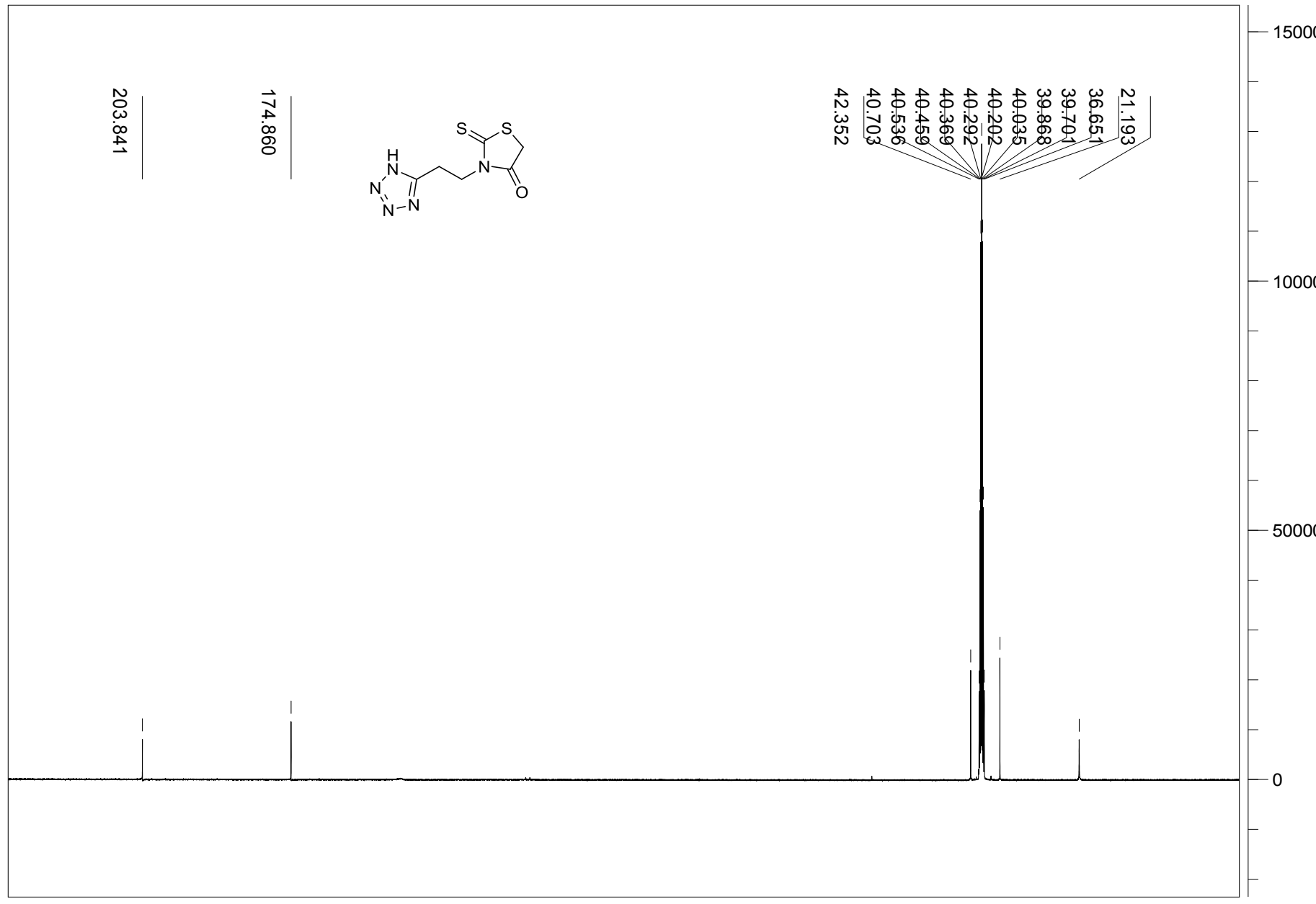
RBPI-12; 3C



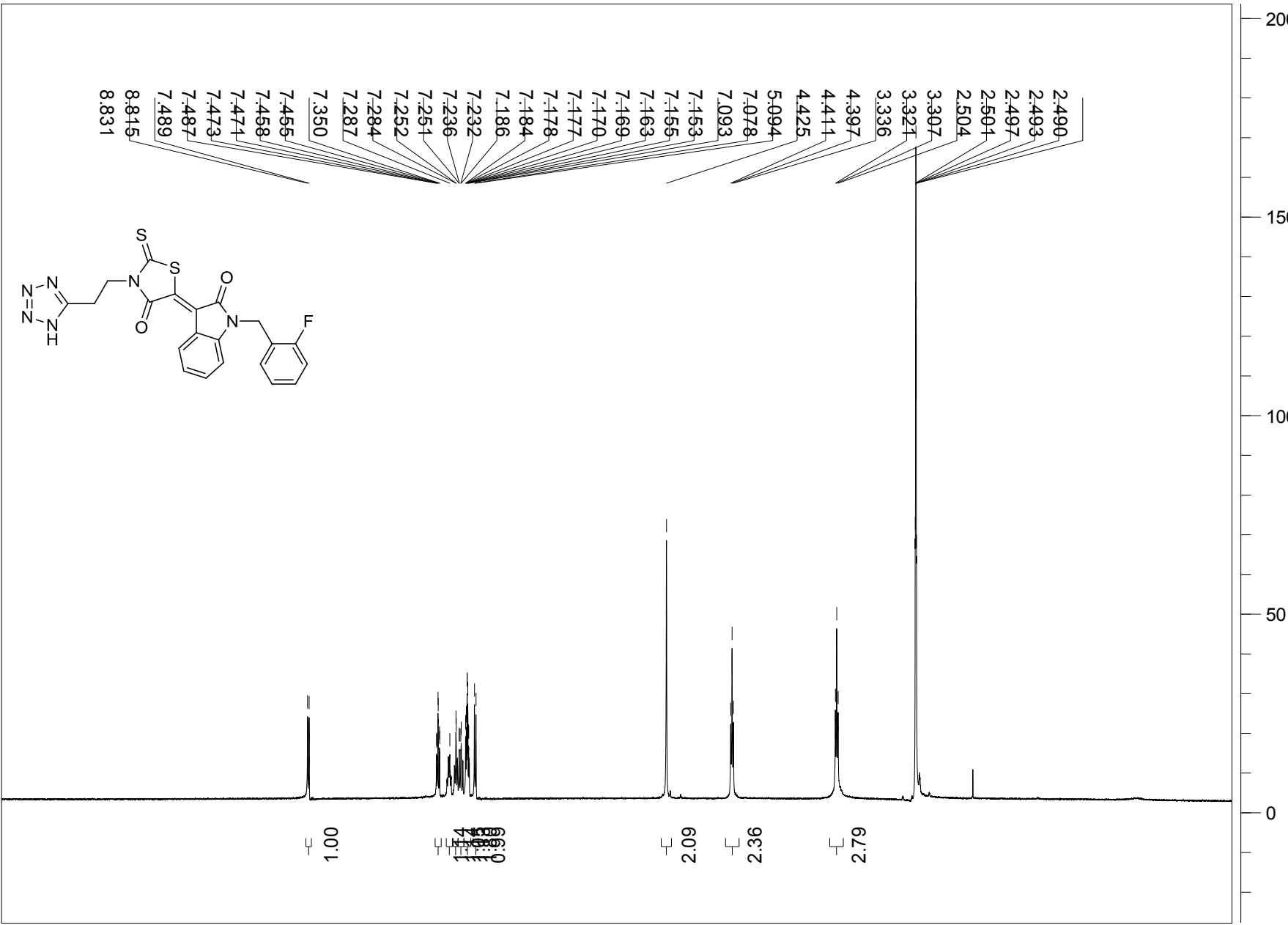
3-(2-(1H-tetrazol-5-yl)ethyl)-2-thioxothiazolidin-4-one; 1H



3-(2-(1H-tetrazol-5-yl)ethyl)-2-thioxothiazolidin-4-one; 13C



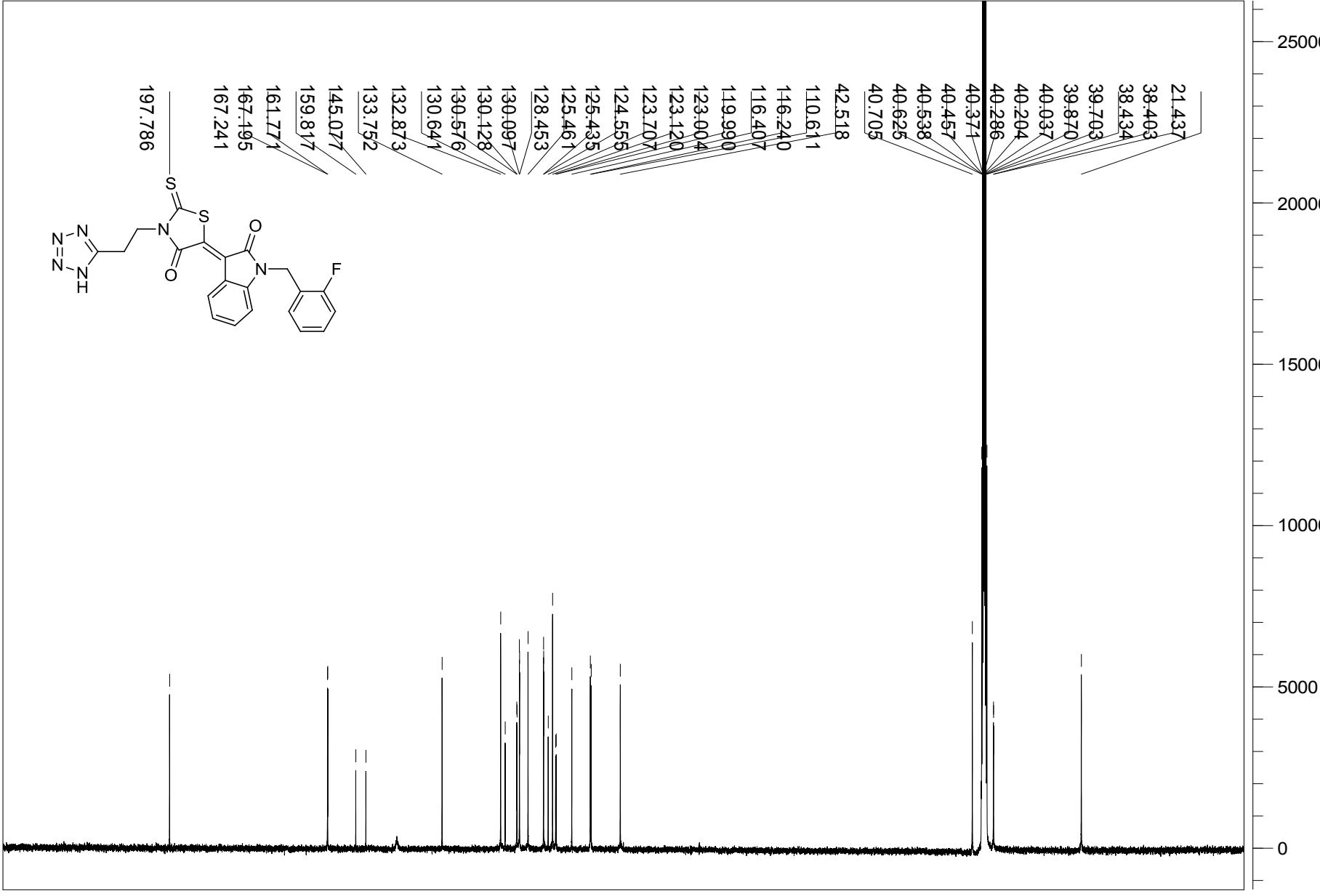
Inactive-2; 1H



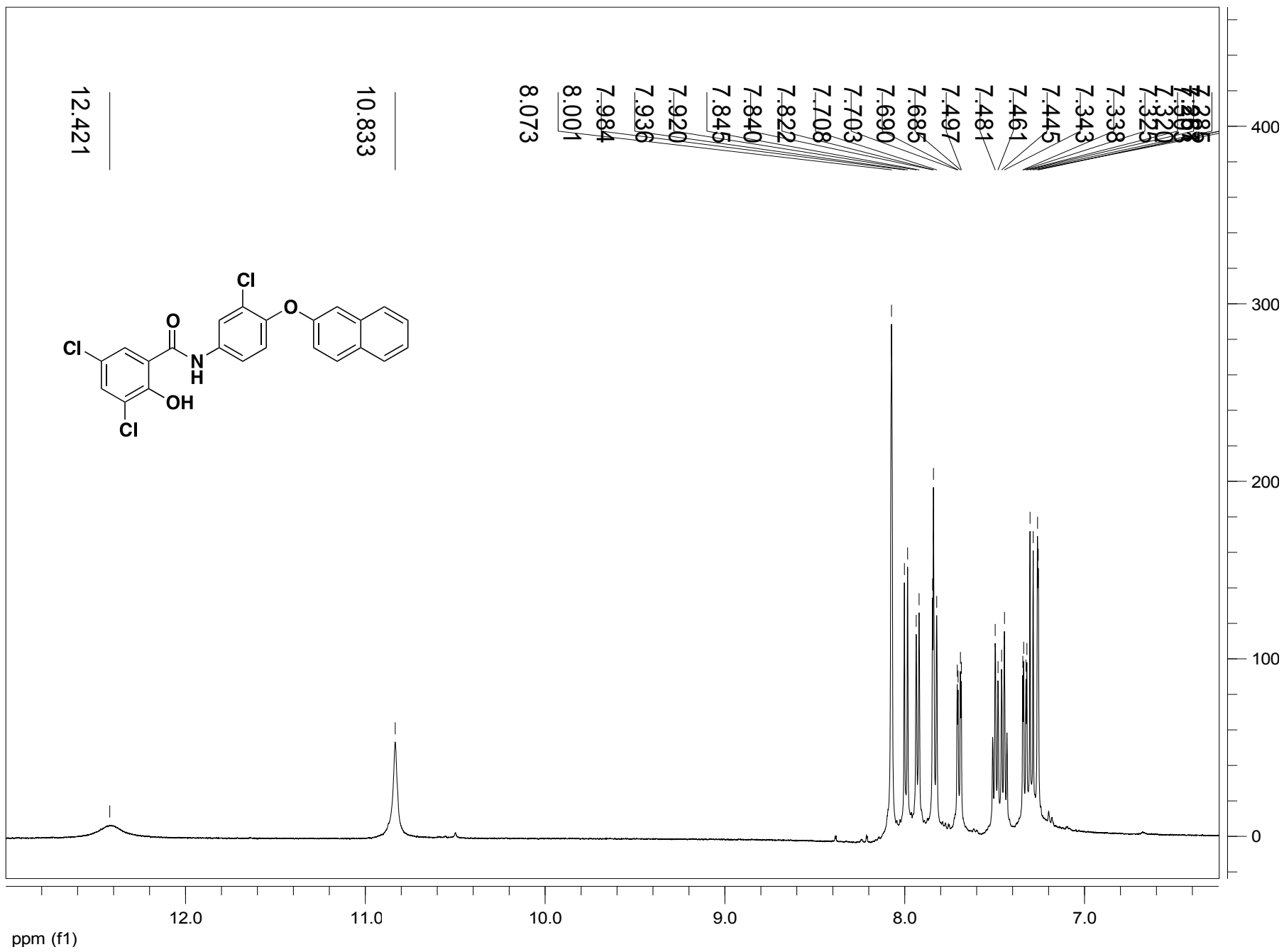
- 2.490
- 2.493
- 2.497
- 2.501
- 2.504
- 3.307
- 3.321
- 3.336
- 4.397
- 4.411
- 4.425
- 5.094
- 7.078
- 7.093
- 7.153
- 7.155
- 7.163
- 7.169
- 7.170
- 7.177
- 7.178
- 7.184
- 7.186
- 7.232
- 7.236
- 7.251
- 7.252
- 7.284
- 7.287
- 7.350
- 7.455
- 7.458
- 7.474
- 7.473
- 7.487
- 7.489
- 8.815
- 8.831

0.01
1.14
1.03
60.2
93.2
67.2

Inactive-2; 13C



6a; 1H



S74

ppm (f1)